# ROLES OF CD28, INDUCIBLE COSTIMULATOR, AND THE INTERLEUKIN-2 RECEPTOR IN HELPER T CELL MEMORY FORMATION

A DISSERTATION
SUBMITTED TO THE FACULTY OF THE GRADUATE SCHOOL
OF THE UNIVERSITY OF MINNESOTA
BY

ANTONIO JOSÉ PAGÁN

IN PARTIAL FULFILLMENT OF THE REQUIREMENTS
FOR THE DEGREE OF
DOCTOR OF PHILOSOPHY

MARC K. JENKINS, ADVISOR

July 2012

**Acknowledgements**

I would like to thank my mentor Dr. Marc Jenkins and my Thesis Committee: Dr. Daniel Mueller, Dr. Stephen Jameson, and Dr. Yoji Shimizu for their guidance throughout my doctoral training. I am also grateful to my laboratory colleagues for sharing their many insights and expertise with me, and Dr. Marion Pepper, in particular, for initiating our collaboration to study helper T cell memory formation and bringing the project to fruition. Lastly, I would like to thank the faculty, staff, and my classmates in the Microbiology, Immunology, and Cancer Biology graduate program and my colleagues in the Center for Immunology for providing an intellectually stimulating and collegial environment in which to grow as a scientist.

## Dedication

I dedicate this dissertation to my parents.  Thank you for instilling in me the joy of learning and always encouraging me to pursue my dreams.

**Abstract**

Numerous studies have suggested that CD28, Inducible Costimulator (ICOS), and Interleukin-2 receptor (IL-2R) signals shape the size and composition of the helper T cell memory pool, but the extent to which these signals regulate specific aspects of memory formation and the precise mechanisms of these processes remain unclear. To address this question, we used a sensitive peptide:Major Histocompatibility Complex II (p:MHCII) tetramer and magnetic bead-based enrichment method to track p:MHCII-specific helper T cells in mice throughout the course of an immune response. We found that CD28, ICOS, and the IL-2R each control unique aspects of helper T cell memory formation. The major defect in CD28-deficient T cells was a failure to sustain the proliferation of effector T cells and not a defect in memory formation per se; CD28-deficient T cells produced memory cells proportionate to the number of effectors present at the peak of the response. Our findings suggest that CD28 mediates this process by enhancing TCR-dependent NFκB signaling independently of the two CD28 cytoplasmic tail sequences previously implicated in clonal expansion. In contrast, ICOS or IL-2R deficiency did not grossly reduce the overall size of the effector or memory cell populations. Instead, they controlled the generation of two distinct subsets of memory T cells from effector cells that were present several days after infection. T-bet$^{high}$ T helper type-1 effector memory (Th1em) cells were generated in an IL-2R-dependent fashion. In contrast, T-bet$^{low}$ CC chemokine receptor 7 (CCR7)$^{+}$ CXC cheomokine receptor 5 (CXCR5)$^{+}$ central memory T (Tcm) cells were formed in a Bcl6- and ICOS-dependent manner from T follicular helper (Tfh) effector cells. Thus, CD28, ICOS, and IL-2R regulate distinct aspects of

helper T cell memory formation.

**Table of Contents**

## List of Figures

**Chapter 2**



**Chapter 3**

**Chapter 4**



**Chapter 5**

# Chapter 1:

# Background and Introduction

## 1.1 Adaptive Immunity

Adaptive, or acquired, immunity is a defining feature of the vertebrate immune system (Boehm, 2011). As posited by Burnet in his clonal selection theory, it is characterized by the selective engagement and expansion of antigen-specific lymphocytes upon binding their relevant antigen (Burnet, 1959). This initial antigen encounter can establish immunological memory, protecting the host from subsequent exposure to the same antigen or pathogen (Ahmed and Gray, 1996). The adaptive immune compartment of mammals consists of millions of B and T lymphocytes, each expressing multiple copies of a unique, randomly-generated antigen receptor (Boehm, 2011). Antigen receptors are generated somatically through a process termed V (D) J recombination, where gene segments in the Variable, Diversity, and Joining regions of the Immunoglobulin and T cell antigen receptor gene loci are "shuffled" in a Recombination Activating Gene (RAG)-1 and RAG-2-dependent manner (Schatz and Ji, 2011). Functional antigen receptors are generated during lymphocyte development without an *a priori* knowledge about their specificity. This dramatically differs from innate immune mechanisms of pathogen recognition, where functional receptors are encoded in the germ line and recognize evolutionarily conserved microbial structures, e.g. lipopolysaccharides, peptidoglycans, and CpG-rich bacterial DNA (Janeway and Medzhitov, 2002). The generation of highly variable antigen receptors enables vertebrates to mount immune responses to virtually any foreign substance (Nikolich-Zugich et al., 2004), but also pose the problem of self versus non-self discrimination

(Siggs et al., 2006). How do lymphocytes acquire tolerance to self, preventing autoimmunity, while preserving the capacity to mount an immune response to a pathogen? This fine balance is achieved during lymphocyte development.

## 1.2 Helper T Cell Development

T cells develop in the thymus, and can be sub-divided into those expressing αβ or γδ T cell antigen receptors (TCRs) (von Boehmer et al., 1998). αβTCR-expressing thymocytes differentiate into CD4 single positive (SP) T cells or CD8SP T cells, which recognize peptides bound to Major Histocompatibility Complex (MHC) II or MHCI, respectively. T cell development commences once bone marrow-derived T lineage progenitor cells seed the thymus (Love and Bhandoola, 2011). These cells then differentiate into thymocytes that undergo V (D) J gene rearrangement in the TCR gene loci. Only T cells that express a functional TCRβ chain, as determined by surface expression of and signal transduction via the pre-TCR, will subsequently rearrange their *Tcrα* loci (von Boehmer et al., 1998). Thymocytes co-expressing CD4 and CD8 molecules survey cortical thymic epithelial cells (cTECs) displaying self-peptides bound to MHCI and MHCII molecules in a process termed Positive Selection. Thymocytes that recognize self-peptide bound to MHCII will transduce pro-survival and differentiation signals through their TCRs and will develop into CD4SP thymocytes (Jameson et al., 1995; Singer et al., 2008). Positive Selection ensures that thymocytes that will continue developing have rearranged functional TCRs. Positively selected thymocytes then migrate to the thymic medulla, where they undergo Negative Selection. At this stage, thymocytes scan medullary thymic epithelial cells (mTECs) and dendritic cells (DCs) displaying ubiquitous and tissue-restricted self-peptides bound to MHC molecules. Importantly, cortical and medullary antigen-presenting cells (APC) process and present different p:MHC (Klein et al., 2009), indicating that the peptide MHC repertoire for selecting functional TCRs and establishing tolerance differ. Another, non-mutually exclusive model posits that the strength of TCR signaling as dictated by TCR affinity for p:MHC (Hogquist et al., 2005), microRNA regulation of TCR-associated phosphatase abundance (Li et al., 2007) and costimulatory molecules (Pobezinsky et al., 2012; Punt et al., 1997; Punt et al., 1994), determine selection outcomes. Most thymocytes that bind too avidly to self p:MHCII will undergo apoptosis or become Foxp3$^+$ regulatory T cells (Hogquist et al., 2005). Only those that weakly bind self p:MHCII will survive, become mature CD4$^+$ T cells, and populate secondary lymphoid tissues like the spleen, lymph nodes, and Peyer's patches. Normal CD4$^+$ T cell development produces a diverse repertoire MHCII-restricted cells that only weakly recognize self p:MHCII, thus ensuring that only mature cells with functional TCRs and low self-reactivity seed the secondary lymphoid tissues. Since foreign p:MHCII are often not involved in thymocyte selection, mature T cells are more likely to respond avidly to a foreign p:MHCII encountered in the secondary lymphoid tissues, as in the case of an infection.

## 1.3 Primary Helper T Cell Response

Naive T cells become activated, or primed, in the secondary lymphoid tissues. Soluble or particulate antigen drains from the infection site into the regional lymph node or is carried into the regional lymph node by migrating DCs, both via afferent lymphatic vessels (Catron et al., 2004; Gonzalez et al., 2011). In infections limited to barrier surfaces such as the skin, gut mucosa, or airways, priming occurs in the tissue-draining lymph node. While in blood-borne infections like *Listeria monocytogenes* infection, priming can occur in the spleen (Khanna and Lefrancois, 2008; Pamer, 2004). Immature DCs in direct contact with microbes or their products sense the infection via pattern recognition receptors, thus inducing their maturation. This process enhances the expression of MHCII and costimulatory ligands such as CD80 (B7-1) and CD86 (B7-2), which bind the surface receptor CD28 on T cells, and induces the synthesis of inflammatory cytokines like interleukin-12 (IL-12) (Greenwald et al., 2005; Janeway and Medzhitov, 2002). Migrating or lymph node resident DCs process pathogen-derived antigens and display pathogen-derived peptide bound to MHCII (p:MHCII) (Jenkins et al., 2001). Antigen presentation in the context of inflammatory and costimulatory signals induces T cell activation, while antigen presentation in a costimulation-poor environment or in the absence of inflammation promotes T cell unresponsiveness also known as anergy (Mueller et al., 1989b). Numerically rare, naive $CD4^+$ T cells with TCRs specific for pathogen-derived p:MHCII (at a frequency of about $1/10^6 – 1/10^5$ of all $CD4^+$ T cells) (Jenkins et al., 2010), but not those with TCRs of irrelevant specificities, will then expand exponentially and concomitantly differentiate into cytokine-producing effector $CD4^+$ T cells that in turn promote phagocyte, B cell, or $CD8^+$ T cell effector function (Jenkins et al., 2001). The specific differentiation program that the $CD4^+$ T cell undergoes depends on the inflammatory context of antigen encounter. For example, pathogens that induce IL-12 production, such as *Mycobacterium tuberculosis*, *Salmonella enterica* serovar Typhimurium, *Leishmania major*, *Toxoplasma gondii*, and *Listeria monocytogenes* promote the generation of interferon-γ $(IFN\text{-}\gamma)^+$ $CD4^+$ cells termed T helper-type 1 (Th1) cells. IFN-γ promotes inducible nitric oxide synthase (iNOS)-mediated microbicidal activity of infected macrophages and dendritic cells (Lazarevic and Glimcher, 2011) and also drives IgG2a isotype switching in B cells (Snapper and Paul, 1987). Other effector functions of $CD4^+$ T cells include CD40 ligand (CD40L)-dependent induction of B cell proliferation, class switch recombination, and somatic hypermutation and cytotoxic T cell activation via direct contact and by activating dendritic cells (Swain et al., 2012). Nonetheless, Th1 cell effector function is not limited to IFN-γ and CD40L; Th1 cells can also promote phagocyte function via production of Tumor Necrosis Factor (TNF) and enhance $CD8^+$ T cell activation through IL-2 secretion (Swain et al., 2012). Some effector $CD4^+$ T cells then egress the secondary lymphoid tissues and migrate into non-lymphoid tissues (Sallusto et al., 2004). While most of the effector cells will die after the pathogen is cleared, a few will persist as memory cells (Ahmed and Gray, 1996).

## 1.4 Helper T Cell Memory Formation

Memory $CD4^+$ T cells exist in at least two subsets referred to as central (Tcm cells) and effector memory cells (Tem cells) (Sallusto et al., 2004; Sallusto et al., 1999). Tem cells express homing receptors needed for migration into non-lymphoid organs, and when stimulated with the relevant p:MHCII ligand, immediately produce microbicidal cytokines (Reinhardt et al., 2001). Tem cells therefore closely resemble lineage-committed effector cells such as Th1 cells and have been shown to derive from these cells in some systems (Harrington et al., 2008; Lohning et al., 2008; Pepper and Jenkins, 2011; Surh and Sprent, 2008). In contrast, Tcm cells express CCR7 and L-selectin (CD62L), which direct recirculation through lymph nodes. When stimulated with the relevant p:MHCII ligand, Tcm cells do not produce microbicidal lymphokines immediately but proliferate to produce new effector cells, which then acquire these functions (Sallusto and Mackay, 2004).

Several factors have been identified that favor the formation of Th1 effector cells and subsequently Th1-like effector memory cells (Th1em). Strong or prolonged TCR signaling has been reported to favor Tem cell formation (Catron et al., 2006; Gudmundsdottir et al., 1999; Sarkar et al., 2007), perhaps as a result of a shift to glycolytic metabolism and activation of mammalian target of rapamycin (Araki et al., 2009; Pearce et al., 2009). IL-2 receptor signaling also plays a role in Th1 development (Khoruts et al., 1998), perhaps as a consequence of STAT5-mediated upregulation of the IL-12 receptor β2-chain and the Th1-associated T-bet (Liao et al., 2011) and Blimp-1 transcription factors (Gong and Malek, 2007; Pipkin et al., 2010), which repress the Bcl6 transcription factor (Oestreich et al., 2012; Shaffer et al., 2002). However, it remains to be determined if this pathway applies to Tem cells generated *in vivo* during infection.

Much less is known about how Tcm cells form. Tcm cells may be the progeny of effector cells that receive weaker TCR signals due to encounters with antigen-presenting cells that display low numbers of p:MHCII ligands, either by chance or due to entry into the relevant secondary lymphoid organs late in the response as the antigen concentration fades(Catron et al., 2006; van Faassen et al., 2005). Recent work indicates that $CD4^+$ Tcm cells defined by expression of CCR7 also express the B cell follicle homing CXCR5 (Chevalier et al., 2011) and are potent helper cells for B cells (Chevalier et al., 2011; MacLeod et al., 2011). These observations suggest that Tcm cells are related to T follicular helper (Tfh) cells (Morita et al., 2011), which depend on Bcl6 and help B cells in germinal centers (Crotty, 2011), but this relationship has not been directly addressed *in vivo*. The link between Bcl6 and Tcm cell development is further strengthened by the observation that Bcl6-deficiency impaired $CD8^+$ Tcm cell formation (Ichii et al., 2004). While the precise mechanism by which Bcl6 promotes $CD8^+$ Tcm cell development is not clear, it might involve repression of Blimp-1, a transcription factor involved in effector T cell differentiation (Kallies et al., 2009; Rutishauser et al., 2009; Shin et al., 2009). Collectively, these observations suggest that signals that promote Th1 effector cell development via Blimp-1 or Tfh cell development through Bcl6 might differentially regulate $CD4^+$ Tem versus Tcm cell formation.

Are $CD4^+$ memory T cells beneficial to the host? The contribution of $CD4^+$ memory T cells to protective immunity is controversial because $CD4^+$ T cells appear to be dispensable for long-term immunity to a variety of infections once $CD8^+$ T cell and/or humoral memory are established (MacLeod et al., 2009). Instead, sustained $CD4^+$ T cell responses are necessary for protective immunity to a variety of persistent infections, which appear to be chiefly mediated by effector $CD4^+$ T cells responses that are maintained by persistent antigen stimulation (Belkaid et al., 2002; Belkaid and Tarbell, 2009). Nonetheless, a few studies have documented the beneficial effects of generating $CD4^+$ memory T cells in response to infection or vaccination. Adoptive transfer of *L. major*-specific $CD4^+$ memory phenotype T cells into naive mice reduced parasite burdens compared to mice that did not receive parasite-specific T cells (Zaph et al., 2004). Similar results were obtained in *L. major*-challenged mice that had been primed with a non-persisting vaccine strain of *L. major* 6 months before challenge (Zaph et al., 2004). Other experiments showed that *Heligmosomoides polygyrus*-specific $CD4^+$ memory T cells in drug-cured helminth-infected mice conferred protection during a secondary infection (Anthony et al., 2006). Similar protective effects have been observed in *M. tuberculosis*-infected mice that had been previously immunized with the BCG vaccine strain of *Mycobacterium bovis* (Jung et al., 2005) or in those where a primary *M. tuberculosis* infection had been cleared with antibiotics (Andersen and Smedegaard, 2000). Bolstering these results, other experiments showed that adoptively transferring $CD4^+$ T cells from drug-cured *M. tuberculosis*-infected mice was sufficient to induce protection in infected T cell-deficient recipients (Andersen and Smedegaard, 2000). Other studies have demonstrated that memory $CD4^+$ T cell responses can facilitate B cell priming compared to naive T cells. Adoptive transfer of Tfh-like memory cells enhanced naive B cell antibody responses compared to mice that did not receive memory cells (MacLeod et al., 2011). Similarly, immunization with a vaccinia virus-derived peptide plus adjuvant produced a large population of antigen-specific $CD4^+$ T cells that enhanced a naive B cell virus-specific, protective humoral immune response compared to mice that had not been immunized with peptide (Sette et al., 2008). Thus, immunization strategies that specifically stimulate memory $CD4^+$ T cell formation might be therapeutically beneficial in the elaboration of optimal cellular and humoral immune responses.

## 1.5 CD28 Costimulation in Helper T cell Priming, Differentiation, and Memory Formation

CD28 is one of the most important stimulatory molecules for activating $CD4^+$ T cells. Naïve T cells and most antigen-experienced T cells express CD28. This surface receptor binds CD80 and CD86 molecules displayed by antigen presenting cells (APCs) like dendritic cells, B cells, and macrophages (Greenwald et al., 2005). APCs mature and increase expression of CD80, CD86, and other T cell-stimulatory molecules upon encountering microbial substances or pro-inflammatory cytokines. The stimulatory function of APCs besides antigen presentation is termed costimulation. Naïve $CD4^+$ T cells that interact with APCs presenting cognate antigen and high levels of CD80 and CD86 activate kinases downstream of the TCR and CD28, proliferate, make interleukin-2 (IL-2), and are responsive to subsequent TCR stimulation. Conversely, $CD4^+$ T cells stimulated in the absence of optimal CD28 engagement *in vitro* or *in vivo* undergo an abortive T cell response characterized by limited kinase activation, reduced proliferation and IL-2 production, and hyporesponsivess to subsequent TCR stimulation, a process termed anergy (Harding et al., 1992; Jenkins et al., 1990; Kearney et al., 1994; Kearney et al., 1995; Khoruts et al., 1998; Mueller et al., 1989a, b; Shahinian et al., 1993). These findings have led to a two-signal model of naïve T cell activation, in which the TCR delivers signal-1 and costimulatory signals, like those conferred through CD28, provide signal-2. This model posits that the context of T cell encounter with antigen dictates the outcome: T cell activation in the presence of costimulation, and tolerance in its absence.

How CD28 induces proper T cell responses remain unresolved. The two-signal model proposes that CD28 provides a unique signal, while another, non-mutually exclusive model argues that CD28 quantitatively enhances TCR signals. The latter involves amplifying or sustaining TCR signals (Acuto and Michel, 2003; Michel et al., 2001). Anti-CD28 treatment alone of T cell leukemia lines induces the transcription of a small set of genes, anti-CD3 stimulation induces an even larger set of genes, and stimulation with both sustains the transcription of the anti-CD3-induced genes (Riley et al., 2002). CD28 also maintains phopho-Lck in the immunological synapse (Holdorf et al., 2002). This is thought to sustain tyrosine phosphorylation of TCR immunoreceptor tyrosine-based activation motifs (ITAMs), thus increasing the activation of second messengers. CD28 signals can also integrate with TCR signals to activate or direct the localization of shared downstream targets (Acuto and Michel, 2003).

CD28 engagement *in vitro* increases $CD4^+$ T cell sensitivity to antigen by reducing the amount of p:MHCII complexes required for activation and accelerating the kinetics of activation (Iezzi et al., 1998; Viola and Lanzavecchia, 1996). Furthermore, increasing the amount of p:MHCII complexes well beyond physiological levels restores early T cell activation and early proliferation (Iezzi et al., 1998). These findings argue that CD28 signaling promotes T cell activation by lowering the threshold of TCR occupancy necessary for inducing a response, and suggest that the strength of TCR signaling sets the requirement for costimulation. However, these findings do not explain why T cells stimulated *in vitro* in the absence of CD28 at high antigen doses fail to make IL-2 or other cytokines and die (Sperling et al., 1996; Thompson et al., 1989). Thus it appears that increasing TCR signal strength does not fully compensate for CD28 deficiency. Early *in vitro* experiments demonstrated that anti-CD28 plus phorbol myristate acetate (PMA) induces IL-2 production and T cell proliferation that are resistant to cyclosporin A, in contrast to anti-CD3 stimulation, suggesting that CD28 can cooperate with Protein Kinase C (PKC) to induce these effects without a requirement to engage $Ca^{2+}$-dependent signaling (June et al., 1987). These observations place constraints on TCR signal amplification model of CD28 costimulation because they illustrate that CD28 can induce IL-2 production and proliferation in a manner that differs biochemically from TCR stimulation. It is possible that the truth may line somewhere between both proposed models, where CD28 amplifies some aspects of TCR signaling and also confers unique signals.

The controversy of how CD28 regulates $CD4^+$ T cell responses is further intensified by an incomplete understanding of the roles of the distinct cytoplasmic motifs of CD28. The cytoplasmic tail of CD28 contains three signaling motifs: a YMNM motif, a C-terminus proline-rich motif (PYAP), and an N-terminus proline-rich motif (PXXP). The YMNM and PYAP motifs are the two most studied, and the only ones with reported functions *in vivo*. The YMNM motif binds phosphoinositide-3-kinase (PI3K) and the adaptors Grb2 and Gads (Pages et al., 1994; Rudd and Schneider, 2003). This motif was required for acute graft-versus-host disease (GVHD), as T cells from CD28-deficient mice expressing a CD28 transgene with a Y→F substitution in its YMNM motif (Y170F) transferred into an MHC-mismatched recipient failed to cause disease (Harada et al., 2001). However, this motif was dispensable for a T-dependent antibody response (Okkenhaug et al., 2001). The basis for the discrepancies for the YMNM motif in these two experimental systems remains unknown. A potential reason could be the induction of other costimulatory molecules with tyrosine-based motifs, like Inducible Costimulator (ICOS), partially compensating for YMNM deficiency in CD28 in the case of T-dependent antibody responses but not induced in the GVHD model. Furthermore, it is not clear whether the defect observed in the GVHD model relates to suboptimal proliferation, survival, or effector function of alloreactive T cells.

CD28 signaling enhances the capacity of T cells responding to antigen to proliferate. This is thought to occur by inducing the expression of genes involved in cell growth and cell cycle progression and increased metabolic processing of nutrients. These processes are thought to be largely mediated by Akt and Akt-dependent activation mammalian Target of Rapamycin (mTOR) (Appleman et al., 2002; Bonnevier and Mueller, 2002; Edinger and Thompson, 2002; Schmelzle and Hall, 2000; Song et al., 2007; Zheng et al., 2007). This pathway controls cell growth, proliferation, and survival, can be induced by CD28 ligation alone, and is poorly induced by TCR signals alone (Appleman et al., 2002; Bonnevier and Mueller, 2002; Frauwirth et al., 2002; Song et al., 2007; Zheng et al., 2007). Activation of Akt induces mammalian Target of Rapamycin (mTOR) activity, which in turn, promotes nutrient uptake, glucose metabolism, macromolecule synthesis, and cell cycle activity (Edinger and Thompson, 2002; Schmelzle and Hall, 2000). Akt signals also induce the transcription of the anti-apoptotic gene *Bcl-x*$_L$ via NFκB (Boise et al., 1995; Khoshnan et al., 2000). The observation that pharmacological inhibition of PI3K limits T cell proliferation and glucose metabolism *in vitro* (8) is consistent with this scenario. Nonetheless, the connections between the YMNM motif and recruitment of PI3K and clonal expansion remain controversial. Some studies demonstrate that Y170F mutants fail to proliferate and make IL-2 in culture upon treatment with anti-CD3/CD28, while in others proliferation and IL-2 production are normal but survival is compromised (Burr et al., 2001; Harada et al., 2001; Okkenhaug et al., 2001). Yet another study showed that genetic disruption of the YMNM motif prevented PI3K binding and phosphorylation of Akt with no effect on IL-2 production, T-cell proliferation, or Bcl-x$_L$ expression (Dodson MCB 2009).

Other reports indicate that CD28 signals through the C-terminal PYAP motif (Friend et al., 2006). Disruption of this site eliminates PKCθ, Filamin A, and Lck recruitment to the CD28 cytoplasmic tail and prevents CD28-dependent enhancement of immunological synapse formation (Andres et al., 2004; Holdorf et al., 1999; Holdorf et al., 2002; Sanchez-Lockhart et al., 2008; Tavano et al., 2006; Viola et al., 1999; Wulfing and Davis, 1998; Wulfing et al., 2002; Yokosuka et al., 2008). These results suggest that CD28 ligation causes cytoskeletal changes that indirectly improve TCR signaling. This model is supported by the report that genetic disruption of the PYAP site reduced phosphorylation of PKCθ and impaired T cell proliferation (Dodson et al., 2009). This motif was also necessary for autoimmunity in CTLA-4-deficient mice (Tai et al., 2007) and for germinal center (GC) formation and T-dependent antibody production (Friend et al., 2006). T cells of mice with P→A mutations in this motif (AYAA) proliferate less and make less cytokines, including IL-2, Interferon-γ, and Tumor Necrosis Factor, than wild-type counterparts when cultured with anti-CD3/CD28 (Burr et al., 2001; Friend et al., 2006; Tai et al., 2005; Tavano et al., 2006). These studies suggest that the PYAP motif plays a critical role in cytokine production. However, it is possible that the proliferation defect observed *in vitro* is a result of little IL-2 production.

Yet other studies show that recruitment of Itk by the N-terminus PXXP motif enhances TCR signaling through NFAT and PLCγ1 (Marengere 1997, Michel Immunity 2001). Genetic disruption of the PXXP motif did not impair T cell proliferation *in vitro*, IL-2 production, or lymphoproliferative disease in CTLA4-deficient mice (Tai et al., 2005; Tai et al., 2007). Furthermore, the importance of Itk recruitment in CD28 signaling has been challenged by experiments showing that CD28 functions normally in Itk-deficient T cells (Li and Berg JI 2005). Thus, the PXXP motif seems less critical for CD28 function than the YMNM and PYAP motifs.

The observation that CD28 signaling enhances effector T cell survival has implications for memory cell formation. T cells primed under costimulation-poor conditions that induce clonal anergy in vivo, such as after peptide immunization in the absence of adjuvant, undergo an exaggerated contraction phase and fail to produce memory cells (Kearney et al., 1994; Walker and Abbas, 2002). While the molecular details of this defect remains unknown, the observation that OX40 deficiency impairs memory formation of $CD4^+$ T cells primed in vitro provides a plausible explanation implicating CD28 in this process (Rogers et al., 2001). CD28 signaling induces OX40 expression and OX40 signaling also promotes Bcl-$x_L$ expression (Rogers et al., 2001). Whether CD28 signaling is required for memory formation under costimulation-rich priming conditions, such as in the context of an infection remains unclear. A couple of studies suggested that CD28-deficient T cells responding to a viral infection showed impaired memory formation compared to CD28-sufficient T cells (Christensen et al., 2002; Fuse et al., 2008). However, these studies were limited by an inability to detect low numbers of antigen-specific T cells *in vivo*, a considerable hurdle when tracking cells that undergo limited clonal expansion, such as CD28-deficient $CD4^+$ T cells. CD28 is also thought to promote the survival of activated $CD4^+$ T cells by inducing the expression of the anti-apoptotic molecules Bcl-$x_L$ and Bcl-2 (Boise et al., 1995; Rogers et al., 2001; Sperling et al., 1996). As mentioned previously, CD28 ligation activates phosphoinositide 3-kinase (PI3K) and Akt to increase the glycolytic rate of T cells stimulated via the TCR (Frauwirth et al., 2002). Thus, CD28 might be required to maintain the metabolic demands of rapidly cycling T cells during the expansion phase. However, in two recent reports, reduction of anabolic metabolism in virus-specific $CD8^+$

T cells increased the proportion of cells that became memory cells (Araki et al., 2009; Pearce et al., 2009). Therefore, it is even possible that CD28 may limit the number of cells that become memory cells by increasing anabolic metabolism. The conflicting predictions set forth by these two lines of thought support revisiting the role of CD28 in memory cell formation.

Defining how CD28 controls $CD4^+$ T cell immunity is important for understanding and manipulating $CD4^+$ T cell responses. Models that posit that CD28 enhances TCR signals and those that argue that it exclusively provides unique signals make opposing predictions as to the requirements for CD28 stimulation within polyclonal $CD4^+$ T cells. If CD28 controls $CD4^+$ T cell activation by enhancing TCR signals, then it is likely that T cells with low affinities for cognate p:MHCII would not respond in the absence of CD28 stimulation. However, if CD28 provides unique signals, then all responding T cells would require CD28 stimulation. If the first model were correct, then only T cell clones below a certain p:MHC affinity threshold would be affected by blockade of CD28 signaling. If the second model were correct, then all responding T cells should be affected by CD28 blockade. Identifying how CD28 controls $CD4^+$ T cell immunity should suggest ways of enhancing or attenuating T cell responses clinically.

## 1.6 ICOS in Helper T Cell Differentiation and in Relation to CD28 Signaling

Inducible Costimulator (ICOS, CD278) is a costimulatory molecule structurally and functionally related to CD28 (Carreno and Collins, 2002; Hutloff et al., 1999; Yoshinaga et al., 1999). It is not expressed by naive T cells but rather induced on T cells upon TCR stimulation in the presence of costimulation (Carreno and Collins, 2002).

While CD28 signaling enhances ICOS expression (McAdam et al., 2000), CD28 is not strictly required for ICOS induction (Suh et al., 2004). In contrast to CD80 and CD86, DC and B cells constitutively express ICOS ligand (ICOSL, CD275) (Carreno and Collins, 2002). ICOS signaling is critical for optimal T-dependent antibody responses. Experiments with ICOS- or ICOSL-deficient mice or involving antibody blockade of ICOS show that ICOS signaling-deficient mice have impaired GC formation and T-dependent antibody production after immunization with protein plus adjuvant (Coyle et al., 2000; Mak et al., 2003; McAdam et al., 2001; Tafuri et al., 2001). Similar defects have been observed in ICOS-deficient humans (Grimbacher et al., 2003). Recent studies in ICOS signaling-deficient mice have attributed these defects in B cell responses to impaired Tfh cell formation (Akiba et al., 2005; Bossaller et al., 2006; Nurieva et al., 2008).

How ICOS specifically induces Tfh cell development is unclear. A comparison of T cells stimulated *in vitro* via their TCR plus CD28 or TCR plus ICOS revealed that ICOS costimulation induces nearly identical gene expression changes to CD28 signaling. A notable exception was the poor induction of *Il2* expression (Riley et al., 2002). This suggests that ICOS chiefly amplifies a TCR and/or CD28 delivered signal rather than transducing a unique signal. One possibility is that ICOS enhances expression of Bcl6, a transcriptional repressor necessary for Tfh cell formation (Johnston et al., 2009; Nurieva et al., 2009; Yu et al., 2009). A recent study by Crotty and colleagues demonstrated that ICOS-deficient $CD4^+$ T cells generated less $Bcl6^+$ cells during the expansion phase, suggesting a link between ICOS and early Bcl6 expression (Choi et al., 2011). However, this study did not identify the molecular basis of this effect. First of all, ICOS-deficiency produced a less dramatic defect in Tfh cell formation than T cell-specific Bcl6 deficiency, indicating that ICOS is not absolutely necessary for Bcl6 induction. Furthermore, it is still unclear whether ICOS directly enhances Bcl6 expression, thereby reinforcing a Tfh cell differentiation program, and/or promotes the survival or proliferation of Tfh cells.

In contrast to the flurry of conflicting data involving CD28 signaling, biochemical and genetic studies of ICOS paint a more cohesive picture of how ICOS signals. This discrepancy could be potentially attributed to the relatively simple structure of the ICOS cytoplasmic tail compared to that of CD28. ICOS contains a tyrosine-based motif but no proline-rich motifs (van Berkel and Oosterwegel, 2006). Thus far, the only signaling molecule known to bind the cytoplasmic tail of ICOS is PI3K, and this is even after conducting a yeast three-hybrid screen (Zang et al., 2006). ICOS recruits PI3K to the immunological synapse via its YMFM motif (Arimura et al., 2002; Coyle et al., 2000; Fos et al., 2008; Parry et al., 2003), suggesting that it acts specifically as an amplifier of TCR-induced PI3K signaling. Importantly, this motif cannot recruit other molecules that the CD28 YMNM motif binds, such as Grb2. This is because the tyrosine-based motif of ICOS lacks the YXNX docking site for Grb2 (Harada et al., 2003). Genetic disruption of the YMFM motif recapitulates the immune defects observed in *Icos*$^{-/-}$ mice (Gigoux et al., 2009), demonstrating that this is the critical signaling site in the cytoplasmic tail. Most, if not all, of the effects of ICOS signaling have been mapped to the PI3K pathway. T cell-specific deletion of the gene encoding the p110δ subunit of PI3K led to impaired Tfh cell development and T-dependent B cell responses, and conversely, genetic ablation of the lipid phosphatase *Pten* in the T cell compartment augmented them (Rolf et al., 2010). Furthermore, T cell-specific expression of constitutively active Akt or PTEN-deficiency

(Rathmell et al., 2003; Suzuki et al., 2001) induced lupus-like antibody-mediated autoimmunity similar to that observed in Roquin-mutant *sanroque* homozygous mice, which exhibit deregulated ICOS expression (Vinuesa et al., 2005). Interestingly, ICOS expression on naive T cells restored T-dependent antibody responses in CD28-deficient mice, thus demonstrating functional redundancy between ICOS and CD28 in promoting T-dependent B cell responses (Linterman et al., 2009). Nonetheless, ICOS overexpression did not restore thymic Foxp3$^{+}$ regulatory T (Treg) cell development in *Cd28*$^{-/-}$ mice (Linterman et al., 2009). Thymic Treg cell development critically depends on the PYAP but not the YMNM motif of CD28 (Lio et al., 2010; Tai et al., 2005; Vang et al., 2010). The inability of ICOS overexpression to rescue Treg cell development suggests that PI3K activity alone is not sufficient to recapitulate the relevant CD28 signals conferred via its PYAP motif. This observation supports the contention that the PYAP motif engages distinct signaling pathways from the YMNM motif and clearly illustrates that CD28 and ICOS signaling are not entirely synonymous.

While the biochemical link between ICOS and PI3K is clear, what is PI3K signaling precisely doing is less evident. In addition to its well-documented effects on Tfh cell differentiation, ICOS has also been shown to enhance clonal expansion; ICOS stimulation of T cells enhanced proliferation *in vitro* (Hutloff et al., 1999; Yoshinaga et al., 1999) and ICOS blockade reduced expansion of superantigen-binding CD4$^{+}$ T cells *in vivo* (Gonzalo et al., 2001), antigen-specific CD8$^{+}$ T cells during *L. monocytogenes* infection (Mittrucker et al., 2002), and limited lymphoproliferation in CTLA4$^{-/-}$ mice (van Berkel et al., 2005). The observations that ICOS can control the size of the effector T cell pool and its potential role in regulating Bcl6 expression, a process that has been implicated in $CD8^+$ Tcm cell generation (Ichii et al., 2004; Pipkin et al., 2010), suggest that ICOS could play a role in memory formation.

### 1.7 IL-2 Signaling in Helper T Cell Immunity

IL-2 is produced by naive T cells upon encountering cognate p:MHC in the context of costimulatory signals. CD28 is critical for IL-2 synthesis, as it both regulates the transcription of *Il-2* as well as the stability of its mRNA (Lindstein et al., 1989; Sanchez-Lockhart et al., 2004; Umlauf et al., 1995), and expression of the IL-2R$\alpha$ (CD25) (Costello et al., 1993). The IL-2R is comprised of an inducible $\alpha$ chain (CD25) and two constitutively expressed $\beta$ and $\gamma_c$ chains (Waldmann, 1989). While the IL-2R$\alpha$ cytoplasmic tail does not recruit signaling molecules, expression of the IL-2R$\alpha$ chain is necessary to form the high-affinity receptor capable of binding IL-2 (Waldmann, 1989). In addition to CD28, IL-2 signaling can enhance CD25 expression via a positive feedback loop (Waldmann, 1989). Seminal *in vitro* studies have shown that IL-2 can promote T cell clonal expansion (Mueller et al., 1989b). However, subsequent experiment tracking antigen-specific T cells in mice have shown conflicting roles for IL-2 in regulating T cell expansion *in vivo*. IL-2 was found to be dispensable for naive $CD4^+$ T cell (Khoruts et al., 1998) and $CD8^+$ T cell (Williams et al., 2006) clonal expansion *in vivo*, yet another group showed that it was necessary to sustain $CD8^+$ T cell expansion *in vivo* (Obar et al., 2010). IL-2 is thought to promote T cell expansion by inducing cell cycle progression (Brennan et al., 1997) as well as by conferring survival signals (Akbar et al., 1996; Dooms et al., 2007). Different structure-function studies attribute these effects to engagement of PI3K, MAPK, and/or STAT5 signaling cascades (Gaffen, 2001). More detailed analyses of IL-2-regulated pathways during an *in vivo* T cell immune response are needed to clarify this controversy. Other studies have shown that IL-2 signaling is required for optimal Th1 cell and cytotoxic T lymphocyte (CTL) differentiation and function. IL-2 signaling deficiency impaired T-bet and IL-12Rβ2 chain expression (Liao et al., 2011), IFN-γ production (Khoruts et al., 1998), CTL terminal differentiation (Kalia et al., 2010), $CD8^+$ memory T cell function (Williams et al., 2006), and induction of trafficking molecules necessary for CTL migration into non-lymphoid tissues (Sinclair et al., 2008). It remains to be determined if IL-2R signaling, which is critical for Th1 differentiation, plays a role in subsequent Th1em memory cell formation.

## 1.8 Detection of Numerically Rare Polyclonal Antigen-specific $CD4^+$ T Cells with p:MHCII Tetramers

The Jenkins laboratory recently developed a method of magnetically enriching rare, polyclonal $CD4^+$ T cells with p:MHCII tetramers and visualizing them by flow cytometry (Moon et al., 2007). This involves staining a single cell suspension of the tissues of interest, typically all spleen and lymph nodes, with fluorochrome-labeled p:MHCII tetramers. Tetramer-bound cells are subsequently stained with magnetic beads decorated with anti-fluorochrome antibodies. The cell suspension is then run through a magnetized column to capture the tetramer-bound cells. This approach has enabled the direct detection and quantification of specific naïve $CD4^+$ T cell precursors and low frequency memory $CD4^+$ T cells within the endogenous repertoire, something unachievable with previous methods. This technique allows one to bypass the need to adoptively transfer TCR transgenic T cells, an experimental manipulation that could affect the kinetics of activation, memory formation, and T cell survival (Badovinac et al., 2007; Garcia et al., 2007; Hataye et al., 2006; Marzo et al., 2005).

## 1.9 Statement of Thesis

Numerous studies have suggested that CD28, ICOS, and IL-2R signals shape the size and composition of the helper T cell memory pool, but the extent to which these signals regulate discrete processes remain unclear. This dissertation tests the hypothesis that CD28, ICOS, and the IL-2R control distinct aspects of the helper T cell memory formation. Using a sensitive p:MHCII tetramer and magnetic bead-based enrichment method to track polyclonal p:MHCII-specific helper T cells in genetically-modified mice throughout the course of an immune response, we found that CD28, ICOS, the IL-2R were necessary for different processes during memory cell formation. CD28 regulated the overall size of the effector T cell pool from which memory T cells emerged, an effect that appears to be achieved by enhancing TCR-induced NFκB activation but independently of the two CD28 cytoplasmic tail sequences previously implicated in clonal expansion. In contrast, ICOS and the IL-2R specifically participated in the generation of distinct memory precursor cell populations. ICOS signaling was necessary to generate Tfh cells from which Tcm cells emerge, and IL-2R signaling was critical to produce Th1 effector cells from which Tem cells form. Collectively, this work supports a model where CD28, ICOS, and the IL-2R act in non-redundant manners in helper T cell memory formation.

# Chapter 2:

## CD28 Promotes $CD4^+$ T Cell Clonal Expansion During Infection Independently of its YMNM and PYAP Sites

CD28 is required for maximal proliferation of $CD4^+$ T cells stimulated through their TCRs. Two sites within the cytoplasmic tail of CD28, a YMNM sequence that recruits PI3K and activates NFκB, and a PYAP sequence that recruits Lck, are candidates as transducers of the signals responsible for these biological effects. We tested this proposition by tracking polyclonal peptide:MHCII-specific $CD4^+$ T cells *in vivo* in mice with mutations in these sites. Mice lacking CD28 or its cytoplasmic tail had the same number of naive T cells specific for a peptide:MHCII ligand as wild-type mice. However, the mutant cells produced one-tenth as many effector and memory cells as wild-type T cells following infection with bacteria expressing the antigenic peptide. Remarkably, T cells with a mutated PI3K binding site, a mutated PYAP site, or both mutations proliferated to the same extent as wild-type T cells. The only observed defect was that T cells with a mutated PYAP or Y170F site proliferated even more weakly in response to peptide without adjuvant than wild-type T cells. These results show that CD28 enhances T cell proliferation during bacterial infection by signals emanating from undiscovered sites in the cytoplasmic tail.

## 2.1 Introduction

The generation of a primary $CD4^+$ T cell response to an infection depends on the display of MHCII-bound pathogen-derived peptides (p:MHCII) on the surface of APCs (Jenkins et al., 2001). Naïve $CD4^+$ T cells that express TCRs specific for these p:MHCII undergo multiple rounds of division and differentiate into effector cells capable of secreting cytokines that promote the microbicidal activity of other cells (Janeway and Medzhitov, 2002). Some of these effector T cells then survive the contraction phase to become long-lived quiescent memory cells capable of protecting the host from a second infection (Ahmed and Gray, 1996).

Although necessary, TCR signaling is not sufficient for maximal clonal expansion; concomitant CD28 signaling in response to its APC-displayed ligands CD80 and CD86 is also required. The importance of CD28 is evidenced by the failure of CD28-deficient mice to produce germinal centers and T cell-dependent antibody responses and to clear certain infections (Ferguson et al., 1996; McSorley and Jenkins, 2000). At the cellular level, it has been proposed that CD28 acts by enhancing cell division by augmenting IL-2 mRNA production or stability (Lindstein et al., 1989; Umlauf et al., 1995), while other reports indicate that CD28 has no effect on proliferation but promotes cell survival by increasing glucose metabolism (Frauwirth et al., 2002) or inducing Bcl-$x_L$ (Boise et al., 1995; Sperling et al., 1996).

CD28 signal transduction is also unclear. Some studies indicate that the biological effects of CD28 depend on a signal cascade emanating from the YMNM site in the CD28 cytoplasmic tail. Phosphatidylinositol 3-kinase (PI3K) has been reported to bind to the YMNM phospho-tyrosine (Pages et al., 1994), resulting in the recruitment of

3-phosphoinositide-dependent protein kinase (PDK1), Akt, and protein kinase C theta (PKCθ) to the immunological synapse (Sanchez-Lockhart et al., 2004; Yokosuka et al., 2008). PDK1 and Akt cooperate with PKCθ to activate the Bcl10/Carma1/Malt1 signalosome and subsequently induce translocation of NFkB to the nucleus and transcription of NFκB target genes encoding IL-2 (Jones et al., 2000; Narayan et al., 2006; Park et al., 2009; Sanchez-Lockhart et al., 2004) and Bcl-$x_L$ (Burr et al., 2001; Chen et al., 2000; Khoshnan et al., 2000). These results suggest a model in which CD28 ligation in the presence of TCR signaling activates NFκB through PI3K. Akt also activates mammalian target of rapamycin (mTOR) resulting in increased cell cycle activity and glucose metabolism (Edinger and Thompson, 2002; Rathmell et al., 2003; Song et al., 2007). The observation that pharmacological inhibition of PI3K limits T cell proliferation and glucose metabolism *in vitro* (Frauwirth et al., 2002) is consistent with this scenario. This model is challenged, however, by the determination that genetic disruption of the YMNM motif prevented PI3K binding and phosphorylation of Akt with no effect on IL-2 production or T-cell proliferation (Dodson et al., 2009; Okkenhaug et al., 2001).

Other reports indicate that CD28 signals through the C-terminal PYAP motif (Friend et al., 2006). Disruption of this site eliminates PKCθ, Filamin A, and Lck recruitment to the CD28 cytoplasmic tail and prevents CD28-dependent enhancement of the immunological synapse (Andres et al., 2004; Holdorf et al., 1999; Holdorf et al., 2002; Sanchez-Lockhart et al., 2008; Tavano et al., 2006; Viola et al., 1999; Wulfing and Davis, 1998; Wulfing et al., 2002; Yokosuka et al., 2008). These results suggest a model in which CD28 ligation signaling causes cytoskeletal changes that indirectly improve

TCR signaling by promoting formation of the immunological synapse. This model is supported by the report that genetic disruption of the PYAP site reduced phosphorylation of PKCθ, IL-2 secretion, and impaired T cell proliferation (Dodson et al., 2009).

It is possible that many of the conflicting reports about CD28 signaling relate to the experimental systems used. Many of the aforementioned studies employed transformed cell lines with aberrant TCR signaling machinery, long-term cultured T cell lines, non-p:MHCII stimuli such as mitogens, agonistic antibodies, or superantigens, and adoptive transfer of large numbers of TCR transgenic T cells, which can alter immune homeostasis (Hataye et al., 2006). We circumvented these limitations by studying the contributions of the YMNM and PYAP sites in CD28 during a physiologically relevant *in vivo* response of polyclonal p:MHCII-specific $CD4^+$ T cells to a bacterial infection. We found that CD28 was required to sustain, but not initiate, naive $CD4^+$ T cell proliferation, and suggest that CD28 achieves this effect by signaling independently of the YMNM and PYAP sites in its cytoplasmic tail.

## 2.2 Materials and Methods

### Mice

Six-to-eight week old C57BL/6 (B6), B6.PL-Thy1$^a$/CyJ (*Thy1.1*) mice, B6.SJL-*Ptprc$^a$ Pepc$^b$*/BoyJ (*Cd45.1*), B6.129S2-*Cd28$^{tm1Mak}$*/J (*Cd28$^{-/-}$*) (Shahinian et al., 1993), and B6.129S7-*Rag1$^{tm1Mom}$*/J (*Rag1$^{-/-}$*) (Mombaerts et al., 1992) mice were purchased from The Jackson Laboratory or the National Cancer Institute. *Cd28$^{-/-}$*, *Cd45.1/.2* heterozygotes, *Thy1.1/.2* heterozygotes, *Cd28$^{AYAA/AYAA}$* (*AYAA*) (Friend et al., 2006) and *Cd28$^{Y170F/Y170F}$* (*Y170F*) (Dodson et al., 2009) mice were bred in-house. Bone marrow from

*Cd28*$^{AYAA/AYAA\ Y170F/Y170F}$ (*AYAA/Y170F*) mice was provided by J. Green, bone marrow from *Cd28*$^{-/-}$ *full-length Cd28* trangenic and *tail-less Cd28* transgenic mice (Tai et al., 2005) was provided by A. Singer. Bone marrow from *Prkcq*$^{-/-}$ (Sun et al., 2000) and *p50*$^{-/-}$ *crel*$^{-/-}$ (Kontgen et al., 1995; Sha et al., 1995) mice was provided by A. Beg, and *Card11*$^{-/-}$ (Egawa et al., 2003) by M. Farrar. Mice were housed in specific pathogen-free conditions according to guidelines from the University of Minnesota and the National Institutes of Health. The Institutional Animal Care and Use Committee of the University of Minnesota approved all animal experiments.

**_L. monocytogenes_ Infection**

Mice were injected intravenously with $10^7$ colony forming units of Δ*actA L. monocytogenes* bacteria expressing a recombinant protein containing the 2W peptide (EAWGALANWAVDSA) fused to chicken ovalbumin (Ertelt et al., 2009).

**p:MHCII Tetramer Production**

Soluble 2W:I-$A^b$ and LLOp:I-$A^b$ molecules were produced and biotinylated in *Drosophila melanogaster* S2 cells and then combined with streptavidin-allophycocyanin or streptavidin-PE (Prozyme) to make tetramers, as previously described (Moon et al., 2007).

**p:MHCII Tetramer Staining and Magnetic Enrichment**

2W:I-$A^b$ and LLOp: I-$A^b$ staining and magnetic enrichment were performed as previously described (Moon et al., 2009). Briefly, single cell suspensions of spleen and lymph nodes were stained with 10 nM allophycocyanin- or PE-labeled 2W:I-$A^b$ or LLOp:I-$A^b$ tetramers for 1 hour at room temperature. Samples were then incubated with magnetic anti-fluorochrome microbeads and run through a magnetized LS column (Miltenyi Biotec).

**Antibodies and Flow Cytometry**

All antibodies were from eBioscience unless noted. Samples were stained at 4°C with Pacific Blue- or eFluor 450-conjugated anti-B220 (RA3-6B2), anti-CD11b (MI-70), anti-CD11c (N418), and anti-F4/80 (BM8, Invitrogen), Pacific Orange-conjugated anti-CD8α (5H10, Invitrogen), FITC-conjugated anti-CD3ε (145-2C11), peridinin chlorophyll protein-cyanine 5.5-conjugated anti-CD3ε (145-2C11), anti-Vα2 (B20.1) or anti-CD4 (RM4-5), Alexa Fluor-conjugated anti-CD44 (IM7), allophycocyanin-Alexa Fluor 750 or allophycocyanin-eFluor 780-conjugated anti-CD4 (RM4-5) antibodies. Samples were run on an LSRII flow cytometer (Becton-Dickinson) and analyzed with FlowJo software (Tree Star).

**DNA Staining and Detection**

Tetramer-enriched samples were stained with antibodies against surface antigens and subsequently fixed and permeabilized with eBioscience Fixation and Permeabilization Buffers. Cells were then stained with 4',6-diamidino-2-phenylindole, dihydrochloride (DAPI) (1μg/ml, Invitrogen) diluted in eBioscience Permeabilization Buffer for one hour at 4°C. The DAPI signal was visualized in linear mode on an LSRII equipped with a UV laser. The DAPI-A and DAPI-W parameters were used to exclude cell aggregates.

**Adoptive Transfer**

Polyclonal $CD4^+$ T cells from the spleen and lymph nodes of wild-type and *Cd28*$^{-/-}$ mice were isolated with a $CD4^+$ T cell isolation kit (Miltenyi Biotec). These were then labeled with CFSE (5μM; Invitrogen) as previously described (Quah et al., 2007). Four x $10^7$ $CD4^+$ T cells were transferred intravenously into individual *Cd90.1* sex-matched recipients. A day after transfer, some mice were infected with Lm-2W bacteria and 2W:I-$A^b$-specific T cells from the spleen and lymph nodes were magnetically enriched and detected as described above. PE-conjugated anti-CD90.2 (53-2.1) was used to identify donor-derived cells.

**Bone Marrow Irradiation Chimeras**

Bone marrow cells were harvested from crushed femurs, tibias, and humeri. T cells were depleted from bone marrow cell suspensions with anti-CD90.2 (30-H12) and low toxicity rabbit complement (Cedarlane Laboratories). To generate 50:50 mixed bone marrow chimeras, equal amounts of bone marrow from each donor strain were combined. Recipient mice were irradiated with 1,000 rads and injected intravenously with 5 – 10 x$10^6$ bone marrow cells. Chimerism in the blood was assessed 8 weeks after reconstitution by determining the percentages of donor-derived B cells or T cells of each strain. FITC-conjugated anti-CD45.2 (104), peridinin chlorophyll protein-cyanine 5.5-conjugated anti-CD45.1 (A20), PE-cyanine 7-conjugated anti-CD90.1 (HIS51), and allophycocyanin-conjugated anti-CD90.2 (53-2.1) antibodies were used to identify donor-derived cells. Variations in the absolute numbers of 2W:I-$A^b$-specific T cells due to minor differences in chimerism were corrected with the formula, c = (r/p) X 50%, where p is the percentage of cells among donor-derived cells obtained experimentally, r is the experimentally-determined absolute number of 2W:I-$A^b$-specific T cells, and c is the absolute number after the correction (Pepper et al., 2011).

**Peptide Immunization**

For analysis of clonal expansion without adjuvant, mice were immunized intravenously with 50μg of 2W peptide (EAWGALANWAVDSA) (GenScript) diluted in PBS.

**RelA Translocation Assay**

OT-II CD90.1$^+$ CD4$^+$ T cells were isolated from spleen and lymph nodes with a CD4$^+$ T cell isolation kit (Myltenyi Biotec) and 0.5-1 x $10^6$ cells were adoptively transferred into CD90.2$^+$ wild-type recipients. The next day, recipient mice were injected intravenously with 5 μg of *Escherichia coli* LPS (List Biological Laboratories) diluted in PBS and then a day later, some mice were iinjected intravenously with 100 μg of chicken ovalbumin peptide 323-339 (OVAp) (Invitrogen) diluted in PBS. Spleens were harvested 20 min after peptide injection, and single cell suspensions of splenocytes were immediately made in 1.5% paraformaldehyde (Electron Microscopy Sciences). CD90.1$^+$ cells were magnetically enriched as previously described (44). Enriched cells were permeabilized in 0.5% saponin (SIGMA) and stained with biotin-conjugated anti-CD90.1 (HIS51), peridinin chlorophyll protein-cyanine 5.5-conjugated streptavidin, PE-conjugated anti-Vβ5 (MR9-4, Pharmingen), AlexaFluor-488-conjugated anti-RelA (F-6, Santa Cruz Biotechnology), and 7-aminoactinomycin D (7AAD) (5μM, Invitrogen). RelA localization was determined with an ImageStream 300 (Amnis Corp.) scanning flow cytometer as previously described (Medeiros et al., 2007).

**Statistical Analyses**

Statistical tests were performed with Microsoft Excel or GraphPad Prism software. P values less than 0.05 were considered statistically significant. Comparisons of absolute cell numbers were done on the $\log_{10}$ of each value (i.e., linearized) to minimize differences in statistical variance of the raw values caused by exponential growth. The two-tailed Student's *t* test was used when comparing two groups, and a one-way analysis of variance (ANOVA) with Bonferroni's post-test was performed when comparing three groups. The one-phase exponential decay was used to calculate the half-life of 2W:I-$A^{b+}$ T cells during the contraction (days 5 - 20) and memory (days 20 - 160) phases. Mean absolute numbers of 2W:I-$A^{b+}$ T cells at each time point within a specified time span were used to determine the best-fit values.

## 2.3 Results

### CD28 Enhances the Expansion of Polyclonal $CD4^+$ T Cells Responding to an *L. monocytogenes*-derived p:MHCII *In Vivo*

We used p:MHCII tetramers and a magnetic bead-based enrichment method to detect endogenous p:MHCII-specific $CD4^+$ T cells (Moon et al., 2009; Moon et al., 2007) responding to bacterial infection in mice expressing the I-$A^b$ MHCII molecule. The *L. monocytogenes* strain used for these experiments was attenuated due to lack of the *actA* gene product needed by the bacteria to spread from one host cell to another (Portnoy et al., 2002), and was engineered to secrete plasmid-encoded chicken ovalbumin fused to a peptide called 2W (AWGALANWA) under control of the *hly* promoter (Lm-2W) (Ertelt et al., 2009). These bacteria also secrete listeriolysin O (LLO) expressed from the endogenous *hly* gene on the bacterial chromosome. The 2W peptide and LLO peptide 190-201 (LLOp) bind to I-$A^b$ MHCII molecules and stimulate $CD4^+$ T cells in C57BL/6 mice (Geginat et al., 2001; Rees et al., 1999). We produced 2W- and LLOp-containing I-$A^b$ streptavidin-fluorochrome tetramers and used them with anti-fluorochrome-conjugated magnetic beads to enrich specific T cells from the spleen and lymph nodes of naïve and infected mice.

We initially sought to determine whether the pre-immune $CD4^+$ T cell repertoires of wild-type and CD28-deficient mice were similar. Uninfected wild-type and CD28-deficient mice contained about 200 2W:I-$A^b$- and 80 LLOp:I-$A^b$-specific $CD4^+$ T cells in the spleen and lymph nodes, most of which were $CD44^{low}$ as expected for naïve cells (Figure 2.1A). No $CD4^+$ T cells bound both tetramers and less than 5 $CD8^+$ T cells per mouse bound either tetramer, demonstrating that tetramer binding was TCR-specific. TCR $V\alpha2^+$ cells were under represented in the 2W:I-$A^b$-specific naive populations but over represented in the LLOp:I-$A^b$-specific naive populations in wild-type and CD28-deficient mice (Figure 2.1B). The fact that 2W:I-$A^b$- and LLOp:I-$A^b$-specific naive populations had similar sizes and compositions in wild-type and CD28-deficient mice indicated that CD28 deficiency did not grossly alter the T cell repertoire.

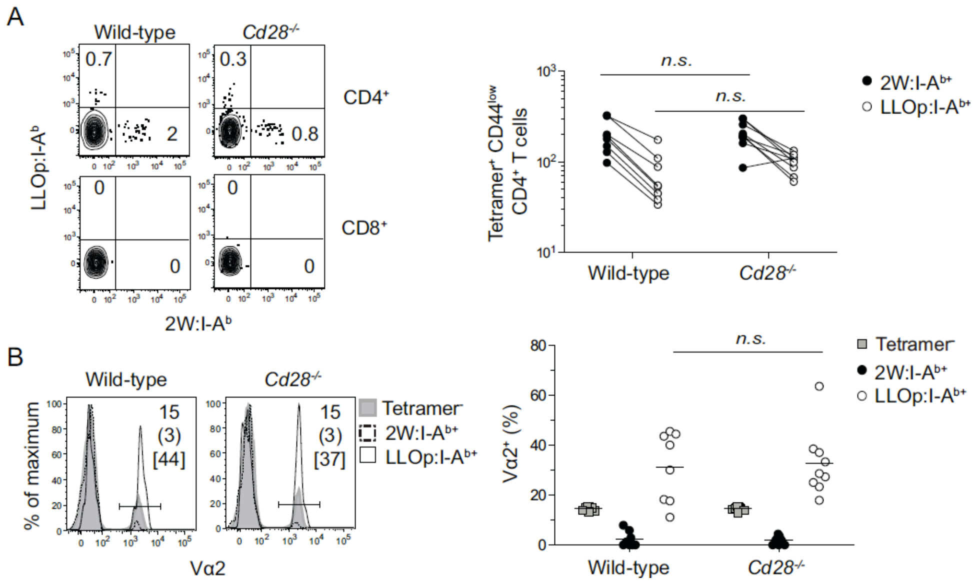


**Figure 2.1. Detection of Naive p:MHCII-specific CD4$^+$ T Cells in Wild-type and CD28-deficient Mice.** 2W:I-A$^{b+}$ and LLOp:I-A$^{b+}$ T cells were magnetically enriched from pooled spleen and lymph nodes and visualized by flow cytometry. (A) Flow cytometry plots of 2W:I-A$^b$ and LLOp:I-A$^b$ tetramer-staining of CD3$^+$ non-T lineage marker$^-$ CD4$^+$ or CD8$^+$ T cells (left), and enumeration of tetramer-stained CD4$^+$ T cells in wild-type and CD28-deficient mice (right). Numbers on the plots depict the percentages of 2W:I-A$^{b+}$ and LLOp:I-A$^b$ within the enriched CD4$^+$ or CD8$^+$ T cells. Lines on the graph connect the number of 2W:I-A$^{b+}$ and LLOp:I-A$^{b+}$ T cells in individual mice. (B) Histograms (left) of Vα2 staining on 2W:I-A$^{b+}$, LLOp:I-A$^{b+}$, and tetramer$^-$ T cells, and the percentage of Vα2$^+$ cells among these three cell types (right). Numbers in histograms show the percentage of Vα2$^+$ cells in tetramer$^-$ T cells (top), 2W:I-A$^{b+}$ T cells (middle), and LLOp:I-A$^{b+}$ T cells (bottom). Horizontal lines on the plot indicate mean values, and each symbol depicts a value from an individual mouse. Groups were compared with a two-tailed Student's *t* test. *n.s.,* not significant, $p > 0.05$. Pooled data from two (A) or four (B) independent experiments are shown.

Wild-type and CD28-deficient mice were then infected intravenously with Lm-2W bacteria to assess the role of CD28 in the activation of naive T cells *in vivo*. The 2W:I-$A^b$-specific cells in each group increased comparably over the first 3 days after Lm-2W infection (Figure 2.2A). However, by day 4 this population was 10-times smaller in CD28-deficient mice than in wild-type mice, a difference that was maintained at the peak on day 5. The 2W:I-$A^b$-specific populations in CD28-deficient and wild-type mice then contracted between days 5 and 20 with a half-life of about 2 days and fell to 10% of their respective maximum values. The 10-fold difference between the two groups was then maintained after day 20 as both populations declined slowly during the memory phase with a half-life of ~50 days (Figure 2.2A). LLOp:I-$A^b$-specific T cells also expanded about 10-fold less well in CD28-deficient than in B6 mice, a difference that was maintained 20 days post infection Figure 2.2B). Thus, CD28 deficiency impaired the extent of $CD4^+$ T cell expansion but did not alter survival during the contraction or memory phases.

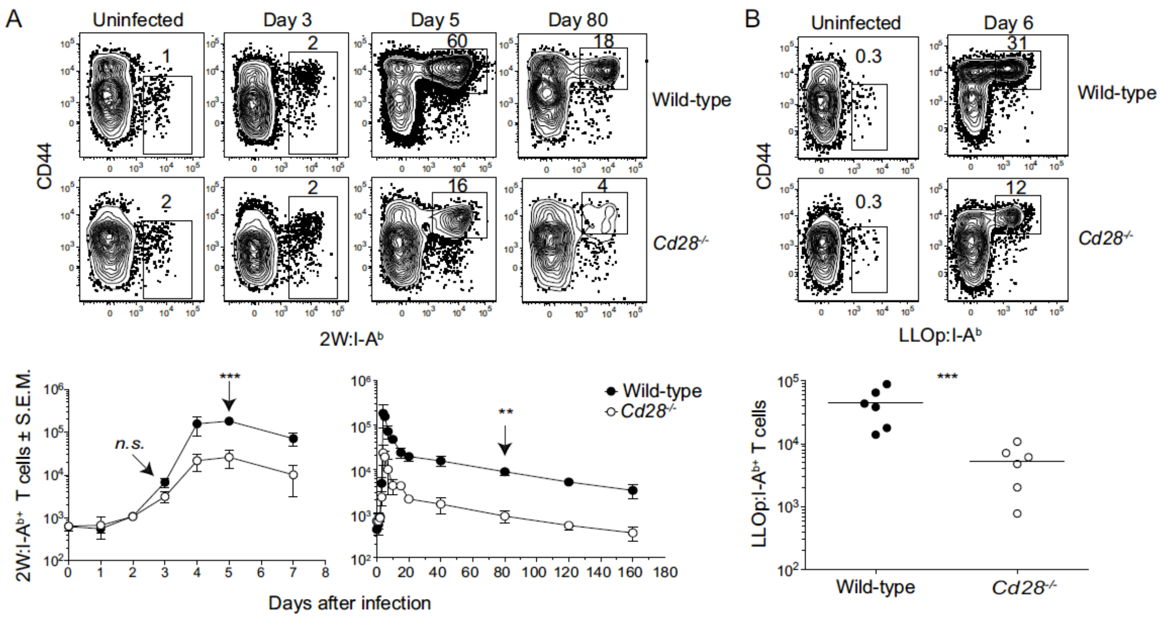


**Figure 2.2. Kinetics of Primary $CD4^+$ T Cell Response to *L. monocytogenes* in Wild-type and CD28-deficient Mice.** 2W:I-$A^{b+}$ or LLOp:I-$A^{b+}$ T cells were magnetically enriched from wild-type and CD28-deficient mice infected intravenously with Lm-2W. (A) and (B) Flow cytometry plots of (A) 2W:I-$A^b$ or (B) LLOp:I-$A^b$ versus CD44 staining on $CD4^+$ T cells from wild-type or CD28-deficient mice (top) with graphs depicting the nmean number ($n \geq 3$) of (A) 2W:I-$A^{b+}$ or (B) LLOp:I-$A^{b+}$ T cells (bottom). A two-tailed Student's *t* test on the $\log_{10}$ values of each group at the indicated time points (arrow) was used to determine statistical significance, *n.s.,* not significant, $p > 0.05$; ** $p < 0.01$, *** $p < 0.001$. Pooled data from six (A) or two (B) independent experiments are shown.

### CD28 Is Necessary to Sustain Cell Cycle Activity of p:MHCII-specific $CD4^+$ T Cells *In Vivo*

CD28 signals enhance cell cycle entry and $G_1$ to S phase cell cycle progression of $CD4^+$ T cells *in vitro* (Appleman et al., 2002; Bonnevier and Mueller, 2002; Bonnevier et al., 2006; Iezzi et al., 1998; Wells et al., 1997) and sustain proliferation of monoclonal T cells *in vivo* (Gudmundsdottir et al., 1999a; Khoruts et al., 2004). DNA replication was measured to determine if CD28 deficiency impaired cell cycle activity in polyclonal p:MHCII-specific $CD4^+$ T cells during infection (Figure 2.3A). All naïve $CD44^{low}$ 2W:I-$A^b$-specific T cells from uninfected wild-type and CD28-deficient mice were in $G_0/G_1$. Similar numbers of 2W:I-$A^b$-specific T cells progressed to S and $G_2/M$ in both groups on day 2. The proportion of cells in S and $G_2/M$ in both groups peaked on day 3, but CD28-deficient mice had fewer cells in S and $G_2/M$ than controls. By day 4, both groups were returning to $G_0/G_1$, with CD28-deficient mice having fewer cycling cells. Thus, CD28 was not needed for entry into S and $G_2/M$ in the early stages of clonal expansion but was required for maintaining cell cycle activity.

To further test whether the requirement of CD28 for sustained T cell cycling was cell-intrinsic, polyclonal $CD4^+$ T cells from the spleen and lymph nodes of wild-type or CD28-deficient mice were labeled with CFSE and transferred into congenic recipients, which were then infected with Lm-2W bacteria. About 100 donor-derived wild-type and CD28-deficient 2W:I-$A^b$-specific T cells were detected in uninfected recipients, and these were $CFSE^{high}$ (Figure 2.3B) as expected for quiescent naïve cells. By day 3, both 2W:I-$A^b$-specific wild-type and CD28-deficient donor T cells had diluted CFSE similarly and expanded about 4-fold (Figure 2.3B). By day 5, most of the wild-type T cells had diluted CFSE beyond the limit of detection. In contrast, most CD28-deficient T cells had not diluted CFSE beyond the levels achieved by day 3. The transferred wild-type T cells expanded about 130-fold above the starting number by day 5, while the CD28-deficient T cells increased only 7-fold (Figure 2.3B). Thus, CD28 was necessary to sustain, but not initiate $CD4^+$ T cell proliferation in response to *L. monocytogenes* infection.

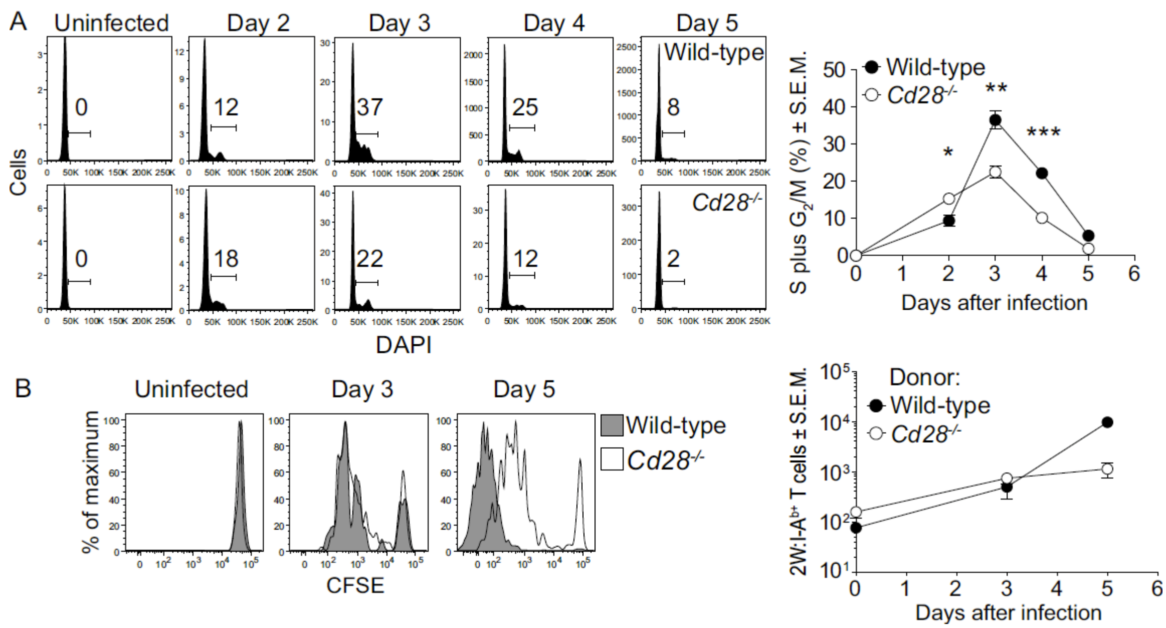


**Figure 2.3. CD28 is Required to Sustain but Not Initiate $CD4^+$ T Cell Proliferation *In Vivo.*** (*A*) Histograms of DAPI staining on 2W:I-$A^{b+}$ T cells from wild-type or CD28-deficient mice infected with Lm-2W bacteria (left). Gates show the percentages of cells in S plus $G_2$/M phases of the cell cycle. Mean percentage ($n \geq 3$) of 2W:I-$A^{b+}$ T cells in S plus $G_2$/M (right). A two-tailed Student's *t* test was used to identify statistical differences between groups, * $p < 0.05$; ** $p < 0.01$, *** $p < 0.001$. (*B*) Histograms of CFSE in 2W:I-$A^{b+}$ T cells from $CD90.2^+$ wild-type or CD28-deficient $CD4^+$ T cells in $CD90.1^+$ wild-type recipients that were subsequently infected with Lm-2W (left) with the mean number (2 - 4 mice per time point) of donor-derived wild-type or CD28-deficient 2W:I-$A^{b+}$ T cells (right). Each graph shows pooled data from three independent experiments.

## The PYAP and Y170F Motifs of CD28 Are Dispensable for CD4$^+$ T Cell Clonal Expansion in Response to *L. monocytogenes* Infection

We next attempted to identify the regions of the CD28 cytoplasmic tail that produced these biological effects. This was done using mixed hematopoietic cell chimeras produced by transplanting lethally irradiated mice with equal numbers of wild-type and CD28-deficient bone marrow cells (Figure 2.4A). These chimeras contained similar numbers of wild-type and CD28-deficient 2W:I-A$^b$-specific naive CD4$^+$ T cells (Figure 4B). In contrast, the wild-type 2W:I-A$^b$-specific CD4$^+$ T cells expanded 50-fold more than the CD28-deficient cells following Lm-2W infection (Figure 2.4B).

The role of the cytoplasmic tail was tested in mixed chimeras containing wild-type T cells and *Cd28*$^{-/-}$ T cells expressing full-length or cytoplasmic tail-deficient (Tail-less) *Cd28* transgenes. The 2W:I-A$^b$-specific CD4$^+$ T cells with tail-less CD28 expanded about 10 times less than the cells with full-length CD28 (Figure 2.4C). Remarkably, however, 2W:I-A$^b$-specific CD4$^+$ T cells with a mutated C-terminal PYAP motif (AYAA), an SH2 domain-binding YMNM motif (Y170F), or both mutations expanded to the same extent as the wild-type CD4$^+$ T cells after Lm-2W infection (Figure 2.4D - F). Thus, the cytoplasmic tail, but neither the PYAP nor the YMNM motifs within the tail were required for the *in vivo* effects of CD28 on clonal expansion after this infection.

It was possible that these negative results were related to the involvement of costimulatory receptors other than CD28, the ligands for which are induced by infection. This possibility was tested by assessing the responsiveness of the CD28-deficient T cells following injection of peptide without an adjuvant. As shown in Figure 2.4G, injection of 2W peptide alone induced expansion of wild-type 2W:I-A$^b$-specific T cells, but at a level that was about 40-fold lower than that induced by Lm-2W infection. The expansion of CD28-deficient 2W:I-$A^b$-specific T cells after injection of 2W peptide alone was 8-fold lower than that of wild-type cells. The expansions of 2W:I-$A^b$-specific $CD4^+$ T cells with mutated PYAP or YMNM motifs were also lower than that of wild-type cells but only by 2-fold. These results indicate that the PYAP and YMNM sites in the cytoplasmic tail of CD28 transduce signals in polyclonal p:MHCII-specific $CD4^+$ T cells under conditions of minimal inflammation.

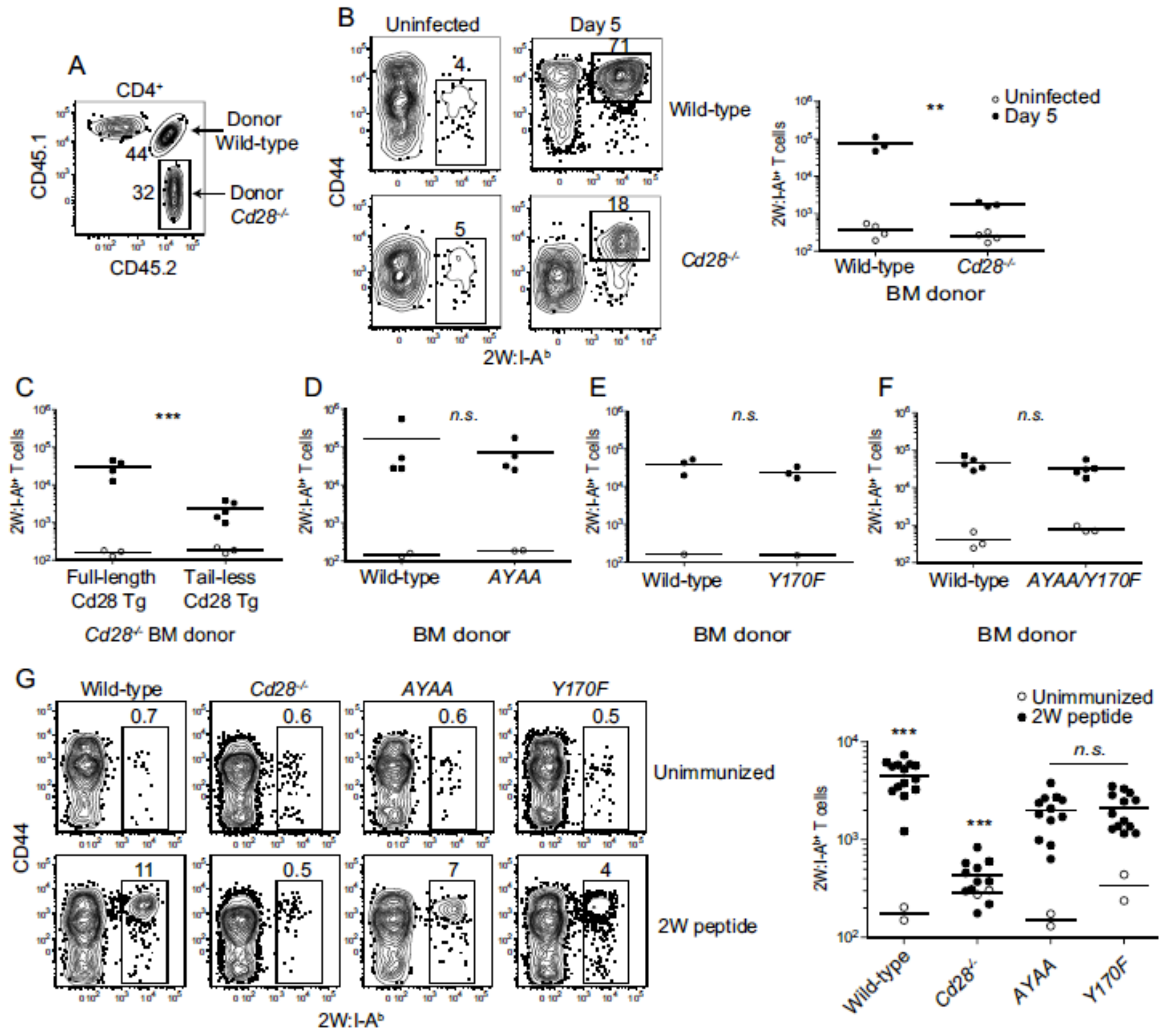


**Figure 2.4. The PYAP and YMNM Motifs of CD28 Are Dispensable for CD28-dependent $CD4^+$ T Cell Clonal Expansion in Response to *L. monocytogenes* Infection.** (A) Flow cytometry plot showing gates used to identify wild-type and CD28-deficient $CD4^+$ T cells in a 2W:I-$A^b$ tetramer-enriched sample from a radiation bone marrow chimeric mouse. Numbers indicate the percentage of donor wild-type or CD28-deficient $CD4^+$ T cells in the enriched sample. (B) Flow cytometry plots of 2W:I-$A^b$ versus CD44 on donor-derived wild-type or CD28-

deficient $CD4^+$ T cells from uninfected or day 5 Lm-2W infected mice (left). (B right plot - F) Numbers of wild-type and CD28 mutant 2W:I-$A^{b+}$ T cells in uninfected and day 5 Lm-2W infected mice. (G) Flow cytometry plots of 2W:I-$A^b$ versus CD44 on $CD4^+$ T cells from the spleens of wild-type or CD28 mutant mice (left) and absolute numbers of 2W:I-$A^{b+}$ T cells in unimmunized mice (open circles) or mice that had been injected intravenously 5 days earlier with 2W peptide without the addition of any adjuvant (filled circles). A two-tailed Student's *t* test was used to compare the $\log_{10}$ values of Lm-2W infected groups and a one-way ANOVA with Bonferroni post-test was used to compare the $\log_{10}$ values of peptide-immunized groups, *n.s.* $p > 0.05$; ** $p < 0.01$, *** $p < 0.001$. Data are from up to five independent experiments.

**CD28 Deficiency Phenotypically Resembles T Cell-intrinsic NFκB Signaling Deficiency During Response to *L. monocytogenes* Infection**

The perplexing finding that neither of the suspected motifs within the tail were required for the *in vivo* effects of CD28 led us to investigate whether NFκB signaling was involved. This was the case as evidenced by the finding that CD28-deficient 2W:I-$A^b$- and LLOp:I-$A^b$-specific T cells did not induce Bcl-$x_L$, an NFκB-regulated gene product, (Chen et al., 2000; Khoshnan et al., 2000), 3 days after Lm-2W infection like control cells (Figure 2.5A). These findings suggested that signals from CD28 contribute to activation of NFκB in this setting. If so, then loss of NFκB signaling would be expected to produce the same defects in T cell activation as CD28 deficiency. This possibility was tested in radiation bone marrow chimeras containing wild-type and *Card11*$^{-/-}$ T cells lacking the CARMA1 component of the NFκB signaling pathway. Like CD28-deficient cells, CARMA1-deficient 2W:I-$A^b$-specific T cells began to expand normally on day 3 after infection but did not continue to expand to day 5 when these T cells exhibited a 40-

fold defect compared to wild-type cells (Figure 2.5B). Similary, CARMA1-deficient failed to induce Bcl-$x_L$ (Figure 2.5B) like CD28-deficient cells. PKCθ- and NFκB1/c-Rel-deficient 2W:I-$A^b$-specific $CD4^+$ T cells had similar clonal expansion defects (Figure 2.5C and D). These results show that the expansion defect of CD28-deficient cells resembles that of NFκB signaling-deficient cells.

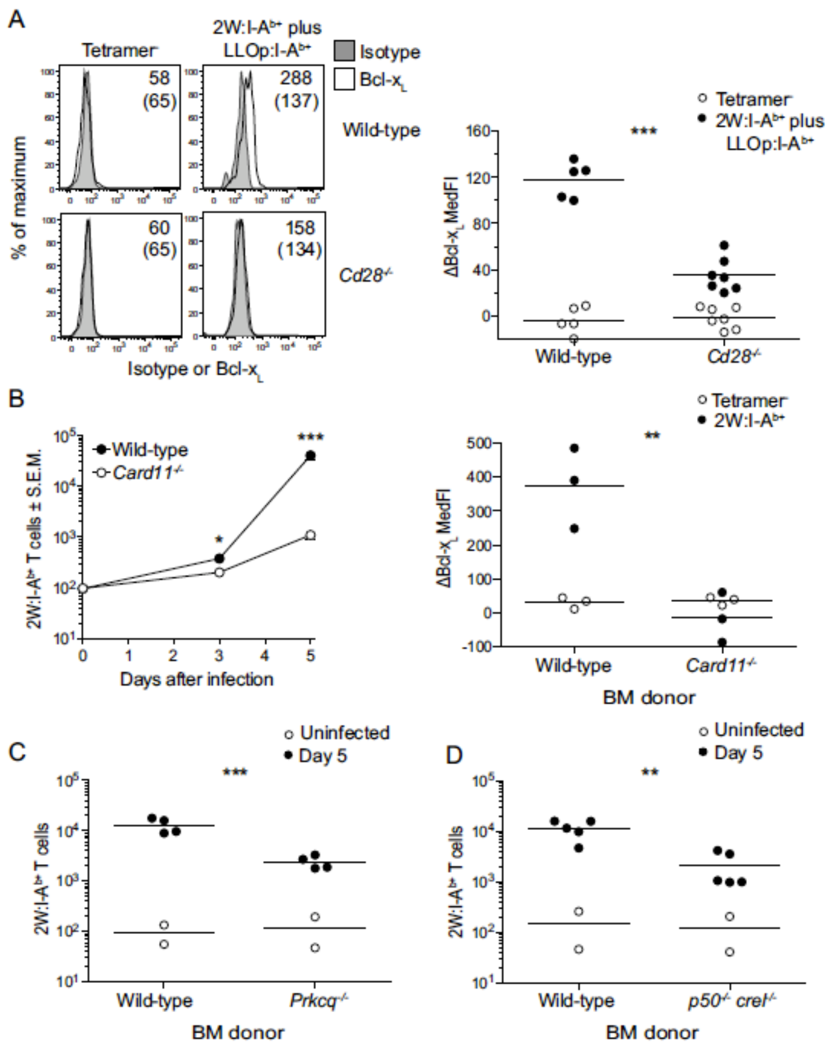


**Figure 2.5. CD28 Deficiency Phenotypically Resembles NFκB Signaling Deficiency *In Vivo.*** (A) Histograms of isotype control or Bcl-$x_L$ staining on tetramer$^-$ CD44$^{low}$ or 2W:I-A$^{b+}$ plus LLOp:I-A$^{b+}$ wild-type or CD28-deficient mice 3 days after Lm-2W infection. Values for median fluorescence intensity of Bcl-$x_L$ staining minus that of isotype control are shown on the right panel of (A). Mixed radiation chimeras made with wild-type and CARMA1-deficient (B), wild-type and PKCθ-deficient (C), or wild-type and p50/c-Rel-deficient (D) bone marrow cells. Mean numbers (n = 2 - 4) of wild-type or CARMA-deficient 2W:I-A$^{b+}$ T cells in uninfected mice and

mice at the indicated times after Lm-2W infection are shown on the left panel of (B). The right panel of (B) shows differences in median fluorescence intensity of Bcl-$x_L$ staining minus that of isotype control for wild-type and CARMA1-deficient cells. Horizontal lines indicate the mean values, and each symbol shows data from an individual mouse. A two-tailed Student's *t* test was used to compare the $log_{10}$ values of tetramer$^+$ cells in Lm-2W infected groups, ** $p < 0.01$, *** $p < 0.001$.

**CD28 Signaling Increases Antigen-dependent Nuclear Translocation of RelA *In Vivo* Independently of the PYAP and YMNM Motifs**

To determine if CD28 signaling indeed enhanced NFκB activation *in vivo*, we used an image scanning flow cytometer to measure nuclear translocation of RelA in CD4$^+$ T cells responding to antigen *in vivo*. We chose to focus on RelA because this NFκB isoform can dimerize with p50 or c-Rel in T cells (Harhaj et al., 1996), translocates into the nucleus upon TCR plus CD28 stimulation, and is a component of a protein complex that can bind the CD28 response element consensus sequence (Ghosh et al., 1993). CD4$^+$ T cells from wild-type or CD28-deficient OVA peptide:I-A$^b$-specific OT-II TCR transgenic mice were transferred into normal mice, which were then injected intravenously with LPS to induce CD80 and CD86 on APC, then with OVA peptide (De Smedt et al., 1996; Khoruts et al., 1998) (Figure 2.6A). RelA was in the cytoplasm of wild-type and CD28-deficient OT-II cells in recipient mice injected with LPS alone (Figure 2.6). In contrast, RelA translocated to the nucleus in OT-II cells 20 minutes after injection of OVA peptide, and this translocation was significantly greater in wild-type than in CD28-deficient cells (Figure 2.6C). Additionally, OT-II expressing CD28 molecules with mutated PYAP or YMNM sites showed the same amount of peptide-induced RelA translocation as wild-type cells (Figure 2.6C). These data demonstrate that CD28 signaling is required for optimal TCR-induced activation of RelA *in vivo* through a pathway that does not involve the YMNM or PYAP sites.

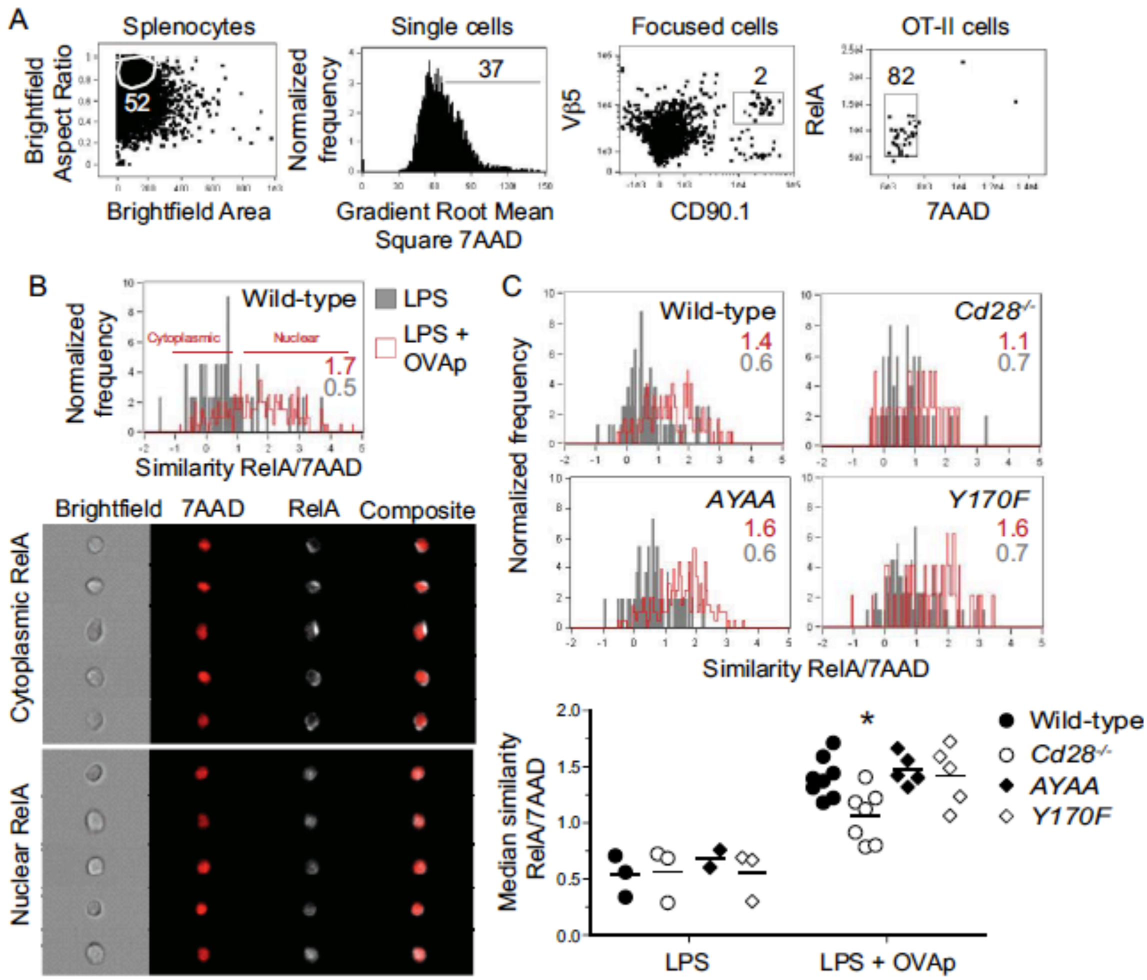


**Figure 2.6. CD28 Enhances p:MHCII-dependent Nuclear Translocation of RelA *In Vivo* Independently of the PYAP and YMNM Motifs.** Wild-type and CD28 mutant CD90.1$^{+}$ OT-II CD4$^{+}$ T cells were transferred intravenously into wild-type recipients. A day later, mice were injected intravenously with LPS. Two days after T cell transfer, some mice were injected intravenously with OVA peptide, and splenocytes were harvested 20 minutes later. (A) Flow cytometry plots show gating strategy used to measure RelA translocation in transferred OT-II cells within CD90.1-enriched samples. (B) Representative histograms of median RelA/7AAD similarity in wild-type OT-II cells from LPS (gray) or LPS plus OVA peptide-injected mice (red) (top). Median RelA/7AAD similarity values are shown on each histogram for samples stimulated

with LPS alone (gray) or LPS plus OVA peptide (red). Sample images of cytoplasmic and nuclear RelA staining in OT-II cells from the LPS plus OVA peptide sample are shown at the bottom. (C) Histograms of median RelA/7AAD similarity in wild-type, CD28-deficient, *AYAA* and *Y170F* OT-II cells from LPS (gray) or LPS plus OVA peptide-injected mice (red). Median values for RelA and 7AAD similarity from individual mice (bottom). Horizontal lines on the graph on the bottom indicate mean values, and each symbol depicts a value from an individual mouse. Groups were compared by one-way ANOVA and Bonferroni post-test, * $p < 0.05$. Graph shows pooled data from four independent experiments.

## 2.4 Discussion

Our results show that the major effect of CD28 signaling on polyclonal p:MHCII-specific T cells responding to an infection was sustained effector cell proliferation. It was surprising to find that CD28-deficient T cells began proliferating *in vivo* at the same rate as wild-type T cells given the many reports that CD28 enhances the production of the early T cell growth factor IL-2. However, this result is less surprising considering evidence that IL-2 is not required for $CD4^+$ T cell proliferation *in vivo* (Khoruts et al., 1998). It is possible that CD28 maintains effector cell proliferation indirectly by sustaining the production of a lymphokine other than IL-2 (Boulougouris et al., 1999) or by directly transducing signals that promote cell cycle progression (Appleman et al., 2002; Bonnevier et al., 2006).

It has been reported that CD28 does not influence *in vitro* T cell proliferation, but rather promotes clonal expansion by opposing apoptosis through induction of Bcl-$x_L$ (Sperling et al., 1996). This was proposed to be an indirect effect of OX40, which promotes memory T cell formation and expression of Bcl-$x_L$ and is induced in a CD28-

dependent fashion (Rogers et al., 2001). In contrast, we found that the polyclonal p:MHCII-specific effector cells that were formed in CD28-deficient mice did not undergo an exaggerated contraction phase and produced memory cells at the expected frequency. This conclusion is supported by the observation of Dahl et al. that over expression of Bcl-$x_L$ failed to restore the clonal expansion of CD28-deficient T cells *in vivo* (Dahl et al., 2000). Therefore, the *in vivo* results indicate that CD28 enhances memory cell generation by sustaining the proliferation of the effector cell population from which memory cells are derived.

It was surprising to find that mutations of the YMNM site had no effect on the production of effector and memory T cells after bacterial infection. The YMNM site has been shown to bind to PI3K, a key molecule in the activation of multiple signaling pathways that regulate cellular metabolism (Akt/mTOR), the immunological synapse (PKCθ), and transcription of genes involved in T cell proliferation and survival (Bcl10/Carma1/Malt1/NFκB) (Burr et al., 2001; Chen et al., 2000; Jones et al., 2000; Khoshnan et al., 2000; Narayan et al., 2006; Park et al., 2009; Sanchez-Lockhart et al., 2004; Yokosuka et al., 2008). Our results are consistent, however, with reports showing that disruption of the YMNM motif and prevention of PI3K binding and phosphorylation of Akt had no effect on IL-2 production *in vitro* or the induction of T cell-dependent airway inflammation or experimental allergic encephalomyelitis *in vivo* (Dodson et al., 2009; Okkenhaug et al., 2001). Our findings extend this work by documenting that the YMNM site is dispensable for the infection-induced proliferation of polyclonal p:MHCII-specific polyclonal $CD4^+$ T cells. Notably, both the PYAP and YMNM sites played a role in T cell expansion induced by peptide without adjuvant, perhaps because fewer costimulatory ligands other than CD80 and CD86 are induced in this case than by infection. It was even more surprising to find that mutations in the PYAP site had no effect on the production of effector and memory T cells after bacterial infection. This site is involved of activation of PDK1 and PKCθ and its disruption impairs *in vivo* T cell functions such as promotion of antibody production and induction of experimental allergic encephalomyelitis. Our observation that p:MHCII-specific $CD4^+$ T cells failed proliferate to the same extent as wild-type cells after injection of peptide alone indicates defective clonal expansion could explain the aforementioned defects. However, the finding that PYAP mutant p:MHCII-specific $CD4^+$ T cells underwent normal clonal expansion under the more inflammatory condition of bacterial infection shows that this site is not critical for T cell proliferation in all immune responses.

Our finding that CD28-deficient T cells did not translocate RelA to the nucleus as well as wild-type T cells following *in vivo* p:MHCII stimulation is consistent with the idea that canonical NFκB activation is a critical component of the CD28 signal that sustains T cell proliferation. Remarkably, however, RelA translocation could not be attributed to the YMNM or PYAP sites, both of which have been implicated in NFκB signaling in some cases. It is therefore possible that CD28 activates the NFκB signaling cascade without recruiting PI3K of other effectors to the YMNM or PYAP sites in its cytoplasmic tail. It is still possible, however, that CD28 triggers NFκB signaling through PI3K without recruiting it to the cytoplasmic tail as suggested by Garçon et al (Garcon et al., 2008). Another possibility is that the tyrosine within the PYAP motif, which is required for PKCθ focusing within the immunological synapse (Sanchez-Lockhart et al., 2008), is necessary for CD28-dependent NFκB activation *in vivo*. In any case, our results point out the need to study CD28 signaling in relevant *in vivo* models and suggest that there is more to be learned about how the cytoplasmic tail transduces signals.

# Chapter 3:

# Opposing Bcl6 and IL-2 Receptor Signals Generate Th1 Central and Effector Memory Cells

*Listeria monocytogenes* infection generates Th1 effector memory cells and $CCR7^+$ cells resembling central memory cells. The factors that promote the simultaneous formation of these different memory cells are unknown. We addressed this issue by tracking endogenous $CD4^+$ T cells specific for *L. monocytogenes* peptides. Two populations of effector cells were already present several days after infection. One population expressed the Th1 transcription factor T-bet, and produced Th1 memory cells in an IL-2 receptor-dependent fashion. The other population expressed CXCR5 and depended on Bcl6 and ICOSL on B cells like follicular helper cells. These effector cells resided in the T cell areas and produced $CCR7^+$ $CXCR5^+$ memory cells that generated diverse effector cell populations in a secondary response. Thus, Th1 effector memory and follicular helper-like central memory cells were produced from early effector cell populations that diverged in response to signals from the IL-2 receptor, Bcl6, and B cells.

## 3.1 Introduction

Bacterial infection generally results in immunity to that infection (Ahmed and Gray, 1996). This immunity is mediated by bacterial antigen-specific lymphocytes that proliferate and differentiate into long-lived memory cells. In the case of $CD4^+$ T cells, this process involves initial proliferation of naïve cells with T cell antigen receptors

(TCR) specific for microbe-derived peptides bound to host major histocompatibility complex II molecules (p:MHCII) (Jenkins et al., 2001). If the innate immune cytokine IL-12 is present, then the effector cell progeny produced by this proliferation acquire the capacity to produce the microbicidal lymphokine IFN-γ and migrate to non-lymphoid sites of infection. Once the infection is cleared, some of the effector cells survive to become long-lived quiescent memory cells (Ahmed and Gray, 1996).

Memory T cells exist in at least two subsets referred to as central (Tcm cells) and effector memory cells (Tem cells) (Sallusto et al., 2004). Tem cells express homing receptors needed for migration into non-lymphoid organs, and when stimulated with the relevant p:MHCII ligand, immediately produce microbicidal lymphokines (Reinhardt et al., 2001). Tem cells therefore closely resemble lineage-committed effector cells such as Th1 cells and have been shown to derive from these cells in some systems (Harrington et al., 2008; Lohning et al., 2008; Pepper and Jenkins, 2011; Surh and Sprent, 2008). Tcm cells express CCR7 and L-selectin, which direct recirculation through lymph nodes. When stimulated with the relevant p:MHCII ligand, Tcm cells do not produce microbicidal lymphokines immediately but proliferate to produce new effector cells, which then acquire these functions (Sallusto et al., 2004).

Several factors have been identified that favor the formation of Th1 effector cells and subsequently Th1-like effector memory cells (Th1em). Strong or prolonged TCR signaling has been reported to favor Tem cell formation (Catron et al., 2006; Gudmundsdottir et al., 1999b; Sarkar et al., 2007), perhaps as a consequence of a shift to glycolytic metabolism and activation of mammalian target of rapamycin (Araki et al., 2009; Pearce et al., 2009). IL-2 receptor signaling also plays a role in Th1 development (Khoruts et al., 1998), perhaps as a consequence of STAT5-mediated upregulation of the IL-12 receptor β2-chain and the Th1-associated T-bet (Liao et al., 2011) and Blimp-1 transcription factors (Gong and Malek, 2007; Pipkin et al., 2010), which repress the Bcl6 transcription factor (Shaffer et al., 2002). It remains to be determined, however, whether this pathway applies to genuine $CD4^+$ effector and memory T cells generated *in vivo* during infection.

Much less is known about the formation of Tcm cells. These cells may be the progeny of effector cells that receive weaker TCR signals due to encounters with antigen-presenting cells that display low numbers of p:MHCII ligands, either by chance or due to entry into the relevant secondary lymphoid organs late in the response as the antigen concentration fades (Catron et al., 2006; van Faassen et al., 2005). Recent work indicates that Tcm cells defined by expression of CCR7 also express the B cell follicle homing CXCR5 (Chevalier et al., 2011) and are potent helper cells for B cells (Chevalier et al., 2011; MacLeod et al., 2011). Although expression of CXCR5 suggests that Tcm cells are related to T follicular helper (Tfh) cells (Morita et al., 2011), which depend on Bcl6 and help B cells in germinal centers (Crotty, 2011), this relationship has not been directly addressed *in vivo*.

We explored the derivation of p:MHCII-specific Tcm and Tem cells induced during acute systemic infection with *Listeria monocytogenes* (Lm). We found that two effector cell populations generated very early after infection preceded these memory cells. One population expressed IL-2 receptor and T-bet, and gave rise to Th1em in an

IL-2-dependent, Bcl6-independent fashion. The other population expressed CXCR5, depended on Bcl6, and produced Tfh or Tcm cells, when signaled by ICOSL on B cells.

## 3.2 Materials and Methods

### Mice

Six- to eight-week-old C57BL/6 (B6), 129x1/SvJ, B6.129S2-*Ighm*$^{tm1Cgn}$/J (μMT) (Kitamura et al., 1991), B6.129P2-*Icos*$^{tm1Mak}$/J (ICOS-deficient) (Tafuri et al., 2001), B6.129P2-*Icosl*$^{tm1Mak}$/J (ICOSL-deficient) (Mak et al., 2003), and B6.SJL-*Ptprc*$^{a}$ *Pep3*$^{b}$/BoyJ (CD45.1) were from the Jackson Laboratory or the National Cancer Institute. B6.129S6-*Bcl6* mice (Bcl6-deficient) (Dent et al., 1997) were obtained from Matthew Mescher (University of Minnesota). Foxp3-GFP *Cd25*$^{-/-}$ CD45.1$^{+}$/CD45.2$^{+}$ mice were obtained from Daniel Campbell (University of Washington). All mice were housed in specific pathogen–free conditions in accordance with guidelines of the University of Minnesota and National Institutes of Health. The Institutional Animal Care and Use Committee of the University of Minnesota approved all animal experiments.

### Generation of r7UP Transgenic Mice

Pierre Chambon (IGBMC) provided the Cre-ERT2 plasmid. Recombination of the Cre-ERT2 coding sequence into the 3′-untranslated region (UTR) of CCR7 in bacterial artificial chromosome clone RP23-80024 (Invitrogen, Carlsbad, CA) was performed as described (Kaplan et al., 2005). Primers used for generation of the recombination cassette were: 5′ A box, 5′- TTAAGGCGCGCCGCTCCTATGCATCAGCATTGA -3′;

3′ A box, 5′- GGCGGATCCCGGATGTGTGCACCACATTAAGGCTC -3′; 5′ B box, 5′-GCCACAGCTTGAGCACAGACTCTCCATCCACCGAA -3′; 3′ B box, 5′-TATTAAGGCCGGCCCTGCAGGTGTATGTGCAAGAC -3′; 5′ I box, 5′-GGTGCACACATCCGGGATCCGCCCCTCTCC -3′; 3′ I box, 5′-AGAGTCTGTGCTCAAGCTGTGGCAGGGAAACCCTC -3′. The recombined construct was injected into the pro-nuclei of B6 mice in the University of Minnesota Mouse Genetics Laboratory. Transgenic mice were then crossed to the B6;129*Gt(ROSA)26Sor*$^{tm2Sho}$/J strain. eYFP expression was induced by daily intraperitoneal injection of tamoxifen (0.05 mg/g) for 5 days.

**Bone Marrow Irradiation Chimeras**

Bone marrow cells were harvested from femurs, tibias, and humeri. T cells were depleted from bone marrow cell suspensions with anti-Thy1.2 (30-H12, Bio X Cell) and low toxicity rabbit complement (Cedarlane Laboratories). Donor bone marrow and recipient mice in Bcl6$^{-/-}$ chimeras were additionally treated with anti-NK1.1(PK136, eBioscience) to deplete NK cells. In some cases, CD45.1$^{+}$/2$^{+}$ wild-type bone marrow cells were mixed with an equal number of CD45.2$^{+}$ *Icos*$^{-/-}$, *Bcl6*$^{-/-}$, or *Bcl6*$^{+/-}$ bone marrow cells. Five-10 x10$^{6}$ total bone marrow cells were injected into lethally-irradiated (1,000 rads) CD45.1$^{+}$ mice. In other cases, CD45.2$^{+}$ wild-type bone marrow cells were mixed with an equal number of CD45.1$^{+}$/2$^{+}$ *Cd25*$^{-/-}$ bone marrow cells and injected into lethally-irradiated (1,000 rads) CD45.1$^{+}$ mice. Chimerism in the blood was assessed 8 weeks after reconstitution by determining the percentages of donor-derived B cells or T cells of each strain. In other cases, wild-type or *Icosl*$^{-/-}$ bone marrow cells were mixed with an equal number of μMT bone marrow cells and 5-10 x$10^6$ total bone marrow cells were injected into lethally-irradiated (1,000 rads) μMT mice. Fluorochrome-conjugated anti-CD45.2 and anti-CD45.1 antibodies were used to identify donor-derived cells. Variations in the absolute numbers of tetramer-binding T cells due to slight differences in chimerism were corrected with the formula, c = (r / p) X 50%, where p is the percent of cells among donor-derived cells obtained experimentally, r is the absolute number of tetramer-binding T cells obtained experimentally, and c is the absolute number after the correction.

**Infections**

Mice were injected intravenously with $10^7$ actA-deficient Lm bacteria engineered to secrete a fusion protein containing an immunogenic peptide called 2W (Lm-2W) (Ertelt et al., 2009).

**Tetramer Production**

Biotin-labeled soluble I-A$^b$ molecules containing 2W (EAWGALANWAVDSA) covalently attached to the I-A$^b$ beta chain were produced in *Drosophila melanogaster* S2 cells, then purified and made into tetramers with streptavidin-phycoerythrin or streptavidin-allophycocyanin (Prozyme) as described (Moon et al., 2007). Biotin-labeled soluble I-A$^b$ molecules containing LLO$_{190\text{-}201}$ (NEKYAQAYPNVS, LLOp) were made in a similar fashion except that the I-A$^b$ alpha chain contained a cysteine substitution at position 72, which allowed a disulfide bond to form between this cysteine and the cysteine 2 residues after the LLOp, in effect locking the peptide into the correct binding register (Stadinski et al., 2010).

**Cell Enrichment and Flow Cytometry**

All antibodies were from eBioscience unless noted. Spleen and lymph node cells were prepared and then were stained for 1 hour at room temperature with LLOp:I-$A^b$- or 2W:I-$A^b$–streptavidin-allophycocyanin tetramers and 2 μg each of peridinin chlorophyll protein–cyanine 5.5–conjugated antibody to CCR7 (anti-CCR7; 4B12) and phycoerythrin-conjugated antibody to CXCR5 (2G8; Becton-Dickinson). Samples were then enriched for bead-bound cells on magnetized columns and a portion was removed for counting as described (Moon et al., 2007). For identification of surface phenotype, the rest of the sample underwent surface staining on ice with a mixture of antibodies specific for B220 (RA3-6B2), CD11b (MI-70), CD11c (N418); CD8α (5H10; Caltag); PD-1 (J43); CD4 (RM4-5); CD3ε (145-2C11); CD25 (PC61.5); CD44 (IM7); CD45.1 (A20), and/or CD45.2 (104), each conjugated with a different fluorochrome. In experiments designed to detect transcription factors, the cells were surface stained with some of the aforementioned antibodies, then treated with Foxp3 Fixation/Permeabilization Concentrate and Diluent (eBioscience), and stained for 1 hour on ice with antibodies against T-bet (4B10; Biolegend) and/or Bcl6 (K112-91; Becton-Dickinson). In experiments designed to detect cytokines, the cells were surface stained, then treated with BD Cytofix/Cytoperm (Becton-Dickinson) overnight, and stained for 1 hour on ice with antibodies against IL-2 (JES6-5H4) and IFN-γ (XMG1.2) in Perm Wash solution (Becton-Dickinson). In all cases, cells were then analyzed on an LSR II or Fortessa (Becton Dickinson) flow cytometer. Data were analyzed with FlowJo software (TreeStar).

### Lymphokine Production

Mice were infected intravenously with Lm-2W bacteria. Ninety-two days later, the mice were injected intravenously with 100 μg of LLOp. Spleen and lymph nodes were analyzed for the presence of intracellular IL-2 and IFN-γ in LLOp:I-$A^b$-specific T cells as described previously (Pepper et al., 2010).

### Cell Transfer

Flow cytometric sorting was used to purify T cell populations before adoptive transfer. For analysis of Tem and Tcm cell function in the secondary response, spleens and lymph nodes were collected from B6 mice infected intravenously at least 20 d earlier with Lm-2W bacteria and stained with fluorochrome-labeled antibodies to CD4, CD44, CCR7, PD-1, and CXCR5. $CD44^{high}$ $CXCR5^-$ $CCR7^-$ $CD4^+$ $Th1_{EM}$ cells and $CD44^{high}$ $CXCR5^+$ $CCR7^+$ $T_{CM}$ cells were then sorted with a FACSAria (Becton Dickinson) flow cytometer. Sorted cells were then injected intravenously into $CD45.1^+$ recipients, which were then infected intravenously with $10^7$ Lm-2W bacteria. Six days later, the phenotype of 2W:I-$A^b$-specific T cells was determined after tetramer-based cell enrichment as described above.

For analysis of Tcm cell location, B6 mice were infected intravenously with Lm-2W bacteria. Eight days later, spleen and lymph node cells from these mice were stained with fluorochrome-labeled antibodies against CD4, CD44, CXCR5, CCR7, and PD-1. $CD4^{+}$ $CD44^{low}$ $CXCR5^{-}$ $CCR7^{-}$ PD-$1^{-}$ Th1 cells, $CXCR5^{intermediate}$ $CCR7^{+}$ PD-$1^{-}$ Tcm cells, and $CXCR5^{high}$ $CCR7^{-}$ PD-$1^{+}$ GC Tfh cells were then sorted and transferred into $CD45.1^{+}$ recipients. One day after transfer, spleens were fixed in 1% formaldehyde dehydrated in 1% sucrose overnight before embedding in O.C.T. Thin sections (7 µm) were cut on a microtome, blocked with culture supernatant containing 24G2 monoclonal antibody plus 1% mouse and 1% rat serum, and stained with fluorescein isothiocyanate-anti-IgD (11-26; eBioscience), biotin-anti-CD4 (GK1.5; eBioscience), and allophycocyanin-anti-CD45.2 (104; eBioscience) antibodies, followed by Cy3-streptavidin (Invitrogen). Stained sections were imaged at 20X as previously described (Pape et al., 2007) with a Leica DM5500B automated upright microscope with a high-precision motorized x/y stage and a Leica DFC340FX Digital Camera. Entire spleen images were reassembled with Leica AF6000 stitching software (Leica) and displayed in Photoshop (Adobe, San Jose, CA).

**Statistical Analysis**

Differences between 2 data sets were analyzed by a paired or unpaired two-tailed Student's *t*-test using Prism (Graphpad) software.

## 3.3 Results

### Detection of LLOp:I-$A^b$-specific $CD4^+$ Memory T cells

We used a p:MHCII tetramer–based approach to identify $CD4^+$ T cells specific for 2 pMHCII ligands produced in C57BL/6 (B6) mice during infection with a vaccine strain of Lm bacteria. This strain, called Lm-2W, contains an attenuating mutation in the *actA* gene (Portnoy et al., 2002), and was engineered to secrete a fusion protein containing the immunogenic 2W peptide (Rees et al., 1999) under the control of the *hly* promoter (Ertelt et al., 2009). Following infection, these bacteria are taken up into phagosomes and then completely eliminated by innate and adaptive immune mechanisms (Portnoy et al., 2002). During this process, the 2W peptide and peptide 190-201 from listeriolysin O (LLOp) are produced by antigen processing and bind to I-$A^b$ MHCII molecules on dendritic cells. These complexes then stimulate $CD4^+$ T cells expressing complementary TCRs, which we detected by staining cells from individual mice with fluorochrome-labeled LLOp:I-$A^b$ or 2W:I-$A^b$ tetramers and anti-fluorochrome magnetic beads and enriching the tetramer-bound cells on a magnetized column (Moon et al., 2007). The cells that bound to the column were stained with antibodies specific for CD3 and a mixture of non–T cell lineage–specific antibodies to aid in identification of genuine $CD3^+$ non–T cell $lineage^-$ T cells (Figure 3.1A).

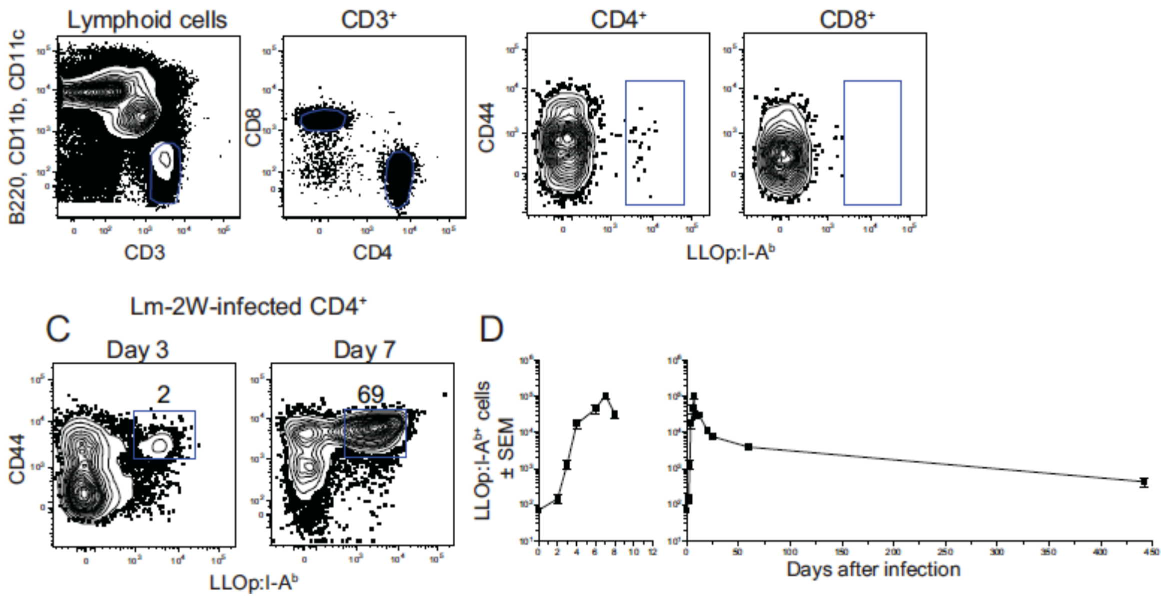


**Figure 3.1. Detection of LLOp:I-A$^b$-specific CD4$^+$ T Cells.** (A) Gate used to identify CD3$^+$ non–T cell lineage$^-$ T cells (left) and CD4$^+$ and CD8$^+$ T cells within that population (right) from the bound fraction after enrichment with LLOp:I-A$^{b+}$ tetramer. (B) CD4$^+$ T cells (left) or CD8$^+$ T cells (right) identified as in (A) from an uninfected B6 mouse with gates on LLOp:I-A$^{b+}$ cells. (C) CD4$^+$ T cells from B6 mice at the indicated times after intravenous infection with Lm-2W bacteria with gates on LLOp:I-A$^{b+}$ cells. The percentages of cells in the indicated gates are shown. (D) Mean number (± SEM, n ≥ 3 for each data point) of CD4$^+$ LLO:I-A$^{b+}$ T cells in the spleen and lymph nodes over the first 8 (left) or 440 days (right) after intravenous infection with Lm-2W bacteria.

We first established the kinetics of the expansion, contraction, and memory phases of the LLOp:I-A$^b$-specific CD4$^+$ T cell population since it had never been detected directly with a tetramer. B6 mice that were not infected contained a small population of LLOp:I-A$^b$ tetramer-binding CD3$^+$ CD4$^+$ cells in the spleen and lymph nodes, most which were CD44$^{low}$ as expected for naive cells (Figure 3.1B). LLOp:I-A$^{b}$ tetramer-binding cells were not detected among the MHCI-restricted CD8$^{+}$ T cells in the bound fraction (Figure 3.1B), indicating that the CD4$^{+}$ cells that bound the tetramer did so via the TCR. Following intravenous injection of $10^{7}$ Lm-2W bacteria, these cells upregulated CD44 and increased in the spleen and lymph nodes as early as day 3 and peaked on day 7 (Figure 3.1C and D). The naïve LLOp:I-A$^{b}$-specific CD4$^{+}$ T cell population in each mouse consisted of about 80 cells, which expanded to ~100,000 cells by day 7 post infection (Figure 3.1D). The population then contracted by day 20 to about 10,000 CD44$^{high}$ memory cells, which then slowly declined over the next 1.5 years (Figure 3.1D). Thus, LLOp:I-A$^{b}$-specific CD4$^{+}$ T cells underwent the expansion, contraction, and slow memory decline phases exhibited by other pMHCII-specific CD4$^{+}$ T cell populations (Homann et al., 2001; Pepper et al., 2010).

**CD4$^{+}$ Memory T Cell Heterogeneity**

Previously, we showed that the 2W:I-A$^{b}$-specific memory T cells induced by intravenous Lm-2W infection consisted of T-bet$^{high}$ CCR7$^{-}$ and Tbet$^{low}$ CCR7$^{+}$ cells (Pepper et al., 2010). We determined whether LLOp:I-A$^{b}$-specific memory cells consisted of similar subsets. Naïve LLOp:I-A$^{b}$-specific cells expressed CCR7 but not T-bet or CXCR5 (Figure 3.2A). In contrast, the LLOp:I-A$^{b}$-specific memory cell population in mice infected 60 days earlier with Lm-2W bacteria consisted of the same T-bet$^{high}$ CCR7$^{-}$ and T-bet$^{low}$ CCR7$^{+}$ subsets observed in the 2W:I-A$^{b}$-specific memory cell population (Pepper et al., 2010). In addition, we found that the CCR7$^{+}$ cells, but not the CCR7$^{-}$ cells expressed CXCR5 (Figure 3.2A).

We next analyzed the peak of the primary response to determine if effector cells with the characteristics of the later memory cells were present. PD-1 was also tested to aid in the detection of germinal center (GC) Tfh cells, which express this marker and the largest amounts of CXCR5 of any CXCR5$^{+}$ population (Crotty, 2011). As shown in Figure 2B, the LLOp:I-A$^{b}$-specific effector cells present on day 8 after infection were split about equally into CXCR5$^{-}$ and CXCR5$^{+}$ populations. The CXCR5$^{-}$ cells were Th1 effector cells based on expression of large amounts of T-bet and lack of CCR7 (Figure 3.2B-D). About 10% of the CXCR5$^{+}$ cells were GC Tfh cells based on expression of PD-1, the largest amounts of CXCR5, and the Tfh lineage-defining transcription factor Bcl6 (Figure 8B and E). These GC Tfh cells expressed more T-bet than naïve cells but less than the Th1 cells (Figure 3.2B and C). The CXCR5$^{+}$ cells that lacked PD-1 also expressed this intermediate amount of T-bet as well as low amounts of Bcl6 (Figure 3.2B, C, and E), as expected for Tfh cells. These cells expressed the most CCR7 of any of the effector cell populations (Figure 3.2B and D). Thus, the LLOp:I-A$^{b}$-specific effector cell population present on day 8 after infection consisted of T-bet$^{high}$ CCR7$^{-}$ and T-bet$^{low}$ CCR7$^{+}$ subsets with the characteristics of the 2 later memory cell populations, along with an additional GC-Tfh cell subset. The T-bet$^{high}$ CCR7$^{-}$ cells present at the peak of the primary response will be referred to as Th1 effector cells and the T-bet$^{low}$ CCR7$^{+}$ CXCR5$^{+}$ PD-1$^{-}$ cells as Tfh cells.

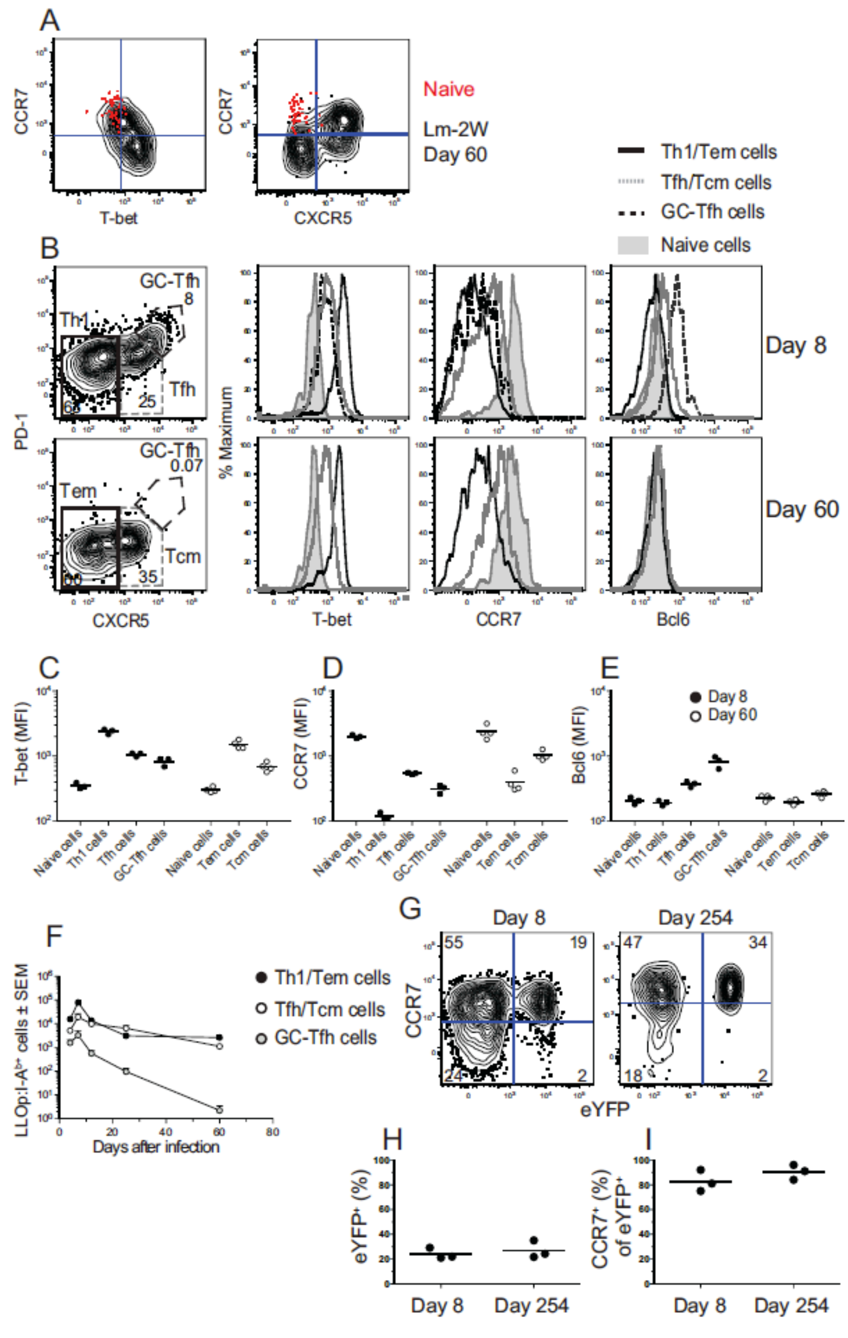


**Figure 3.2. Identification of Tem and Tcm Cells.** (A) Representative plots of CCR7 versus T-bet (left) or CXCR5 (right) on LLOp:I-A$^b$-specific CD44$^{low}$ naïve cells from uninfected B6 mice (red dots) or LLOp:I-A$^b$-specific CD44$^{high}$ memory cells from mice infected with Lm-2W bacteria

60 days before analysis (black contours). (B) Representative plots of CXCR5 versus PD-1 used to identify CXCR5$^{-}$ PD-1$^{-}$ Th1/Tem cells, CXCR5$^{intermediate}$ PD-1$^{-}$ Tfh/Tcm cells, and CXCR5$^{high}$ PD-1$^{+}$ GC-Tfh cells on days 8 or 60 after intravenous infection with Lm-2W bacteria, with histograms of T-bet, CCR7, and Bcl6 on Th1/Tem cells (black line), Tfh/Tcm cells (gray line), GC-Tfh cells (dashed line), or CD44$^{low}$ naïve cells (shaded histogram). (C-E) Mean fluorescence intensities (MFI) of T-bet (C), CCR7 (D), and Bcl6 (E) on the indicated cell types from 3 individual mice on days 8 (filled circles) or 60 (open circles) after intravenous infection with Lm-2W bacteria. (F) Mean number (± SEM, n ≥ 3) of LLO:I-A$^{b}$-specific Th1/Tem (filled circles), Tfh/Tcm (open circles), or GC-Tfh (gray circles) cells identified as shown in (B). (G) CCR7 and eYFP expression by 2W:I-A$^{b}$-specific CD4$^{+}$ T cells in 2W:I-A$^{b}$ tetramer-enriched samples from r7UP mice infected with Lm-2W bacteria, treated with tamoxifen on days 4-8 post-infection, and analyzed on days 8 or 254 post-infection. (H, I) Percentage of eYFP$^{+}$ cells among 2W:I-A$^{b}$-specific cells (H) or CCR7$^{+}$ cells among eYFP$^{+}$ 2W:I-A$^{b}$-specific cells (I) from individual mice.

This analysis was repeated 60 days after infection to determine if any of the effector populations entered the memory pool. At this time, about half of the memory cells resembled the Th1 effector cell population (Figure 3.2B-E) and will therefore be referred to as Th1em cells. The other memory cells closely resembled the CXCR5$^{+}$ T-bet$^{low}$ CCR7$^{+}$ Tfh cells present on day 8, with the exception of reduced expression of Bcl6 (Figure 3.2B-E). The CXCR5$^{+}$ PD-1$^{+}$ Bcl6$^{high}$ GC-Tfh cell population that was present at the peak of the response was not detected in the memory cell pool 60 days after infection (Figure 3.2B). A more detailed time course experiment showed that T-bet$^{high}$ CXCR5$^{-}$ Th1and CXCR5$^{+}$ PD-1$^{-}$ CCR7$^{+}$ Tfh cells, putative Tcm precursors, peaked at day 7 and contracted to lower numbers by days 12-25 that were maintained until day 60 (Figure 8F). In contrast, the CXCR5$^{+}$ PD-1$^{+}$ Bcl6$^{high}$ GC-Tfh cell population peaked at day 7 but declined progressively until disappearing by day 60 (Figure 3.2F). These results suggested that some of the Th1 effector cells survived the contraction phase to become Tem cells, while some Tfh cells became Tcm cells. In contrast, although GC Tfh cells were generated during the effector phase of the response they appeared to contribute very little to the memory cell pool.

We produced a new transgenic mouse (called the r7UP mouse) to formally test the possibility that some Tfh cells survived the contraction phase to become Tcm cells. These mice contain a bacterial artificial chromosome with an internal ribosome entry site (IRES) and Cre-recombinase-estrogen receptor 2-fusion protein sequence (Cre-ERT2) inserted between exon 3 and the 3' untranslated region of the *Ccr7* gene (Supplemental Figure 3.1A). These mice also contain an enhanced yellow fluorescent protein (*eYFP)* (Tsien, 1998) transgene with a floxed stop cassette controlled by the constitutive ROSA 26 promoter (Srinivas et al., 2001) (Supplemental Figure 3.1A). eYFP is not expressed in the absence of tamoxifen because the Cre-ERT2 molecule is sequestered in the cytosol (Srinivas et al., 2001). Administration of tamoxifen allows the Cre-ERT2 protein to enter the nucleus, leading to excision of the stop cassette and permanent expression of eYFP in cells that expressed CCR7 at the time of tamoxifen treatment. All of the progeny of the marked cells retain expression of eYFP, even if CCR7 is subsequently shut off.

As shown in Supplemental Figure 3.1B, about half of the CCR7$^{+}$ CD4$^{+}$ T cells in uninfected r7UP mice treated with tamoxifen for 5 days expressed eYFP. In contrast, none of the CCR7$^{-}$ CD4$^{+}$ T cells in these mice and none of the CD4$^{+}$ T cells in tamoxifen-treated B6 mice expressed eYFP (Supplemental Figure 3.1B). Similarly, the population of LLOp:I-A$^{b}$-specific memory cells in r7UP mice treated with tamoxifen for 5 days beginning 18 days after infection with Lm-2W bacteria contained a subset of eYFP$^{+}$ cells, all of which expressed CCR7 (Supplemental Figure 3.1B) and CXCR5 (Supplemental Figure 3.1C**)**, while none of the LLOp:I-A$^{b}$-specific CCR7$^{-}$ memory cells expressed these molecules (Supplemental Figure 3.1B and C**)**. The CCR7$^{+}$ eYFP$^{-}$ CD4$^{+}$ T cells in tamoxifen-treated r7UP mice were likely cells that had not yet deleted the stop cassette upstream of the eYFP gene after 5 days of tamoxifen treatment as observed in T cells in other Cre-ERT2 transgenic mice (Rubtsov et al., 2010). Despite this incomplete labeling, it was clear that the LLOp:I-A$^{b}$-specific cells that did turn on eYFP after tamoxifen treatment several weeks after infection were CCR7$^{+}$ memory cells.

To test the capacity of CCR7$^{+}$ effector cells to become memory cells, r7UP mice were infected with Lm-2W bacteria and labeled with tamoxifen during the period of maximal effector cell generation from days 4-8. We focused on the 2W:I-A$^{b}$-specific population because its larger size provided a practical advantage. About 25% of the 2W:I-A$^{b}$-specific effector cells present on day 8 were eYFP$^{+}$ (Figure 3.2G and H) and most of these cells expressed CCR7 (Figure 8G and I). Two hundred and fifty four days after infection and 246 days after the cessation of tamoxifen treatment, about 30% of the 2W:I-A$^{b}$-specific memory cells were again eYFP$^{+}$ (Figure 8G and H) and the vast majority retained CCR7 (Figure 3.2G and I). Therefore, some CCR7$^{+}$ effector cells on day 8 gave rise exclusively to stable $CCR7^+$ memory cells present 254 days after infection.

## $CXCR5^+$ Memory Cells Are Tcm Cells

Expression of CXCR5 suggested that Tcm precursor cells might be a variety of GC-Tfh cell. If so, then by definition these cells would be expected to located in B cell-rich follicles. This possibility was assessed in an adoptive transfer experiment. $CD44^{high}$ $CD4^+$ $CXCR5^-$ PD-$1^-$ Th1, $CXCR5^{intermediate}$ PD-$1^-$ Tcm, and $CXCR5^{high}$ PD-$1^+$ GC-Tfh cells (Figure 3.3A) were purified by flow cytometric sorting (Figure 3.3B) from $CD45.2^+$ B6 mice 10 days after infection with Lm-2W organisms and injected into naive $CD45.1^+$ recipients. These populations contained effector cells specific for Lm-2W-derived p:MHCII ligands and other memory cells. Spleen sections from recipient mice were then stained with fluorochrome-labeled anti-CD4, anti-IgD, and anti-CD45.2 antibodies 1 day after cell transfer. The locations of the cells in the T cell areas (dense $CD4^+$ cells), follicles (dense $IgD^+$ cells), or red pulp/marginal zone (sparse $CD4^+$ cells and $IgD^+$ cells) were assessed by microscopy (Figure 3.3C). Th1 cells were located predominantly in the red pulp and T cell areas, while GC-Tfh cells were located primarily in follicles (Figure 3.3D). I n contrast, $CXCR5^+$ PD-$1^-$ Tcm cells were located predominantly in the T cell areas (Figure 3.3D). This location outside of the follicles formally demonstrated that Tcm cells were not GC Tfh cells.

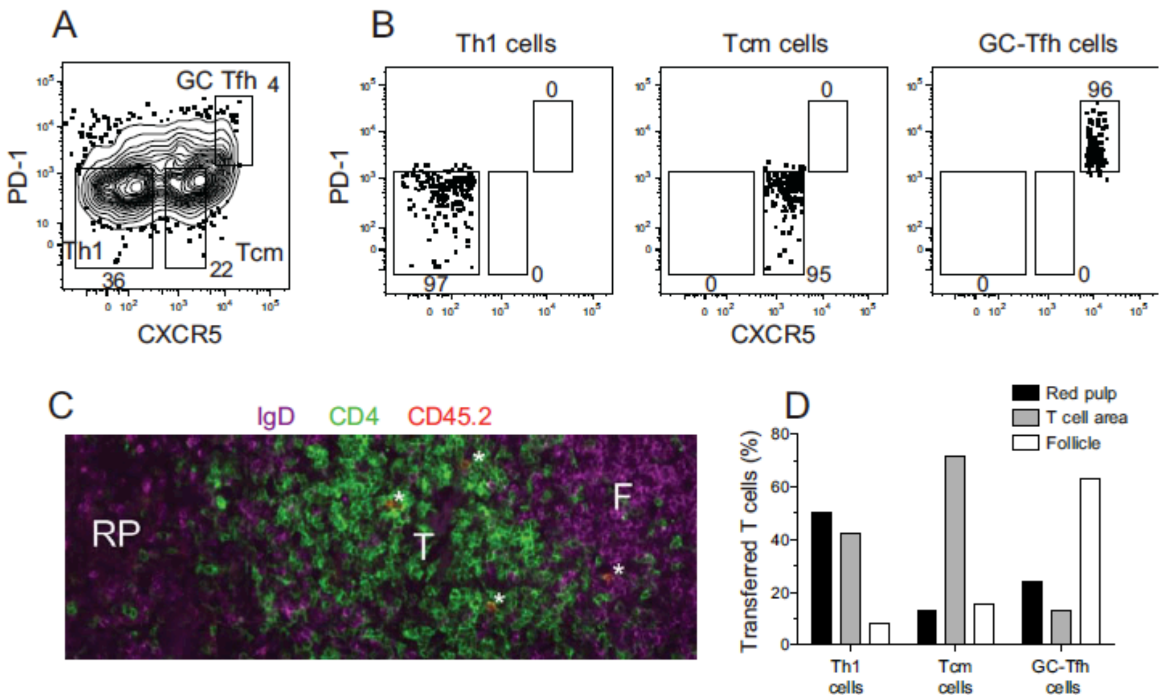


**Figure 3.3. Tcm Precursor Cells are Located in the T Cell Areas.** (A) Gates used to sort purify the indicated subsets from the spleen and lymph nodes of B6 mice 10 days after Lm-2W infection. CCR7 staining was also used as a sorting parameter (not shown) with Th1 cells sorted as CCR7$^-$ cells, Tcm cells as CCR7$^+$ cells, and GC-Tfh cells as CCR7$^{low}$ cells. (B) Post-sort analysis of the indicated populations. Four x $10^6$ Th1, 3 x $10^6$ Tcm, or $10^6$ GC-Tfh cells were transferred into CD45.1$^+$ recipients. (C) CD4 (green), IgD (purple), and CD45.2 (red) expression in a representative spleen section from a naïve B6 mouse that received $T_{CM}$ cells one day before analysis. CD45.2$^+$ cells that were also CD4$^+$ appeared orange. A T cell area (T), follicle (F), and red pulp/marginal zone area (RP) are indicated. Three CD4$^+$ CD45.2$^+$ transferred T cells in the T cell area and one in the follicle are labeled with asterisks. (D) Percentage of Th1 (151 cells), Tcm (91 cells), and GC-Tfh cells (38 cells) located in the indicated areas one day after transfer.

We also determined whether CXCR5$^{+}$ memory cells behaved like Tcm cells with respect to lymphokine production (Sallusto et al., 2004). Mice infected with Lm-2W bacteria 92 days earlier were injected intravenously with LLOp to restimulate LLOp:I-A$^{b}$-specific memory cells. As shown in Figure 4A and B, neither the T-bet$^{high}$ CXCR5$^{-}$ Th1 nor the T-bet$^{low}$ CXCR5$^{+}$ LLOp:I-A$^{b}$-specific memory cells were producing IL-2 or IFN-γ before peptide injection. Both memory cell types retained their pre-injection patterns of T-bet and CXCR5 expression 2 hours after LLOp challenge (Figure 3.4A), allowing analysis of their lymphokine production. About 60% of the T-bet$^{+}$ CXCR5$^{-}$ Th1 memory cells produced IFN-γ and IL-2 and ~20% made IL-2 but not IFN-γ 2 hours after injection of LLOp (Figure 3.4A and B). In contrast, about 10% of the T-bet$^{low}$ CXCR5$^{+}$ memory cells produced IFN-γ and IL-2 while ~60% made IL-2 but not IFN-γ. Therefore, the LLOp:I-A$^{b}$-specific CXCR5$^{+}$ memory cells were less potent IFN-γ producers than Th1em cells and rapidly produced IL-2 as expected for Tcm cells.

Finally, we used an adoptive transfer approach to test whether CXCR5$^{+}$ memory cells produced diverse effector cell progeny during the secondary response as expected for Tcm cells (Sallusto et al., 2004). CD44$^{high}$ CD4$^{+}$ CXCR5$^{+}$ (containing 2W:I-A$^{b}$-specfiic Tcm cells) and CD44$^{high}$ CD4$^{+}$ CXCR5$^{-}$ (containing 2W:I-A$^{b}$-specfiic Th1em cells) cells were sorted from B6 mice 40 days after infection with Lm-2W organisms and injected into naive CD45.1$^{+}$ recipients. The recipient mice were then challenged with Lm-2W organisms, and the phenotype of the donor and recipient 2W:I-A$^{b}$-specific T cells (Figure 3.4C) was assessed 6 days later. As shown in Figure 3.4C and D, 96% of the effector cell progeny of CCR7$^{-}$ CXCR5$^{-}$ Th1em cells were Th1 cells. In contrast, the progeny of $CXCR5^+$ memory cells consisted of 70% Th1 cells, 21% Tfh cells, and 5% GC-Tfh cells, whereas the naïve cells of the recipients produced 44% Th1, 43% Tfh, and 8% GC-Tfh cells. Therefore, although $CXCR5^+$ memory cells had a tendency to produce Th1 effector cells, they more efficient than Tem cells at generating Tfh cells and GC-Tfh cells.

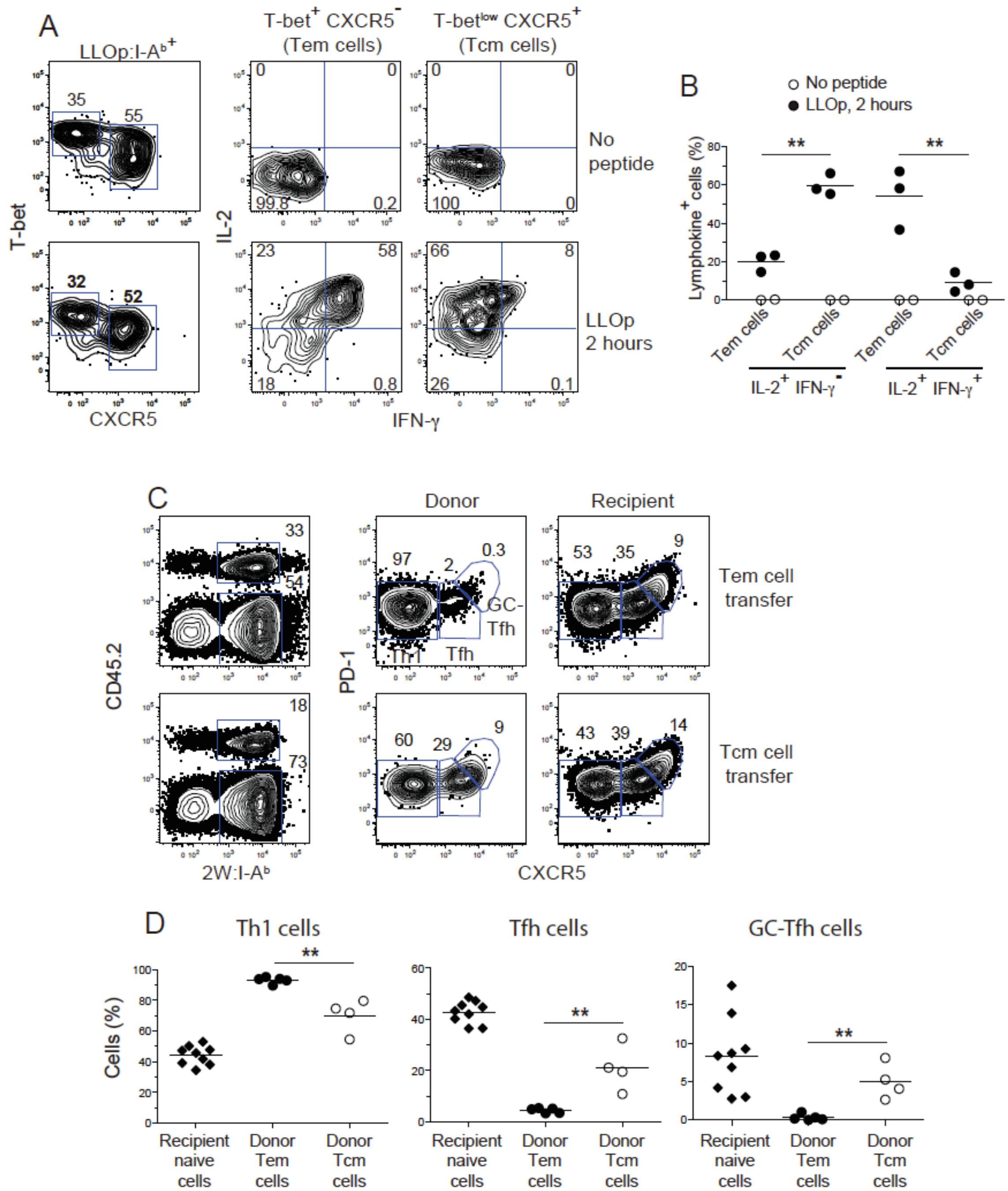


**Figure 3.4. Secondary Responses by Memory Cells.** (A) Contour plots showing T-bet and CXCR5 expression by LLOp:I-A$^b$-specific T cells (left panels), or intracellular IFN-γ and IL-2 staining (lower panels) in LLOp:I-A$^b$-specific Tem (middle panels) or Tcm cells (right panels)

from day 92 Lm-2W-infected mice before (upper panels) or 2 hours after intravenous injection of LLOp (lower panels). (B) Percentage of LLOp:I-$A^b$-specific Tcm or Tem cells producing the indicated lymphokines before (filled circles) or 2 hours after intravenous injection of LLOp (open circles). **, $p < 0.01$. (C) 4.8 x $10^5$ $CD44^{high}$ $CD4^+$ $CCR7^+$ $CXCR5^+$ PD-$1^-$ Tcm or 4.3 x $10^5$ $CD44^{high}$ $CD4^+$ $CCR7^-$ $CXCR5^-$ PD-$1^-$ $T_{em}$ cells were sorted from $CD45.2^+$ B6 mice infected 30 days earlier with Lm-2W bacteria, and transferred into $CD45.1^+$ mice, which were then challenged with Lm-2W bacteria. Representative plots used to identify donor (upper gates, left panels) or recipient (lower gates, left panels) 2W:I-$A^b$-specific cells 6 days after challenge are shown, along with plots of PD-1 versus CXCR5 used to identify Th1 effector cells, Tfh, and GC-Tfh cells of donor (middle) or recipient (right) origin. (D) Percentage of Th1 effector, Tfh, or GC-Tfh cell progeny from donor Tem, donor Tcm, or recipient naïve cells. **, $p < 0.01$.

### Development of Tem and Tcm Cells

The results were consistent with the possibility that Th1 effector and Tcm precursor cells generated early in the primary response gave rise to Th1em and Tcm cells. We examined very early times after Lm-2W infection to get insight into the origins of these populations. The IL-2 receptor alpha chain (CD25) was included in the analysis because it has been implicated in Th1 development in other systems (Khoruts et al., 1998; Liao et al., 2011). Naïve LLOp:I-$A^b$-specific cells in uninfected mice did not express CXCR5 or CD25 (Figure 3.5A). Remarkably, the LLOp:I-$A^b$-specific population had already split equally into $CXCR5^-$ and $CXCR5^+$ subsets only 3 days after infection (Figure 3.5A) when expansion of LLOp:I-$A^b$-specific T cells was first detected (Figure 3.1D). Notably, most of the $CXCR5^-$ cells also expressed CD25 and most of the

CXCR5$^+$ cells did not (Figure 3.5A). On day 4 after infection, the CXCR5$^-$ cells expressed more T-bet than CXCR5$^+$ cells (Figure 3.5B).

These findings raised the possibility that CD25 was required for the development of the CXCR5$^-$ effector cells by augmenting T-bet after day 3. This premise was tested in chimeras containing a mixture of wild-type and CD25-deficient T cells so that both populations could be monitored under conditions where normal regulatory T cells were present to prevent the autoimmunity that occurs in intact CD25-deficient mice (Willerford et al., 1995). As shown in Figure 3.5C and D, CD25-deficient LLOp:I-A$^b$-specific naïve cells were about one tenth as good as wild-type cells at generating T-bet$^{high}$ CXCR5$^-$ Th1 cells in these chimeras 5 days after Lm-2W infection, but were as good as wild-type cells at generating CXCR5$^+$ PD-1$^-$ Tfh cells (Tcm precursor cells) and CXCR5$^+$ PD-1$^+$ GC-Tfh cells. CD25 was therefore required for the optimal development of the T-bet$^{high}$ CXCR5$^-$ Th1 but not the other effector cell populations.

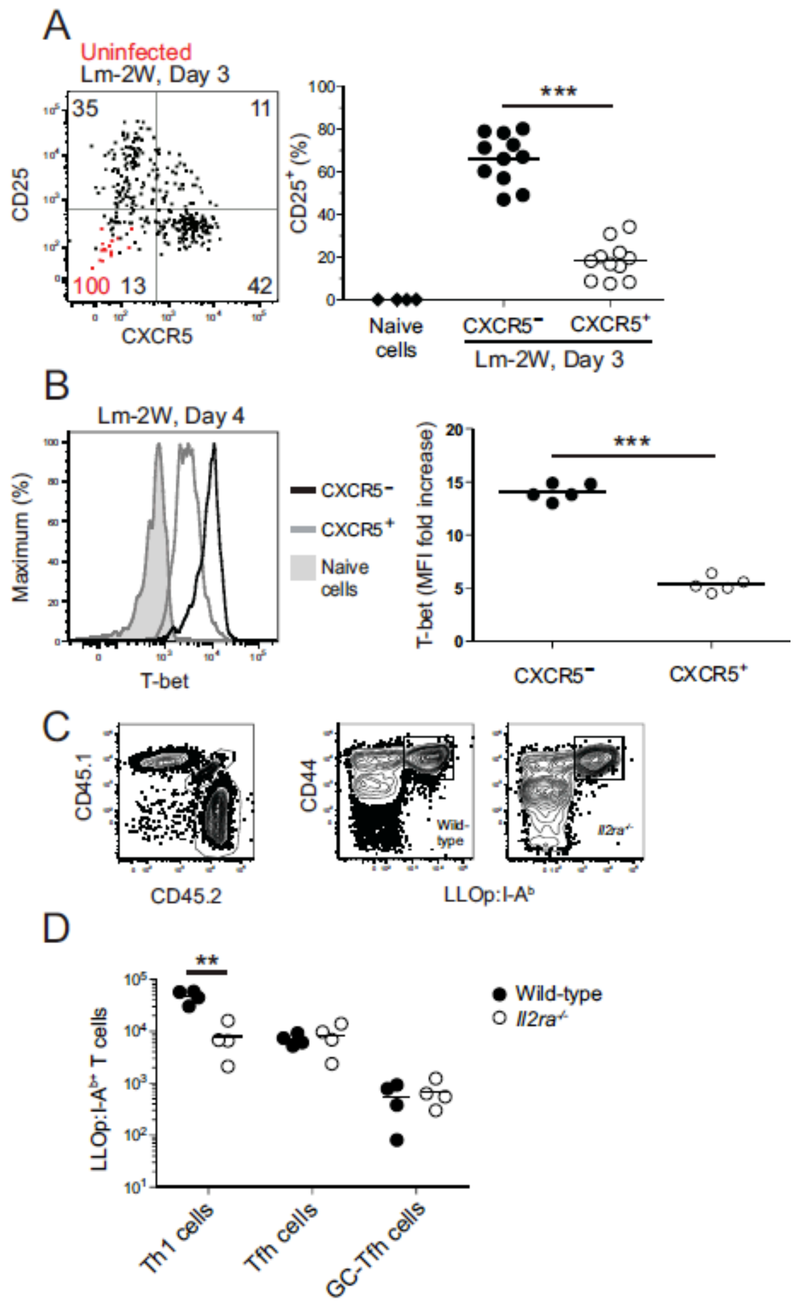


**Figure 3.5. Development of Th1 Effector Cells Depends on CD25**. (A) Representative dot plots of CD25 versus CXCR5 expression by LLOp:I-A$^b$-specific cells from naïve mice (red dots) or from mice 3 days after intravenous infection with Lm-2W bacteria (black dots). The values on

the plots represent the percentage of cells in the indicated quadrants from naïve (red) or Lm-2W-infected (black) mice. The scatter plot shows the percentage of $CD25^+$ total naïve $CD4^+$ T cells from uninfected B6 mice (diamonds) or $CXCR5^-$ (filled circles) or $CXCR5^+$ (open circles) LLOp:I-$A^b$-specific cells from mice 3 days after intravenous infection with Lm-2W bacteria. ***, $p < 0.001$. (B) T-bet expression in total naïve $CD4^+$ T cells from uninfected B6 mice (shaded), or $CXCR5^-$ (black) or $CXCR5^+$ (gray) LLOp:I-$A^b$-specific cells from mice 4 days after intravenous infection with Lm-2W bacteria, with a scatter plot showing the fold increase of T-bet mean fluorescence intensity (MFI) of the indicated LLOp:I-$A^b$-specific populations over the T-bet MFI of naïve $CD4^+$ T cells. ***, $p < 0.001$. (C) Representative plots of CD45.1 versus CD45.2 expression and CD44 expression versus LLOp:I-$A^b$ tetramer staining of $CD4^+$ T cells in a tetramer-enriched sample from a radiation chimera produced with $CD45.2^+$ wild-type and $CD45.1^+/2^+$ *Cd25*$^{-/-}$ bone marrow, 5 days after intravenous infection with Lm-2W bacteria. (D) Number of LLOp:I-$A^b$-specific Th1, Tcm, and GC-Tfh cells identified as in Figure 2B of wild-type (filled circles) or *Cd25*$^{-/-}$ (open circles) origin from individual mice, 5 days after intravenous infection with Lm-2W bacteria. **, $p < 0.01$.

We also examined the expression of Bcl6 as a prelude to assessing its role in the development of Tcm cells. Bcl6 was expressed in higher amounts in the $CXCR5^+$ subset of LLOp:I-$A^b$-specific cells 3 days after Lm-2W infection than in the $CXCR5^-$ subset (Figure 3.6A). Radiation bone marrow chimeras containing a mixture of wild-type and *Bcl6*$^{-/-}$ (Dent et al., 1997) cells were used to test whether Bcl6 was required for the formation of $CXCR5^+$ T cells. Indeed, Bcl6-deficient $CD4^+$ T cells failed to generate early LLOp:I-$A^b$-specific $CXCR5^+$ cells on day 3 (Figure 3.6A and B). Similarly, CXCR5$^{+}$ PD-1$^{-}$ Tfh cells and CXCR5$^{+}$ PD-1$^{+}$ GC-Tfh cells were generated at least 100-fold less well from Bcl6-deficient than from wild-type CD4$^{+}$ T cells 7 days after Lm-2W infection (Figure 3.6C and D). The Bcl6-deficient LLOp:I-A$^{b}$-specific T cells present on day 7 were all T-bet$^{high}$ indicating that T-bet$^{low}$ Tcm precursors were truly absent and had not simply lost CXCR5 (Figure 3.6C). We also produced radiation bone marrow chimeras containing a mixture of wild-type and *Bcl6*$^{+/-}$ T cells to test the dependence of the two types of CXCR5$^{+}$ effector cells on the amount of Bcl6 expressed. As shown in Figure 3.6D, LLOp:I-A$^{b}$-specific *Bcl6*$^{+/-}$ Tfh cells formed normally 7 days after Lm-2W infection, while *Bcl6*$^{+/-}$ GC-Tfh cells exhibited a 10-fold defect compared to wild-type T cells. These results demonstrated that Tfh and GC-Tfh cells both depended on Bcl6 although Tfh cells were less dependent.

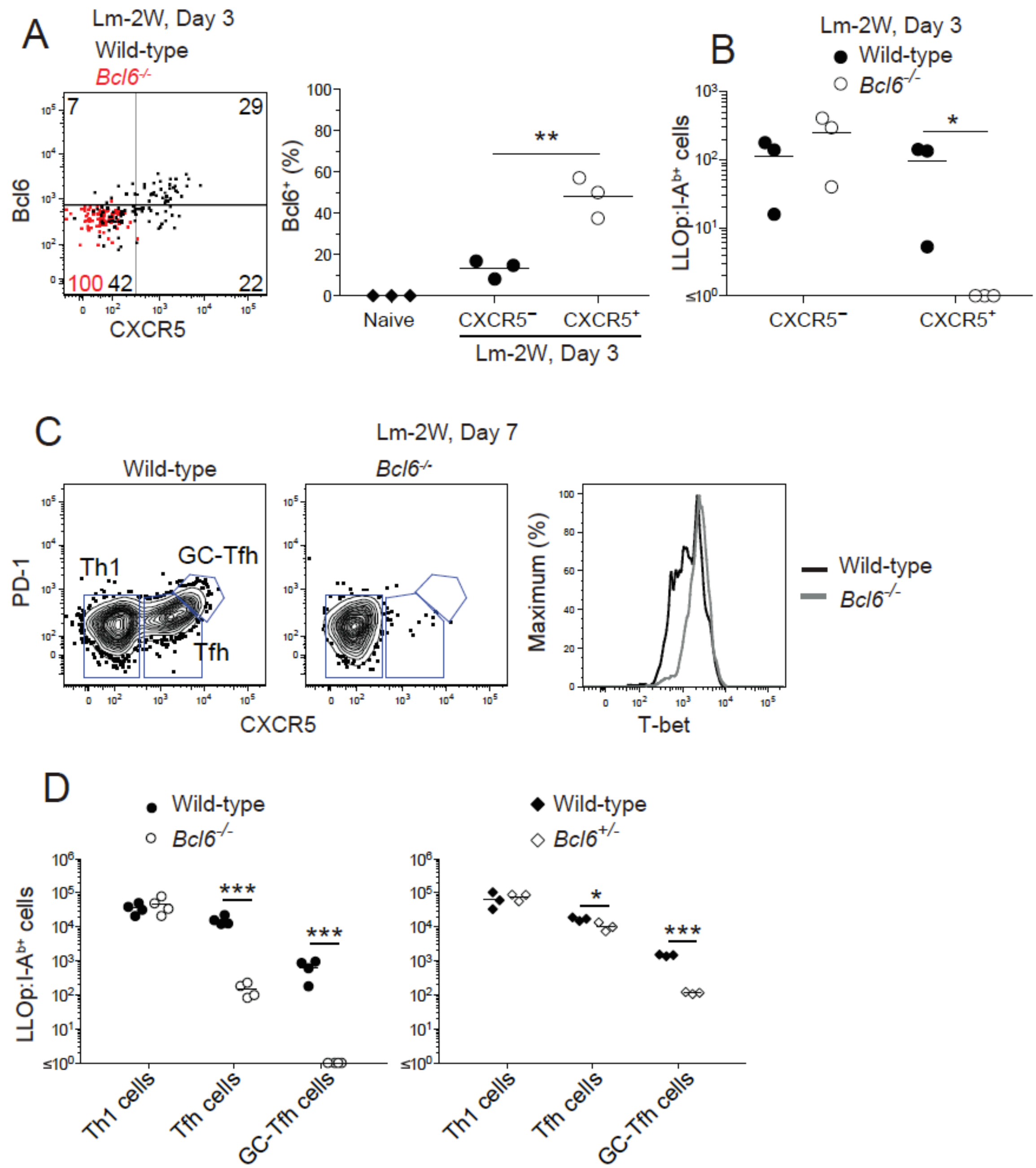


**Figure 3.6. Development of Tcm Cells Depends on Bcl6**. (A) Representative plot of Bcl6 versus CXCR5 expression by wild-type (black dots) or *Bcl6*$^{-/-}$ (red dots) LLOp:I-A$^{b}$-specific cells from a wild-type/*Bcl6*$^{-/-}$ mixed radiation bone marrow 3 days after intravenous infection with Lm-

2W bacteria with a scatter plot showing the percentage of $Bcl6^{+}$ naïve $CD4^{+}$ T cells from uninfected B6 mice (diamonds) or $CXCR5^{-}$ (filled circles) or $CXCR5^{+}$ (open circles) LLOp:I-$A^{b}$-specific cells from wild-type mice 3 days after infection. (B) Number of wild-type (filled circles) or *Bcl6*$^{-/-}$ (open circles) $CXCR5^{-}$ or $CXCR5^{+}$ LLOp:I-$A^{b}$-specific cells from 3 wild-type/*Bcl6*$^{-/-}$ mixed radiation bone marrow chimeras, 3 days after intravenous infection with Lm-2W bacteria. *, $p < 0.05$. (C) Representative plots of CXCR5 versus PD-1 staining used to identify wild-type or *Bcl6*$^{-/-}$ LLOp:I-$A^{b}$-specific Th1 effector cells, Tfh cells (Tcm precursors), and GC-Tfh cells from wild-type/*Bcl6*$^{-/-}$ mixed radiation bone marrow chimeras 7 days after Lm-2W infection. T-bet expression by wild-type or *Bcl6*$^{-/-}$ LLOp:I-$A^{b}$-specific cells in these chimeras is also shown. (D) Number of LLOp:I-$A^{b}$-specific Th1, Tfh, and GC-Tfh cells identified as in (C) from individual wild-type/*Bcl6*$^{-/-}$ (left) or wild-type/*Bcl6*$^{+/-}$ (right) mixed radiation bone marrow chimeras, 7 days after intravenous infection with Lm-2W bacteria. *, $p < 0.05$, ***, $p < 0.001$.

## ICOS Signals from B cells Sustain Tcm Cell Differentiation

The Bcl6 requirement of Tfh cells and GC-Tfh cells prompted us to determine whether Tcm precursors also required signals from B cells and the ICOS costimulatory receptor (Akiba et al., 2005; Vinuesa et al., 2005) as described for GC Tfh cells (Nurieva et al., 2008). Seven and 25 days after Lm-2W infection, the numbers of LLOp:I-$A^{b}$-specific Tcm cells and GC-Tfh cells were 3-10-fold lower in μMT mice lacking B cells (Kitamura et al., 1991) than in wild-type mice (Figure 3.7A). Therefore, B cells were necessary for optimal generation of Tcm and GC-Tfh cells.

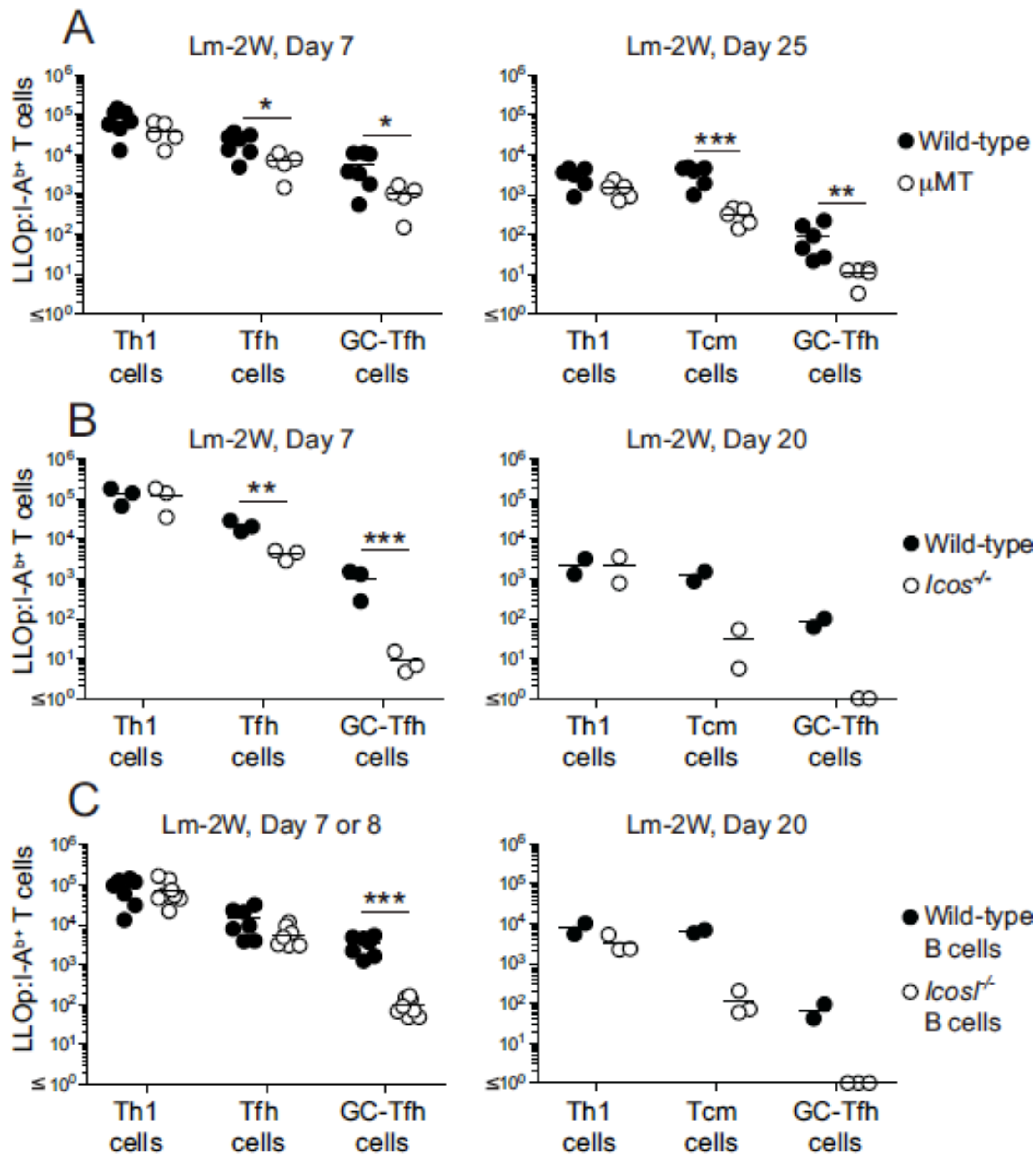


**Figure 3.7. Development of Tcm Cells Depends on ICOS Signals from B cells.** (A) Number of LLOp:I-A$^b$-specific Th1/Tem, Tfh/Tcm, and GC-Tfh cells identified as in Figure 2B from individual wild-type or B cell-deficient μMT mice, 7 or 25 days after intravenous infection with Lm-2W bacteria. (B) Number of LLOp:I-A$^b$-specific Th1/Tem, Tfh/Tcm, and GC-Tfh cells from

individual wild-type/*Icos*$^{-/-}$ mixed radiation bone marrow chimeras, 7 or 20 days after intravenous infection with Lm-2W bacteria. (C) Number of LLOp:I-A$^{b}$-specific Th1, Tcm, and GC-Tfh cells from individual wild-type/μMT or *Icosl*$^{-/-}$/μMT mixed radiation bone marrow chimeras, 7 or 8, or 20 days after intravenous infection with Lm-2W bacteria. *, $p < 0.05$, **, $p < 0.01$, ***, $p < 0.001$

The role of ICOS was tested in bone marrow chimeras reconstituted with an equal mixture of ICOS-deficient (Tafuri et al., 2001) and wild-type bone marrow cells so that ICOS-deficient T cells could be analyzed under conditions where wild-type T cells were present to promote a normal germinal center response. ICOS-deficient and wild-type Th1 effector cells were generated equally 7 days after Lm-2W infection, and maintained as Th1em cells on day 20 (Figure 3.7B). In contrast, ICOS-deficient Tfh cells were generated at about 3-fold less well on day 7 and survived as Tcm cells on day 20 about 30-fold less well than the comparable wild-type populations. GC-Tfh cells were even more dependent on ICOS, forming 100-fold less well on days 7 and 20 in the absence of ICOS than in its presence.

We next determined whether B cells were the critical source of ICOSL. Chimeras were made by reconstituting lethally irradiated B6 mice with an equal mixture of ICOSL-deficient (Mak et al., 2003) and wild-type or μMT bone marrow cells incapable of forming B cells (Kitamura et al., 1991). All of the B cells in the chimeras made with wild-type bone marrow expressed ICOSL, and all of the B cells in the chimeras made with ICOSL-deficient bone marrow cells lacked ICOSL, while half of the dendritic cells in those chimeras expressed ICOSL. Seven or 8 days after Lm-2W infection, the number of LLOp:I-$A^b$-specific Tfh cells was slightly but not significantly lower in chimeras containing ICOSL-deficient B cells than in chimeras containing wild-type B cells (Figure 3.7C). However, by day 20, the number of LLOp:I-$A^b$-specific Tcm cells was 100-fold lower in chimeras containing ICOSL-deficient B cells than in chimeras containing wild-type B cells (Figure 3.7C). GC-Tfh cells were generated 100-fold less efficiently on days 7 or 8 in chimeras containing ICOSL-deficient B cells than in chimeras containing wild-type B cells. The formation of Tcm cells and GC-Tfh cells in chimeras lacking ICOSL on B cells therefore mirrored the production of these populations from ICOS-deficient T cells. Together, these experiments demonstrate that the interaction of ICOS on the T cells with ICOSL on B cells is necessary for optimal generation of GC-Tfh cells and the maintenance of Tcm cells.

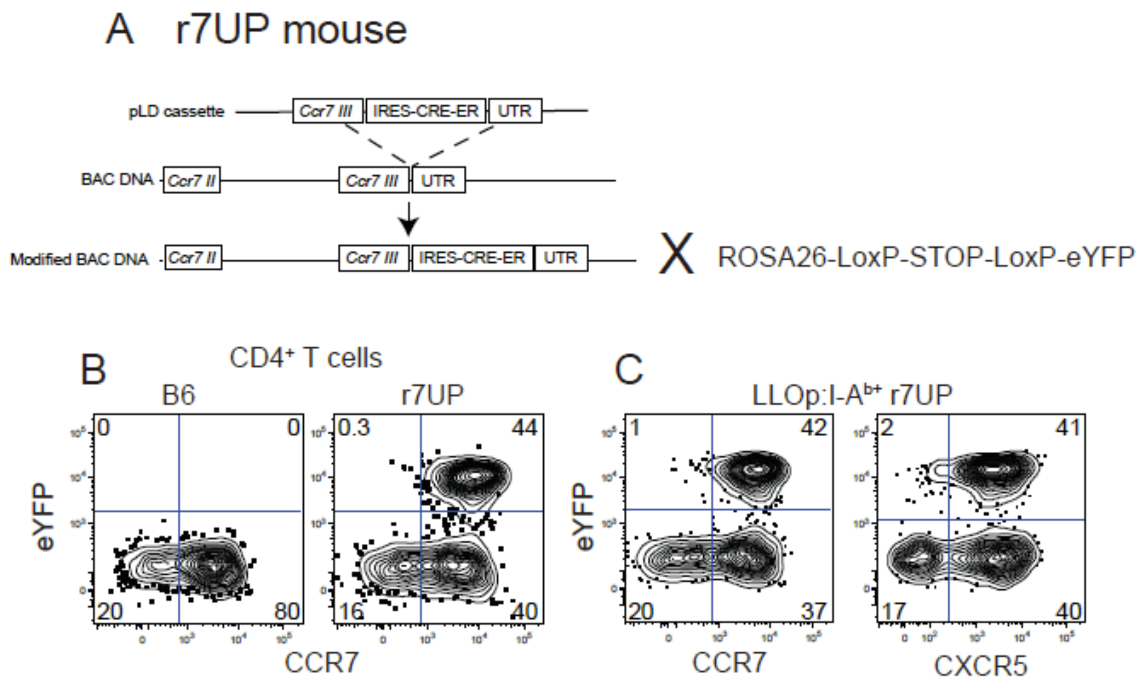


**Supplemental Figure 3.1. Characterization of r7UP mice.** (A) Schematic representation of strategy used to create the r7UP mouse. (B) Representative plot of eYFP versus CCR7 expression by total $CD4^+$ T cells from uninfected B6 (left) or r7UP mice (right) after 5 days of tamoxifen treatment. (C) eYFP versus CCR7 (left) or CXCR5 (right) expression by tetramer-enriched LLOp:I-$A^b$-specific $CD4^+$ T cells from r7UP mice 20 days after Lm-2W infection. All mice were analyzed after 5 days of tamoxifen treatment.

### 3.4 Discussion

Our results demonstrate that LLOp:I-$A^b$-specific T-$bet^{high}$ $CXCR5^-$ and T-$bet^{low}$ $CXCR5^+$ $CD4^+$ T cells were already present at the peak of the primary response to a vaccine strain of Lm. Several observations indicate that some of these effector cells survived the contraction phase to become Th1em and Tcm cells. First, the 2 memory cell populations that survived the contraction phase had phenotypes that were very similar to the 2 effector cell populations with the exception that T-bet$^{low}$ CXCR5$^{+}$ memory cells lacked Bcl6. Second, several other groups demonstrated that memory cells can be derived from IFN-γ-producing Th1 effector cells (Harrington et al., 2008; Lohning et al., 2008). Third, our studies of the r7UP mouse revealed that CCR7$^{+}$ Tcm cells were derived from CCR7$^{+}$ effector cells present at the peak of clonal expansion. Our results indicate that GC-Tfh cells fail to enter the memory cell pool although we cannot rule out that possibility that small numbers of these cells lose expression of PD-1 and contribute to the CXCR5$^{+}$ memory cell population.

The bifurcation of Lm p:MHCII-specific effector cells into CXCR5$^{-}$ and CXCR5$^{+}$ subsets was already apparent at the time of the earliest proliferation at day 3 as recently described in another CD4$^{+}$ T cell response (Choi et al., 2011). Although it is not clear what caused this early bifurcation, an asymmetric division of a CD25$^{+}$ mother cell into CD25$^{+}$ and CD25$^{-}$ daughter cells is a possibility (Chang et al., 2007). Once this split occurred, then work by others suggests a scenario in which IL-2 receptor signaling in the CD25$^{+}$ cells activated STAT5 (Hou et al., 1995; Lin et al., 1995), which induced the IL-12 receptor and T-bet (Liao et al., 2011), and suppressed Bcl6 and CXCR5 by inducing Blimp-1 (Gong and Malek, 2007; Shaffer et al., 2000). This sequence of events would be predicted to cause the early CD25$^{+}$ CXCR5$^{-}$ cells to retain T-bet and differentiate into Th1 effector cells, a fraction of which then survived as Th1em cells.

Conversely, the lack of IL-2 receptor signaling in the early CD25$^{-}$ cells may have been conducive to Bcl6 expression, which was essential for formation of early CXCR5$^{+}$

effector cells and subsequent PD-1$^{-}$ Tfh cell and PD-1$^{+}$ GC-Tfh cell progeny. Although it is not clear what drives the split between PD-1$^{-}$ Tfh cells and PD-1$^{+}$ GC-Tfh cells, the requirement of GC-Tfh cells for more Bcl6 and earlier ICOS signals than Tfh cells may be a clue. GC-Tfh cells tend to express TCRs with higher affinity for pMHCII ligands than other cells in the population (Fazilleau et al., 2009). The formation of these cells is also promoted by additional p:MHCII presentation by B cells (Deenick et al., 2010; Johnston et al., 2009). Therefore, early CXCR5$^{+}$ effector cells that receive very strong TCR and ICOS signals may express and maintain the large amounts of Bcl6 needed to commit to the GC-Tfh fate. Other early CXCR5$^{+}$ effector cells that receive less strong TCR and ICOS signals may express enough Bcl6 needed to become Tfh cells, and subsequently Tcm cells, but not enough to maintain Bcl6 and become GC-Tfh cells.

Although Tcm and GC-Tfh cells express CXCR5 and share some activation requirements, our results show that these are different cells. For example, Tcm cells were located at the T cell areas, not the follicles like GC-Tfh cells (Crotty, 2011). In addition, Tcm cells did not express Bcl6 and were relatively inefficient at producing GC-Tfh cells during the secondary response. Indeed, Th1 effector cells were the dominant progeny produced by Tcm cells when exposed to antigen. These properties may be related to the fact that Tcm cells expressed low amounts of T-bet at the time of challenge, and thus were partially committed to the Th1 lineage. Notably, however, Tcm cells produced some CXCR5$^{+}$ effector cells indicating that they were more flexible than Th1em cells, which only produced Th1 effector cells. The reports that CXCR5$^{+}$ Bcl6$^{-}$ Tcm-like memory cells present in humans (Chevalier et al., 2011), and similar cells in mice immunized with soluble antigen (MacLeod et al., 2011) or *Salmonella* infection (Lee et al., 2011) are potent helpers of B cell proliferation and antibody production is further evidence of the poly-functionality of Tcm cells.

An implication of this work is that B cells enhance the production of Tcm cells, adding to other studies showing a role for B cells in memory T cell formation (Linton et al., 2000; Whitmire et al., 2009). In our study, it was very likely that many B cells in the spleen had access to Lm bacteria soon after intravenous injection. In contrast, B cells may have less access to bacteria like *Mycobacteria* and *Salmonella*, which often initially enter the body in very small numbers and then multiply inside the phagosomes of macrophages and dendritic cells (Cosma et al., 2003; Monack et al., 2004) and induce poor germinal center responses (Cunningham et al., 2007; Racine et al., 2010). Our results suggest that poor B cell activation in these infections produces primarily Th1em cells. In contrast, immunization with soluble antigens and adjuvants, which freely activate B cells, may produce primarily Tcm and GC-Tfh cells. Therefore, subunit vaccines of this type may not produce protective immunity to *Mycobacteria* and *Salmonella* infections because they induce the wrong type of memory T cells. The challenge facing vaccines for this type of infection will therefore be to deliver the antigen in a way that maximizes IL-2 production and minimizes activation of B cells.

# Chapter 4:

# Germinal Center T Follicular Helper Cells Form Central Memory T Cells with an Increased Capacity to Produce CXCR5$^+$ Effector Cells

Acute, systemic *Listeria monocytogenes* or lymphocitic choriomeningitis virus (LCMV) infections generate three kinds of CD4$^+$ effector cells; Th1 cells and two CXCR5$^+$ follicular helper subsets, one expressing PD-1 and located in germinal centers (GC-Tfh) and another lacking PD-1 and located at the border between the T and B cell areas (Tfh). However, the memory cell population that survives after the contraction phase only contains Th1 cells and CC chemokine receptor 7 (CCR7)$^+$ central memory T (Tcm) cells phenotypically resembling Tfh cells.  Thus, it is not clear whether GC-Tfh cells present early in the response contribute to the memory cell pool. Here we used a peptide:MHCII tetramer-based cell enrichment method to discover that GC-Tfh cells generated in response to lymphocitic choriomeningitis virus (LCMV) infection become memory cells but lose PD-1 expression.  Like memory cells originating from Tfh cells, GC-Tfh -derived memory cells produced diverse effector cell subsets in a secondary response but were better at making Tfh and GC-Tfh cells than the Tfh-derived memory cells.  Thus, both Tfh and GC-Tfh cells contribute to the Tcm pool but the GC-Tfh-derived memory cells have an increased potential to generate CXCR5$^+$ effector T cells.

## 4.1 Introduction

Naïve $CD4^+$ T cells that encounter dendritic cells displaying the relevant peptide:MHC II ligand (p:MHCII) proliferate and produce effector cells, some of which survive long-term as memory cells. During acute infections with *Listeria monocytogenes* or lymphocitic choriomeningitis virus (LCMV), the effector cell population consists of Th1 cells, $CXCR5^{high}$ $PD\text{-}1^{high}$ T follicular helper cells that are located in germinal centers (GC-Tfh) and $CXCR5^{int}$ $PD\text{-}1^{low}$ Tfh cells that are located at the border between the T and B cell zones. Two phenotypically-distinct memory cell populations remain following the contraction phase of the response, one resembling the Th1 effector cells and one resembling the Tfh effector cells. We recently demonstrated that the latter memory T cells correspond to classically-defined central memory T (Tcm) cells (Sallusto et al., 1999) based on expression of CCR7, location within T cell areas of secondary lymphoid tissue, ability to rapidly produce IL-2 but not IFN-γ upon re-stimulation with cognate p:MHCII ligand, and production of Th1 cells, Tfh cells, and GC-Tfh cells in a secondary response (Pepper et al., 2011). Similar $CXCR5^+$ $CD4^+$ memory T cells with B cell helper function have been described in humans and other murine systems (Chevalier et al., 2011; MacLeod et al., 2011; Morita et al., 2011).

The absence of memory cells with the GC-Tfh phenotype raised the possibilities that the GC-Tfh effector cells died and the $CXCR5^+$ Tcm cells were derived exclusively from Tfh effector cells. The observation that tonsilar GC-Tfh cells are prone to apoptosis *in vitro* (Rasheed et al., 2006) supports this perspective. However, it was also possible that some GC-Tfh effector cells lose expression of PD-1 and enter the memory pool along with some Tfh effector cells. A recent imaging study by Okada and colleagues showing that GC-Tfh cells can downregulate PD-1 and Bcl6, become quiescent, and express memory markers during the resolution of a primary immune response (Kitano et al., 2011) is consistent with this possibility.

We sought to resolve the issue of whether Tfh cells or GC-Tfh cells are the precursors of Tcm cells by using p:MHCII tetramers and a magnetic bead-based enrichment method to directly compare the fate of p:MHCII-specific Tfh cells and GC-Tfh cells generated in response to an acute systemic LCMV infection. We demonstrate that both Tfh and GC-Tfh effector cells contribute to the Tcm cell pool. In addition, we found that memory cells generated from both types of effector cells produce Th1 effector cells, Tfh cells, and GC-Tfh cells in a secondary response but that GC-Tfh cell-derived memory cells were superior at producing $CXCR5^+$ effector cells. Our results indicate that Tfh and GC-Tfh cells contribute to the Tcm cell pool and highlight a difference in their secondary response potential.

## 4.2 Materials and Methods

### Mice

Six- to eight-week old B6 and B6.SJL-*Ptprc*$^a$ *Pep3*$^b$/BoyJ (CD45.1) mice were purchased from the Jackson Laboratory or the National Cancer Institute and housed in a specific pathogen-free facility in accordance to guidelines from the National Institutes of Health and the University of Minnesota. The Institutional Animal Care and Use Committee of the University of Minnesota approved all experiments.

**Infections**

Mice were infected i.p. with 2 x $10^5$ plaque-forming units of the LCMV Armstrong strain (D. Masopust, University of Minnesota) as previously described (Homann et al., 2001).

**Tetramer Production**

Soluble biotin-labeled I-$A^b$ molecules containing LCMV glycoprotein $(GP)_{66\text{-}77}$ peptide (DIYKGVYQFKSV) covalently linked to the I-$A^b\beta$ chain were produced in *Drosophila melanogaster* S2 cells, purified, and made into tetramers with allophycocyanin-conjugated streptavidin (Prozyme) as described (Moon et al., 2007).

**Cell Enrichment and Flow Cytometry**

All antibodies were from eBioscience unless indicated. Single-cell suspensions from spleen and lymph nodes were stained for 1 hour at room temperature with allophycocyanin-conjugated streptavidin GP66:I-$A^b$ tetramers and 2μg of phycoerythrin-labeled anti-CXCR5 (2G8; BD Bioscience) and peridinin chlorophyll protein-cyanine 5.5-conjugated anti-CCR7. Samples were then enriched with magnetic bead-coupled anti-allophycocyanin over a magnetized LS column (Miltenyi), and a portion was removed for cell counting with fluorescent counting beads (Invitrogen) as described (Moon Immunity 2007). Enriched samples were stained for 30 minutes at 4°C with antibodies specific for B220 (RA3-6B2), CD11b (MI-70), CD11c (N418), CD8α (5H10; Invitrogen), PD-1 (J43), CD4 (RM4-5), CD3ε (145-2C11), CD44 (IM7), CD45.1 (A20), and/or CD45.2 (104) each labeled with a different fluorochrome. To detect transcription factors, some samples were subsequently treated with Foxp3 Fixation/Permeabilization Concentrate and Diluent (eBioscience) and stained for 1 hour at 4°C with antibodies against T-bet (4B10; Biolegend) and/or Bcl6 (K112-91; BD Bioscience).

**Fluorescence-activated Cell Sorting and Adoptive Transfers**

$CD4^+$ T cells from the spleen and lymph nodes of LCMV-infected CD45.1 mice were negatively selected with the $CD4^+$ T cell Isolation Kit II (Miltenyi) over a magnetized LS column (Miltenyi). Single cell suspensions were stained with a cocktail of antibodies against B220, CD11b, CD11c, CD8α to exclude non-$CD4^+$ T cells and antibodies to CXCR5, CCR7, and PD-1 to identify $CD4^+$ T cell subsets of interest. Cells of interest were sorted with a FACSAria (Becton Dickinson) flow cytometer. Tem cells were identified as $CXCR5^-$, $CCR7^-$, $PD\text{-}1^-$; Tfh cells and Tcm cells were identified as $CXCR5^{int}$, $CCR7^+$, $PD\text{-}1^-$; and GC-Tfh cells were identified as $CXCR5^{high}$, $CCR7^-$, $PD\text{-}1^{high}$. In some experiments, samples were also stained with antibodies against CD4 and CD44. To determine the frequency of GP66:I-$A^b$-specific T cells within the sample to be sorted, an aliquot of the $CD4^+$ T cell-enriched sample was stained with GP66:I-$A^b$ tetramer and antibodies as described above. For experiments comparing the secondary responses of Tem cells and Tcm cells, cell suspensions containing 8,000 Tem or Tcm GP66:I-$A^{b+}$ T cells were injected into B6 mice i.v. Recipient mice were immediately infected i.p. with LCMV as indicated above. For experiments evaluating Tfh cell and GC-Tfh cell entry into the memory pool, 37,000 Tfh cells or GC-Tfh cells were injected i.v. into B6 mice. Twenty-seven days after transfer, a cohort of recipient mice was infected with LCMV as indicated above. In some experiments, transferred CD45.1$^+$ cells were enriched for analysis as previously described (Hataye et al., 2006). In other experiments, cells from B6 mice were sorted and transferred into CD45.1$^+$ mice.

**Statistical Analyses**

Statistical tests were performed in Prism (GraphPad). For comparisons between two groups, a two-tailed, unpaired Student's *t* test was used. For comparisons involving three groups, a two-tailed, unpaired, one-way Analysis of Variance (ANOVA) with Bonferroni post-test was used. *P* values less than 0.05 were considered statistically significant.

## 4.3 Results

**Detection of Polyclonal GP66:I-A$^b$-specific CD4$^+$ T Cells**

We used p:MHCII tetramers and a magnetic bead-based enrichment method (Moon et al., 2009; Moon et al., 2007) to detect polyclonal CD4$^+$ T cells specific for the LCMV glycoprotein peptide 66-77 (DIYKGVYQFKSV) bound to the I-A$^b$ MHCII molecule (GP66:I-A$^b$) (Homann et al., 2001). We then tracked the primary response of GP66:I-A$^b$-specific T cells in I-A$^{b+}$ C57BL/6 (B6) mice following intraperitoneal inoculation with the Armstrong strain of LCMV, which produces a systemic infection that is cleared in about a week (Wherry et al., 2003). Tetramer-enriched spleen and lymph node single cell suspensions were stained with anti-CD3 and a cocktail of antibodies to non-T lineage markers to identify T cells (Figure 4.1A). About 150 GP66:I-A$^b$-specific T cells were detected among the CD4$^+$ T cells in enriched samples from uninfected mice, while none were detected in the CD8$^+$ T cell population (Figure 4.1B and D). Tetramer-binding cells in uninfected mice were CD44$^{low}$ as expected for naive cells. By day 8 after infection, GP66:I-A$^b$-specific cells had expanded about 4,000-fold and were CD44$^{high}$ as expected for antigen-experienced cells (Figure 4.1C and D). The number of GP66:I-A$^b$-specific T cells then contracted to about 10% of peak numbers by day 31 and gradually declined over the following several hundred days (Figure 4.1D). The dynamics of this response were therefore similar to those described for p:MHCII-specific CD4$^+$ T cells responding to LCMV Armstrong (Homann et al., 2001) or systemic infection with a vaccine strain of *L. monocytogenes* (Pepper et al., 2010; Pepper et al., 2011).

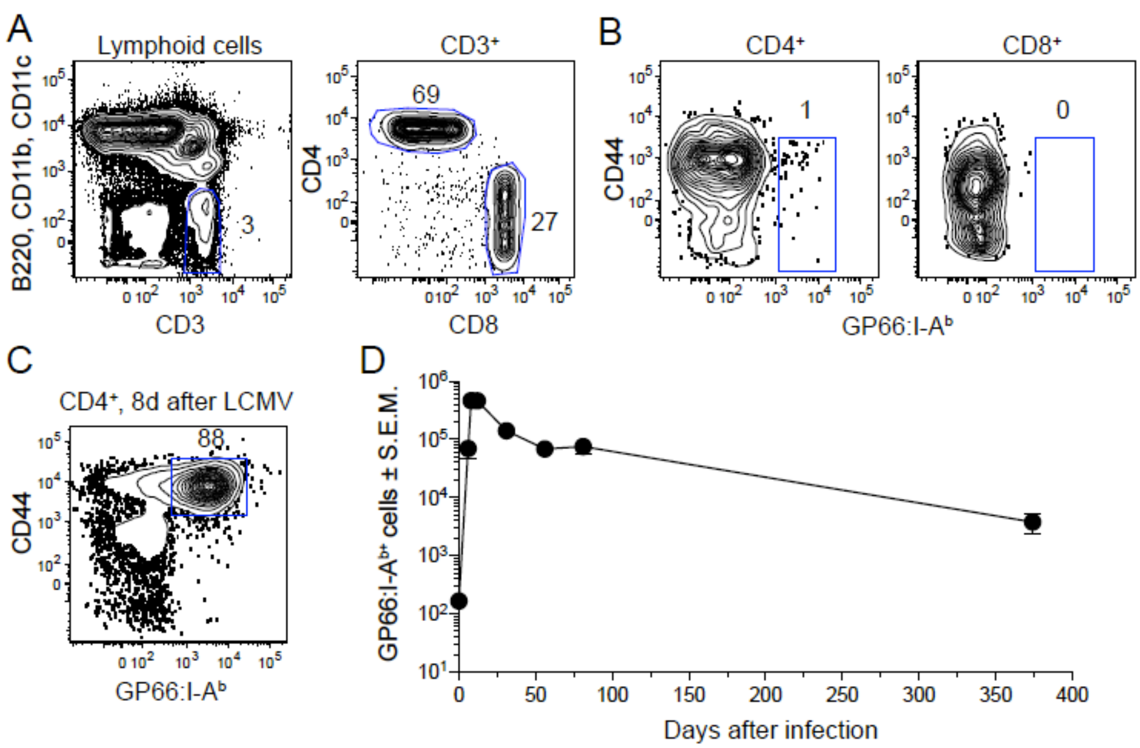

**Figure 4.1. Identification of GP66:I-A$^b$-specific T Cells.** GP66:I-A$^{b+}$ T cells were magnetically enriched from pooled spleen and lymph nodes from uninfected or LCMV-infected B6 mice and visualized by flow cytometry. (A) T cells were identified as CD3$^+$ events that did not bind non-T lineage-specific antibodies. CD4$^+$ and CD8$^+$ subsets were identified within the CD3$^+$ population. (B) GP66:I-A$^b$ tetramer versus CD44 staining for CD4$^+$ T cells (left) or CD8$^+$ T cells (right) in a tetramer-enriched sample of an uninfected mouse or (C) CD4$^+$ T cells 8 days after LCMV infection. The numbers on each plot represent the percentage of cells in the indicated gates. (D) Mean number of GP66:I-A$^{b+}$ T cells (3 - 6 mice per time point) at the indicated times after LCMV infection. Error bars represent standard error of the mean. Pooled data from three different experiments are shown.

## Characterization of CD4$^+$ T Cell Response to LCMV Armstrong Infection

We then sought to determine if LCMV Armstrong infection produced Th1 effector cells, Tfh cells, and GC-Tfh cells similar to those generated after systemic infection with attenuated *L. monocytogenes* (Pepper et al., 2011). Eight days after LCMV infection, three subsets of GP66:I-A$^b$-specific T cells could be defined by expression of CXCR5 and PD-1 (Figure 16A). All three subsets expressed more T-bet than naive cells, with CXCR5$^{low}$ PD-1$^{low}$ cells expressing the most (Figure 4.2B and C). CXCR5$^{int}$ PD-1$^{low}$ and CXCR5$^{high}$ PD-1$^{high}$ cells expressed more CCR7 than CXCR5$^-$ PD-1$^{low}$ cells but less than naive cells (Figure 4.2B and D). Both CXCR5$^+$ subsets but not CXCR5$^-$ PD-1$^{low}$ or the naive cells expressed Bcl6, with CXCR5$^{high}$ PD-1$^{high}$ cells expressing the largest amounts (Figure 4.2B and E). About 10% of the CXCR5$^-$ and CXCR5$^{int}$ PD-1$^{low}$ effector cells survived the contraction phase and produced cells resembling the Tem and Tcm cells described after *L. monocytogenes* infection (Pepper et al., 2011). In contrast, cells with a GC-Tfh cell phenotype did not persist into the memory phase, as indicated by the loss of PD-1$^{high}$ and Bcl6$^{+}$ cells (Figure 4.2B, D, E). Thus, LCMV infection produced CXCR5$^{-}$ PD-1$^{low}$ Th1 effector cells, CXCR5$^{+}$ PD-1$^{low}$ Tfh cells, and CXCR5$^{+}$ PD-1$^{high}$ GC-Tfh cells but only CXCR5$^{-}$ PD-1$^{low}$ and CXCR5$^{+}$ PD-1$^{low}$ memory cells like *L. monocytogenes* infection (Pepper et al., 2011). These GP66:I-A$^{b}$-specific T cell subsets also resembled those recently defined by Marshall and colleagues based on PSGL-1 and Ly6C expression (Marshall et al., 2011).

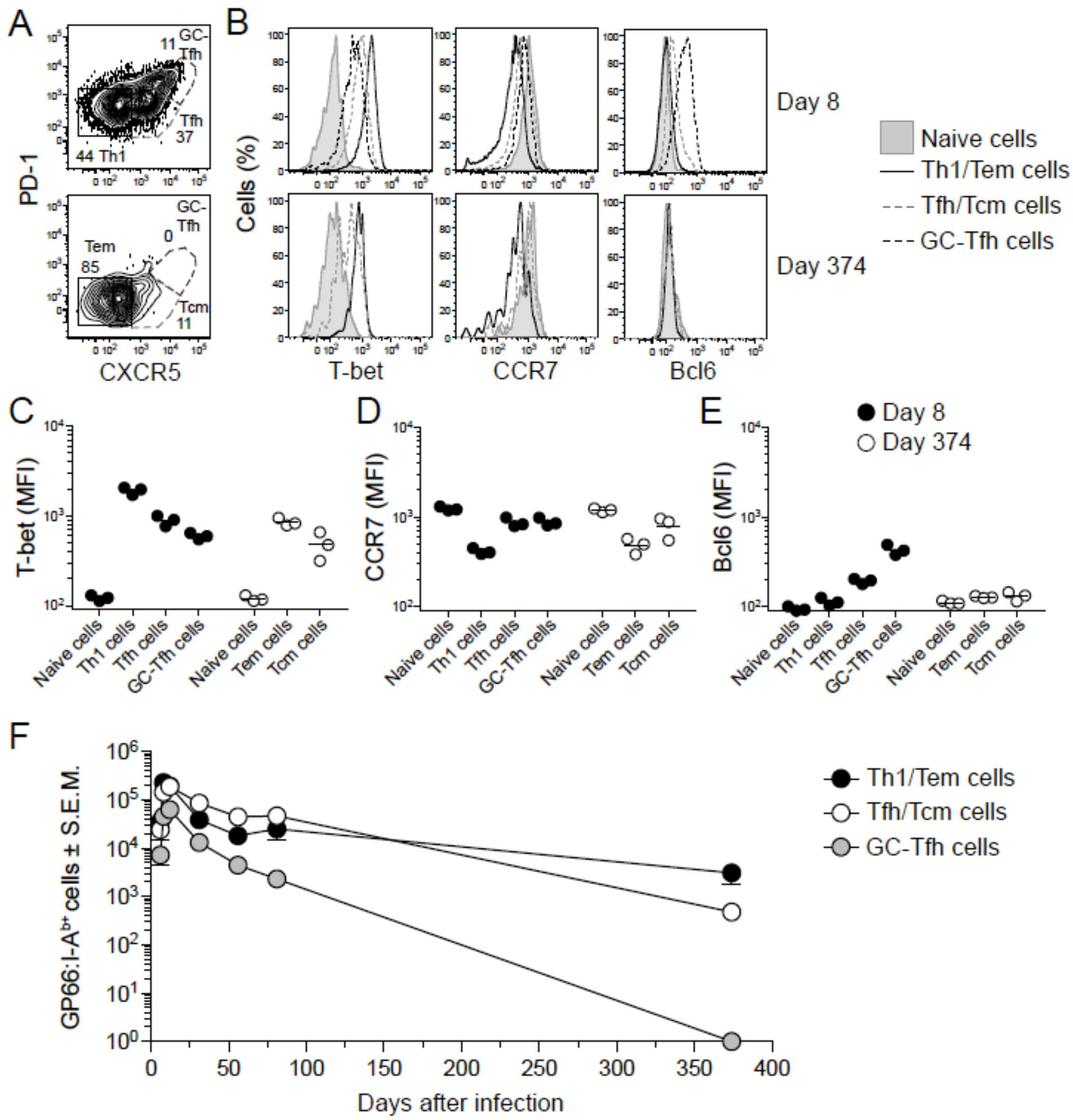


**Figure 4.2. Characterization of $CD4^+$ T Cell Subsets after LCMV Armstrong Infection.** (A) Plots identifying $CXCR5^-$ $PD\text{-}1^-$ Th1/Tem cells, $CXCR5^+$ $PD\text{-}1^{low}$ Tfh/Tcm cells, and $CXCR5^+$ $PD\text{-}1^{high}$ GC-Tfh cells within GP66:I-$A^{b+}$ T cells 8 or 374 days after LCMV infection. (B) Histograms of T-bet, CCR7, and Bcl6 expression on naive, day 8 effector cells, or day 374 memory cells. Mean fluorescence intensity (MFI) of (C) T-bet, (D) CCR7, or (E) Bcl6 on GP66:I-$A^{b+}$ T cells 8 or 374 days after infection. Histograms for $CD44^{low}$ $tetramer^-$ naïve cells are

also shown for comparison. (F) Mean number of GP66:I-$A^{b+}$ Th1 effector/Tem cells, Tfh/Tcm cells, and GC-Tfh cells after LCMV infection. Data from a single experiment (A – E) or three experiments (F) with three mice per group are shown.

### Secondary Responses by GP66:I-$A^b$-specific Effector Memory and Central Memory T Cells

We then investigated whether the cells in the memory phase that phenotypically resembled Tem cells and Tcm cells behaved as such in a secondary response. Tem cells and Tcm cells were sorted from day 29 LCMV-infected mice based on the $CD4^+$, $CD44^{high}$, $CCR7^-$, $CXCR5^-$, PD-$1^-$ and $CD4^+$, $CD44^{high}$, $CCR7^+$, $CXCR5^+$, PD-$1^-$ phenotypes, respectively (Figure 4.3A and B), and transferred into uninfected, congenic recipients that were then infected with LCMV Armstrong. GP66:I-$A^b$-binding T cells were then detected among the $CD4^+$ T cells of donor or recipient origin 7 days after infection (Figure 4.3C). As expected, the recipient's naive cells produced Th1 cells, Tfh cells, and GC-Tfh cells (Figure 4.3C – F). Donor-derived Tem cells chiefly produced Th1 cells. In contrast, Tcm cells formed Th1 cells, Tfh cells, and GC-Tfh cells similarly to the recipient's naive cells. Thus, LCMV Armstrong infection produces memory subsets that are very similar to those generated after attenuated *L. monocytogenes* infection (Pepper Immunity 2011).

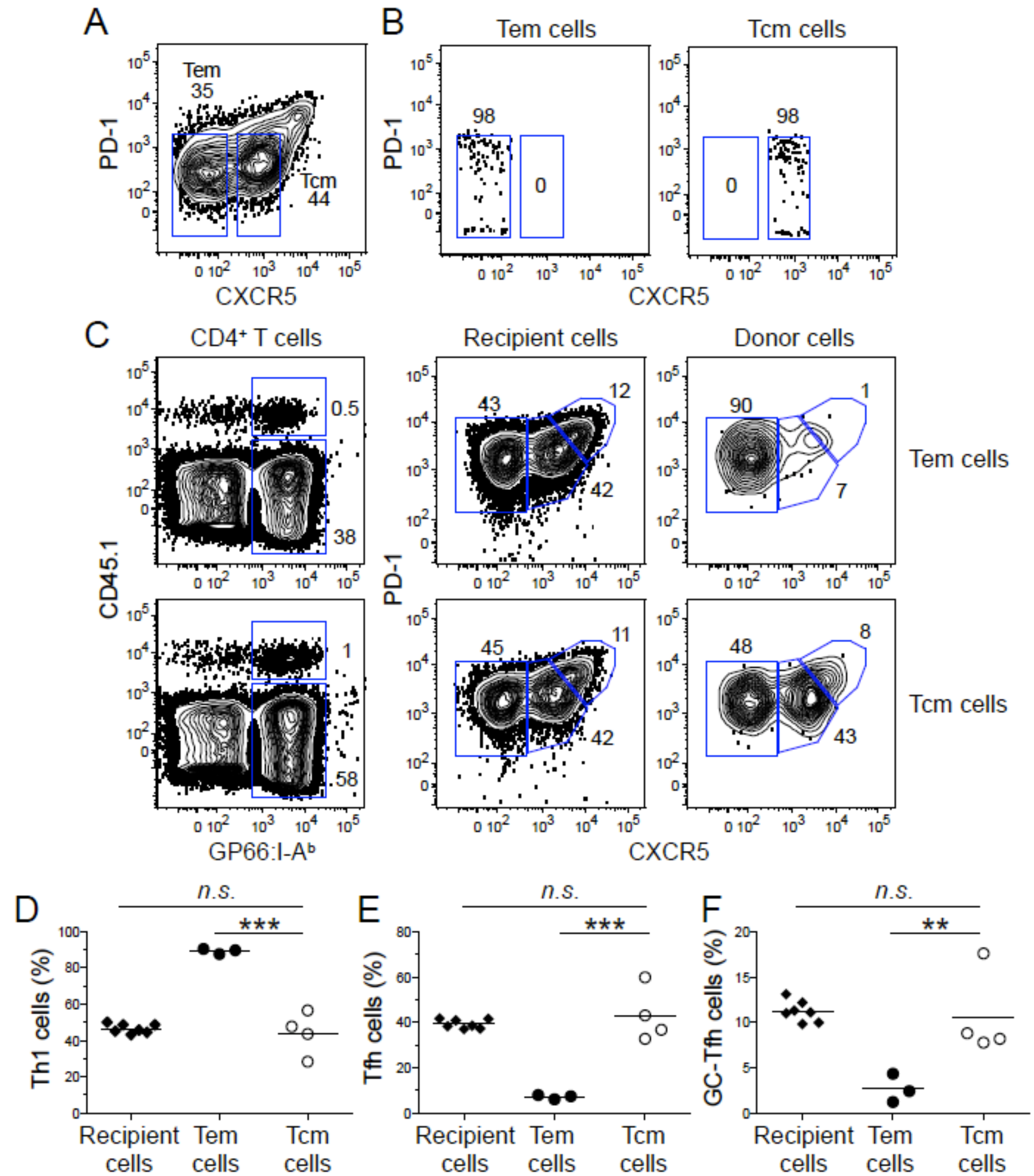


**Figure 4.3. Secondary Responses by GP66:I-A$^{b}$-specific Memory T Cells.** CD4$^{+}$ Tem cells and Tcm cells from the spleen and lymph nodes of CD45.1$^{+}$ mice 29 days after LCMV infection were sort purified as described in the text. Eight-thousand GP66:I-A$^{b+}$ T cells were transferred

i.v. into B6 recipients, which were immediately infected with LCMV. Seven days after transfer, GP66:I-$A^{b+}$ T cells were enriched magnetically and analyzed by flow cytometry. (A) Plot illustrating gating strategy used for sorting subsets of $CD44^{high}$ $CD4^{+}$ T cells. CCR7 staining was also used as a sorting parameter with Tem cells identified as $CCR7^{-}$ and Tcm cells identified as $CCR7^{+}$. (B) Post sort analysis of the indicated populations. (C) Plots show gating strategy to identify recipient and donor GP66:I-$A^{b+}$ T cells, and Th1/Tfh/GC-Tfh subsets within the GP66:I-$A^{b+}$ T cell populations (right). (D) Percentages of Th1 cells, Tfh cells, and GC-Tfh cells from individual mice after LCMV infection. One-way ANOVA with Bonferroni post-test was used to determine statistical significance. ($p > 0.05$, not significant, *n.s.*; $p < 0.01$, **; $p < 0.001$, ***). Each symbol represents an individual mouse. Data from one experiment with 3 – 4 mice per group are shown.

**GC-Tfh Cells that Persist into the Memory Phase Lose PD-1 Expression**

We next developed a sensitive adoptive transfer method to assess whether GC-Tfh effector cells enter the memory pool. Six $x10^{6}$ purified $CD4^{+}$ T cells from naive or day 82 LCMV-infected $CD45.1^{+}$ mice were transferred into uninfected $CD45.2^{+}$ recipients. A day after transfer, donor-derived $CD4^{+}$ T cells were enriched with CD45.1 antibody and stained with GP66:I-$A^{b}$ tetramer. GP66:I-$A^{b}$-binding $CD44^{high}$ T cells of donor origin were detected in the mice that received $CD4^{+}$ T cells from LCMV-infected mice but not naive mice (Figure 4.4A and B), thereby demonstrating the specific detection of transferred memory cells. The $CD44^{high}$ tetramer-binding cells detected in the recipients accounted for about 1% of the GP66:I-$A^{b+}$ memory cells that were present in the transferred population from day 82 LCMV-infected donor mice. These results demonstrated that small numbers of GP66:I-$A^{b+}$-specific memory T cells could be detected after adoptive transfer.

To address whether GC-Tfh effector cells enter the memory pool, we sorted $CCR7^{+}$ $CXCR5^{int}$ PD-$1^{low}$ Tfh cells and $CCR7^{-}$ $CXCR5^{high}$ PD-$1^{high}$ GC-Tfh cells from day 13 LCMV-infected mice (Figure 4.4C and D), and transferred these cells into uninfected congenic recipients. CCR7 was included in the sorting strategy because Tfh cells expressed two-fold more CCR7 on day 13 than GC-Tfh cells (data not shown). A day after transfer, donor GP66:I-$A^{b}$-specific T cells could be detected in recipient mice (Figure 4.4E and F), and these cells retained their respective Tfh and GC-Tfh cell phenotypes (Figure 4.4G and H). Twenty-seven days after transfer, corresponding to 40 days after infection, donor GP66:I-$A^{b}$-specific T cells could still be detected in both groups (Figure 4.4E and F). GC-Tfh cells seeded the secondary lymphoid tissues at about 10% the efficiency of the Tfh cells, perhaps as a consequence of sorting $CCR7^{-}$ cells. However, the GC-Tfh cells that seeded the secondary lymphoid tissues survived over the following 27 days to the same degree as the transferred Tfh cells (Figure 4.4F). Importantly, GC-Tfh cells lost PD-1 expression and resembled the Tfh cells at the end of the 27 day transfer period (Figure 4.4G and H). These results demonstrate that Tfh cells and GC-Tfh cells produce phenotypically similar memory cells.

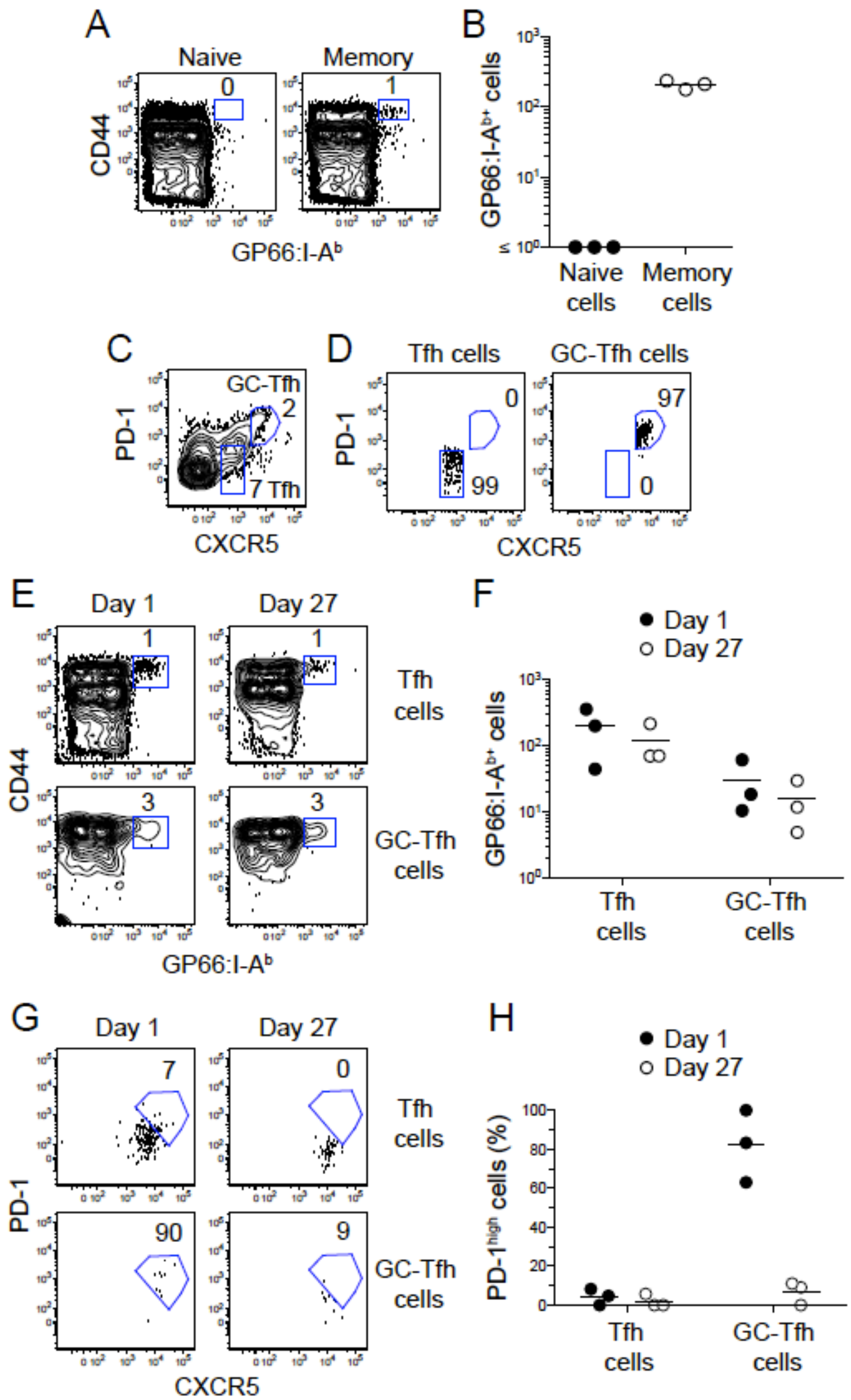


**Figure 4.4. GC-Tfh Cells Can Enter the Memory Pool.** (A – B) CD4$^+$ T cells from the spleen and lymph nodes of uninfected CD45.1$^+$ mice or CD45.1$^+$ mice that were infected with LCMV 82

days earlier were transferred into uninfected B6 mice. A day after transfer, $CD45.1^+$ cells in the spleen and lymph nodes of the recipient mice were enriched with CD45.1 antibody. (A) Plots of GP66:I-$A^b$ tetramer versus CD44 staining on enriched $CD4^+$ T cells. (B) Enumeration of donor-derived GP66:I-$A^{b+}$ $CD44^{high}$ cells. (C – H) $CD4^+$ Tfh and GC-Tfh cells were sort purified from the spleen and lymph nodes of $CD45.1^+$ mice 12 or 13 days after LCMV infection and samples containing 37,000 GP66:I-$A^{b+}$ T cells were transferred i.v. into uninfected B6 recipients. (C) Gating strategy used for sorting Tfh and GC-Tfh cells. (D) Post sort analysis of the indicated populations. (E) Identification of GP66:I-$A^{b+}$ T cells within transferred $CD45.1^+$ $CD4^+$ T cells. (F) Enumeration of transferred GP66:I-$A^{b+}$ T cells 1 or 27 days after transfer. (G) Phenotype of transferred GP66:I-$A^{b+}$ T cells. (E and G) Plots of two concatenated samples for each transferred population are shown for days 1 and 27 after transfer. (H) Percent of PD-$1^{high}$ GP66:I-$A^{b+}$ Tfh or GC-Tfh cells 1 or 27 days after transfer. Each symbol represents an individual mouse. Pooled data from two experiments are shown.

**Secondary Response Potential of Memory Cells Derived from Tfh Cells or GC-Tfh Cells**

We then sought to determine if the memory cells derived from Tfh cells or GC-Tfh cells differed in their secondary response potential. To address this point, we rechallenged mice containing transferred Tfh-, or GC-Tfh-derived memory,cells with LCMV Armstrong. Seven days after infection, expanded populations of donor-derived and recipient GP66:I-$A^b$-specific T cells could be detected in the spleen and lymph nodes (Figure 4.5A). As expected, the naive GP66:I-$A^b$-specific T cells of recipient origin in both transfer groups generated Th1 effector cells, Tfh cells, and GC-Tfh cells (Figure 4.5A – D). Both Tfh - and GC-Tfh -derived memory cells produced Th1 cells, Tfh cells, and GC-Tfh cells (Figure 4.5A – D), and thus behaved like Tcm cells. The Th1, Tfh, and GC-Tfh effector cell progeny derived from the recipient's naive cells or Tfh or GC-Tfh memory cells showed similar graded expression of T-bet with Th1 effector cells expressing the most and GC-Tfh cells expression the least (Figure 4.5E). Thus, the effector cells derived from the memory populations were qualitatively similar to those generated in a primary response. However, GC-Tfh-derived memory cells generated more Tfh and GC-Tfh effector cells than Tfh cell-derived memory cells and fewer Th1 effector cells (Figure 4.5A – D).

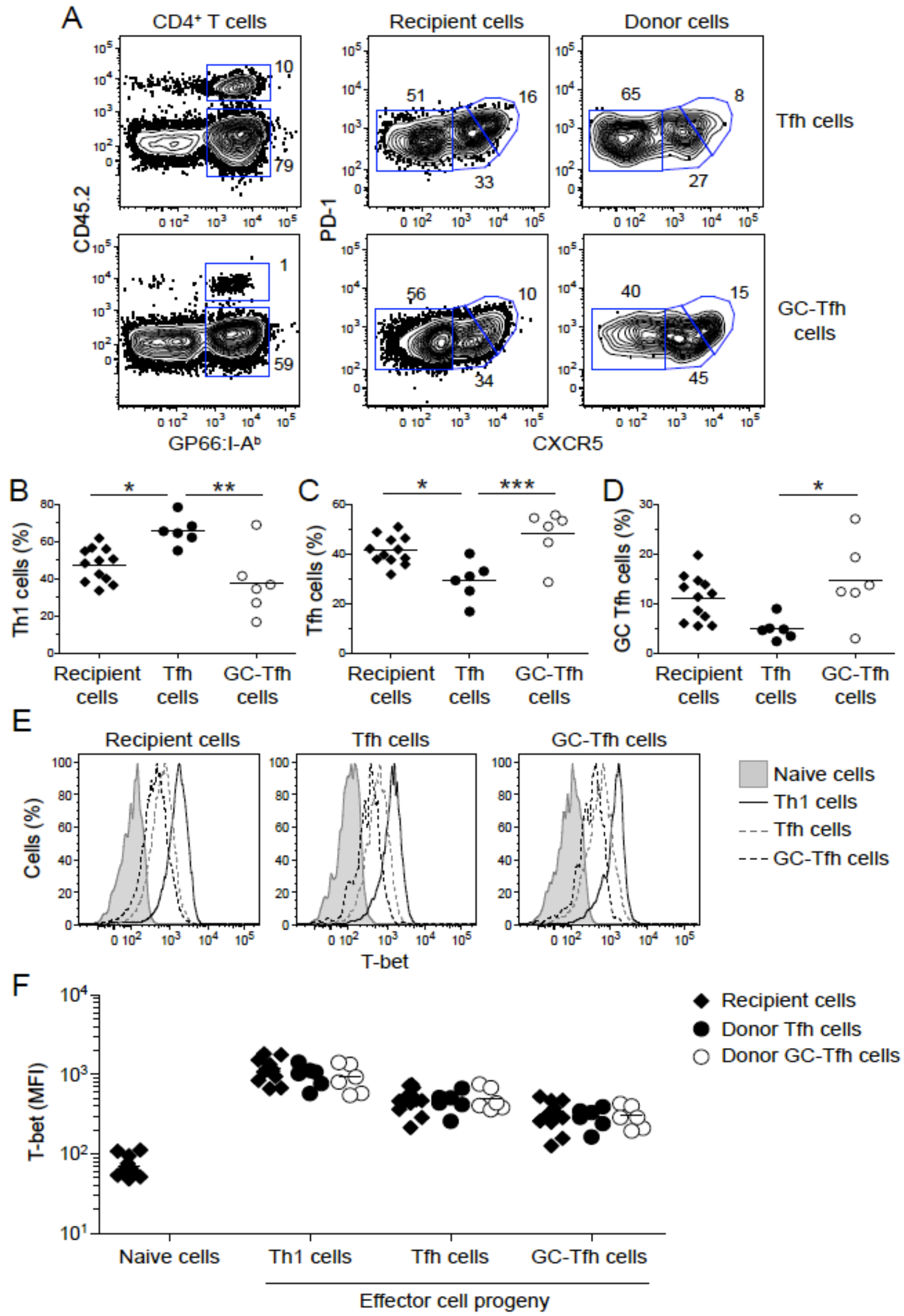


**Figure 4.5. Secondary Responses of Memory Cells Derived from Tfh Cells or GC-Tfh Cells.**

Twenty-eight days after transfer, corresponding to 40 days after infection, memory cells derived from Tfh cells or GC-Tfh cells were challenged with LCMV. (A) Gating strategy to identify $CD45.2^-$ recipient and $CD45.2^+$ donor GP66:I-$A^{b+}$ T cells (left), and Th1/Tfh/GC-Tfh subsets within GP66:I-$A^{b+}$ T cells present 7 days after LCMV challenge (right). Percentages of (B) Th1 cells, (C) Tfh cells, and (D) GC-Tfh cells within recipient or donor GP66:I-$A^{b+}$ T cell populations. (E) Histograms of T-bet expression in $CD44^{low}$ GP66:I-$A^{b-}$ naive $CD4^+$ T cells and GP66:I-$A^{b+}$ Th1 cells, Tfh cells, and GC-Tfh cells derived from the recipients' naive cells or the transferred Tfh or GC-Tfh cells. (F) MFI of T-bet expression in recipient and donor $CD4^+$ T cells. Each symbol represents an individual mouse, and horizontal lines indicate mean values. One-way ANOVA with Bonferroni post-test was used to determine statistical significance ($p <$ 0.01, **; $p < 0.001$, ***). Pooled data from two experiments are shown.

## 4.4 Discussion

The results presented here clarify the precursor-product relationship between $CXCR5^+$ effector cell subsets and Tcm cells by showing that both Tfh and GC-Tfh effector cell populations generate cells that become Tcm cells. The GC-Tfh effector cells that do so lose PD-1 and thus become indistinguishable from Tfh-derived Tcm cells. This conclusion is supported by the recent work of Nutt and colleagues showing that the GC-Tfh effector cells marked by expression of IL-21 become PD-$1^-$ memory cells (Luthje et al., 2012). Although both $CXCR5^+$ populations contribute cells to the Tcm pool, it is likely that Tfh effector cells contribute more since they outnumber GC-Tfh effector cells about 5 to 1 at the peak of the response.

Another important conclusion of our study is that GC-Tfh-derived memory cells are better at generating $CXCR5^+$ effector cells than Tfh-derived memory cells. This advantage might relate to a more advanced stage of differentiation. Recent studies suggest that GC-Tfh cells rely more heavily on Bcl6, ICOS, SAP, and p:MHCII presentation by B cell than Tfh cells (Baumjohann et al., 2011; Choi et al., 2011; Goenka et al., 2011; Pepper et al., 2011; Yusuf et al., 2010), supporting the idea that GC-Tfh cells constitute a more differentiated subset within a developmental continuum of Tfh cells (Crotty, 2011). GC-Tfh cells may garner higher amounts of ICOS by receiving stronger signals through their TCRs, which have been shown to have higher affinities for p:MHCII ligands than other T cells in the population (Fazilleau et al., 2009). In addition, the lower expression of T-bet by GC-Tfh cell-derived Tcm cells might preclude them from efficiently generating Th1 effector cells by limiting their capacity to repress Bcl-6 (Nakayamada et al., 2011; Oestreich et al., 2012). The fact that GC-Tfh effector cells produce memory cells that are poised to produce more GC-Tfh effector cells indicates that vaccines that rely on T cell-dependent antibodies should aim to generate this T cell subset.

# Chapter 5:

# Conclusions

## 5.1 Summary

Our *in vivo* experiments tracking antigen-specific CD4$^+$ T cells in gene-targeted mice during the course of Lm infection show that CD28, ICOS, IL-2R signals control different aspects of helper T cell memory formation, and suggest the following model (Figure 5.1). Naive p:MHCII-specific CD4$^+$ T cells begin to expand upon encountering DC in T cell areas displaying cognate pMHCII and high-levels of CD80 and CD86. While CD28 signaling is not necessary for initial expansion, its engagement enhances TCR-induced NFκB activation, which sustains clonal expansion by inducing the expression of genes that promote cell cycle progression and survival. While the cytoplasmic tail of CD28 was necessary for this effect, neither the often-studied YMNM nor PYAP motifs were required. Since both DC and B cells express CD80 and CD86 (Jenkins et al., 2001), it is likely that CD28 signaling will be engaged every time a T cell encounters cognate pMHCII displayed by these APCs. This suggests that CD28 might amplify NFκB signaling throughout the extent of the expansion phase but not during the contraction or memory phases. Once antigen is cleared, most effector T cells will die during the contraction phase and about 10% will persist as memory cells. Importantly, the number of memory cells that is generated whether in the presence or absence of CD28 signaling proportional to the number of effector cells at the peak of the response, indicating that CD28 is dispensable for establishing memory cell survival gene expression program or overcoming clonal anergy in the context of an immune response to infection. Future structure-function studies should identify the critical motif on the tail of CD28 responsible for regulating clonal expansion *in vivo* and engaging the NFκB pathway.

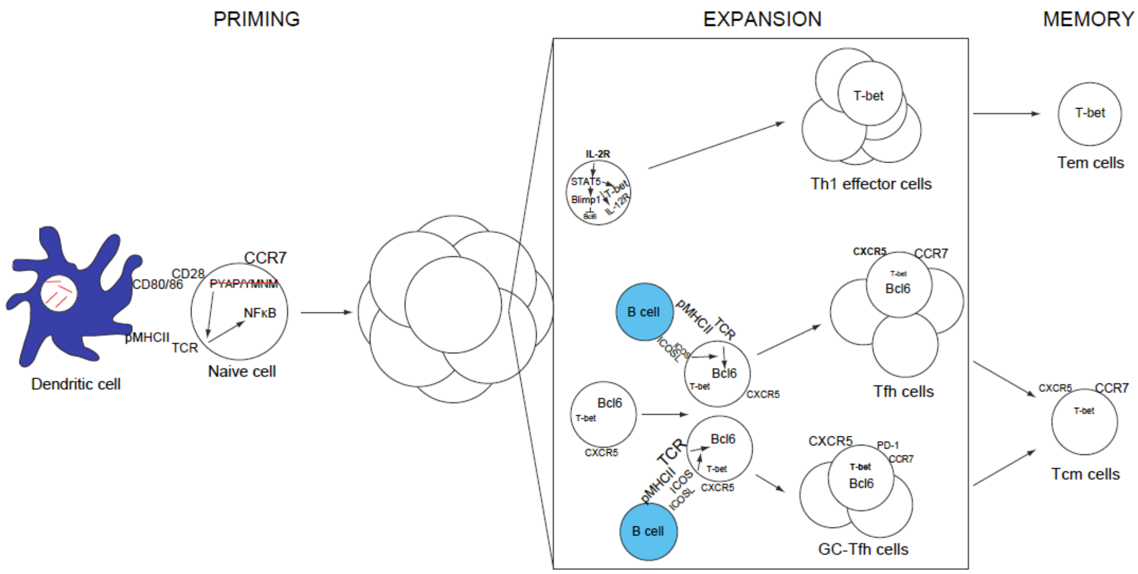


**Figure 5.1. Model of CD28, ICOS, and IL-2R Function in Helper T Cell Memory Formation.** Naive $CD4^+$ T cells specific for a pathogen-derived peptide bound to MHCII expand clonally upon encountering DC displaying the relevant p:MHCII and CD80/CD86 molecules. CD28 signaling enhances expansion by amplifying TCR-induced NFκB activation independently of its PYAP and YMNM motifs. During the expansion phase, IL-2R signaling promotes Th1 effector cell differentiation and inhibits Tfh cell differentiation. Conversely, ICOSL expression by B cells supports Bcl-6-dependent Tfh and GC-Tfh cell differentiation. A few Th1 effector cells survive the contraction phase, producing Tem cells. In contrast, the few Tfh cells and GC-Tfh cells that survive the contraction phase persist as Tcm cells.

TCR plus costimulation then induces the expression of ICOS, CD25, and IL-2, which exert their effects on T cell differentiation throughout the week following initial pMHCII encounter. In contrast to CD28, these molecules do not act as global regulators of $CD4^+$ effector T cell expansion; CD28-deficient T cells in competitive chimeras with normal T cells showed a 50-fold expansion defect, while ICOS- or CD25-deficient cells showed less than a 3-fold defect in expansion. Instead, the major functions of ICOS and IL-2R signaling appear to be to support Bcl6 or Blimp-1/T-bet differentiation programs, respectively. Choi et al. and our work show that two molecularly distinct populations of effector cells emerge within the first 3 days of infection. One expresses Bcl6, CXCR5, and low levels of T-bet while the other one expresses Blimp-1, CD25, and higher levels of T-bet (Choi et al., 2011; Pepper et al., 2011). Sequential ICOS stimulation by ICOSL-expressing DC and B cells, once primed T cells migrate to the T-B border, likely enhances Bcl6 expression on the early $CXCR5^+$ Tfh cells, thus repressing Blimp-1 (Johnston et al., 2009). Alternatively, ICOS supports TCR-driven survival or proliferation of Tfh cells. Future biochemical studies should help resolve this controversy. Regardless of the specific mechanism, ICOS signaling cements Tfh cell fate. The observation that effector cells in the earliest stages of priming express some Bcl6 suggests that Bcl6 induction might constitute a "default" process initiated by TCR signaling plus an early wave of IL-12-induced STAT4 signaling (Baumjohann et al., 2011; Choi et al., 2011; Goenka et al., 2011; Kerfoot et al., 2011; Nakayamada et al., 2011). Tfh cells with the highest affinity TCR might outcompete the lower affinity clones for B cells presenting cognate pMHCII (Fazilleau et al., 2009), thus receiving sustained TCR signaling plus ICOS costimulation, which drive full polarization of these Tfh cells into IL-21-secreting $Bcl6^{high}$ $CXCR5^{high}$ $PD\text{-}1^{high}$ GC-Tfh cells (Deenick et al., 2010; Luthje et al., 2012; Yusuf et al., 2010). Fully differentiated GC-Tfh cells then help cognate B cells undergo somatic hypermutation and class switch recombination in germinal centers (Crotty, 2011). Within the following 2 – 4 weeks as antigen is cleared, most Tfh and GC-Tfh cells undergo apoptosis but a few will persist as Tcm cells, losing expression of Bcl6 and PD-1 (Kitano et al., 2011). The fact that Tfh cells are more numerous than GC-Tfh cells suggests that Tfh cells are the major Tcm precursor cell population. Importantly, however, GC-Tfh cell-derived Tcm cells have a greater capacity to produce $CXCR5^{+}$ effector cells upon secondary challenge than Tfh cell-derived Tcm cells, suggesting that more differentiated status of GC-Tfh cells compared to Tfh cells makes them more resistant to Th1-inducing signals during secondary challenge. In contrast to ICOS and Bcl6, IL-2 signaling in $CXCR5^{-}$ early effector cells promotes Th1 effector cell differentiation by simultaneously inducing Th1-specific genes in a STAT5-dependent manner and repressing the Bcl6 that was expressed early in the priming phase (Ballesteros-Tato et al., 2012; Johnston et al., 2012; Liao et al., 2011; Nakayamada et al., 2011; Nurieva et al., 2012; Oestreich et al., 2012; Pepper et al., 2011). Nonetheless, whether other signals emanating from the IL-2R besides STAT5 activation (i.e., PI3K and MAPK signals) participate in Th1 differentiation *in vivo* remains unclear. Once antigen is cleared, some of these Th1 effector cells persist as Tem cells. Thus, ICOS and IL-2R signals elaborate two distinct effector differentiation programs that are initiated early in the expansion phase and that produce two unique memory cell populations.

## 5.2 Therapeutic Implications

The observation that CD28 and ICOS control different aspects of helper T cell priming suggest that novel clinical interventions targeting ICOS signaling or both CD28 and ICOS pathways might be beneficial in the treatment of T-dependent antibody-mediated autoimmune diseases like rheumatoid arthritis. While blockade of CD28 signaling with a CTLA-4 receptor-immunoglobulin fusion protein (CTLA-4:Ig, abatacept) is often a safe and effective treatment for severe rheumatoid arthritis, it did increase the incidence of serious bacterial infections in patients receiving CTLA-4:Ig plus other anti-rheumatic therapies compared to patients receiving therapies other than CTLA-4:Ig (Weinblatt et al., 2006). ICOS receptor-immunoglobulin fusion proteins (ICOS:Ig) or ICOSL blocking antibodies (Iwai et al., 2002) might therefore constitute an alternative treatment approach for preventing T-dependent antibody responses without inducing the massive T cell immunosuppression that CTLA-4:Ig might produce in humans. Nonetheless, since CD28 is not strictly required for ICOS expression and these two pathways are not fully redundant (Linterman et al., 2009; Suh et al., 2004), combination therapies that block CD28 and ICOS signaling pathways might be viable alternatives for patients that do not respond favorably to CTLA-4:Ig treatment alone since it would both target clonal expansion and Tfh cell formation.

The conclusion that ICOS and IL-2R signaling affect distinct aspects of T cell differentiation and subsequent memory formation also bring to light implications for vaccine design. To enhance GC-Tfh formation and T-dependent antibody-mediated immunity, such as when aiming to produce neutralizing antibodies to a virus or a bacterial toxin with a subunit vaccine, antigen could be targeted to B cells with CD19-specific antibodies (Yan et al., 2005) and neutralizing antibodies against IL-2 (Boyman and Sprent, 2012) could be used concurrently to inhibit Th1 differentiation. Since GC-Tfh cells can produce Tcm cells that preferentially differentiate into Tfh cells and GC-Tfh cells upon secondary challenge, this immunization regimen should be compatible with vaccine boosting strategies. In contrast, immunization against intracellular pathogens like *M. tuberculosis* should aim to minimize Tfh cell development and instead promote robust Th1 effector and Tem cell generation. This goal could be achieved by combining strategies targeting antigen to dendritic cells (Trumpfheller et al., 2012), stimulating IL-2R signaling in effector $CD4^+$ T cells, and blocking ICOS signaling.

## References


Acuto, O., and Michel, F. (2003). CD28-mediated co-stimulation: a quantitative support for TCR signalling. Nat Rev Immunol *3*, 939-951.

Ahmed, R., and Gray, D. (1996). Immunological memory and protective immunity: understanding their relation. Science *272*, 54-60.

Akbar, A.N., Borthwick, N.J., Wickremasinghe, R.G., Panayoitidis, P., Pilling, D., Bofill, M., Krajewski, S., Reed, J.C., and Salmon, M. (1996). Interleukin-2 receptor common gamma-chain signaling cytokines regulate activated T cell apoptosis in response to growth factor withdrawal: selective induction of anti-apoptotic (bcl-2, bcl-xL) but not pro-apoptotic (bax, bcl-xS) gene expression. Eur J Immunol *26*, 294-299.

Akiba, H., Takeda, K., Kojima, Y., Usui, Y., Harada, N., Yamazaki, T., Ma, J., Tezuka, K., Yagita, H., and Okumura, K. (2005). The role of ICOS in the CXCR5+ follicular B helper T cell maintenance in vivo. J Immunol *175*, 2340-2348.

Andersen, P., and Smedegaard, B. (2000). CD4(+) T-cell subsets that mediate immunological memory to Mycobacterium tuberculosis infection in mice. Infect Immun *68*, 621-629.

Anthony, R.M., Urban, J.F., Jr., Alem, F., Hamed, H.A., Rozo, C.T., Boucher, J.L., Van Rooijen, N., and Gause, W.C. (2006). Memory T(H)2 cells induce alternatively activated macrophages to mediate protection against nematode parasites. Nat Med *12*, 955-960.

Appleman, L.J., van Puijenbroek, A.A., Shu, K.M., Nadler, L.M., and Boussiotis, V.A. (2002). CD28 costimulation mediates down-regulation of p27kip1 and cell cycle progression by activation of the PI3K/PKB signaling pathway in primary human T cells. J Immunol *168*, 2729-2736.

Araki, K., Turner, A.P., Shaffer, V.O., Gangappa, S., Keller, S.A., Bachmann, M.F., Larsen, C.P., and Ahmed, R. (2009). mTOR regulates memory CD8 T-cell differentiation. Nature *460*, 108-112.

Arimura, Y., Kato, H., Dianzani, U., Okamoto, T., Kamekura, S., Buonfiglio, D., Miyoshi-Akiyama, T., Uchiyama, T., and Yagi, J. (2002). A co-stimulatory molecule on activated T cells, H4/ICOS, delivers specific signals in T(h) cells and regulates their responses. Int Immunol *14*, 555-566.

Badovinac, V.P., Haring, J.S., and Harty, J.T. (2007). Initial T cell receptor transgenic cell precursor frequency dictates critical aspects of the CD8(+) T cell response to infection. Immunity *26*, 827-841.

Ballesteros-Tato, A., Leon, B., Graf, B.A., Moquin, A., Adams, P.S., Lund, F.E., and Randall, T.D. (2012). Interleukin-2 inhibits germinal center formation by limiting T follicular helper cell differentiation. Immunity *36*, 847-856.

Baumjohann, D., Okada, T., and Ansel, K.M. (2011). Cutting Edge: Distinct waves of BCL6 expression during T follicular helper cell development. J Immunol *187*, 2089-2092.

Belkaid, Y., Piccirillo, C.A., Mendez, S., Shevach, E.M., and Sacks, D.L. (2002). CD4+CD25+ regulatory T cells control Leishmania major persistence and immunity. Nature *420*, 502-507.

Belkaid, Y., and Tarbell, K. (2009). Regulatory T cells in the control of host-microorganism interactions (*). Annu Rev Immunol *27*, 551-589.

Boehm, T. (2011). Design principles of adaptive immune systems. Nat Rev Immunol *11*, 307-317.

Boise, L.H., Minn, A.J., Noel, P.J., June, C.H., Accavitti, M.A., Lindsten, T., and Thompson, C.B. (1995). CD28 costimulation can promote T cell survival by enhancing the expression of Bcl-XL. Immunity *3*, 87-98.

Bonnevier, J.L., and Mueller, D.L. (2002). Cutting edge: B7/CD28 interactions regulate cell cycle progression independent of the strength of TCR signaling. J Immunol *169*, 6659-6663.

Bonnevier, J.L., Yarke, C.A., and Mueller, D.L. (2006). Sustained B7/CD28 interactions and resultant phosphatidylinositol 3-kinase activity maintain G1-->S phase transitions at an optimal rate. Eur J Immunol *36*, 1583-1597.

Bossaller, L., Burger, J., Draeger, R., Grimbacher, B., Knoth, R., Plebani, A., Durandy, A., Baumann, U., Schlesier, M., Welcher, A.A.*, et al.* (2006). ICOS deficiency is associated with a severe reduction of CXCR5+CD4 germinal center Th cells. J Immunol *177*, 4927-4932.

Boulougouris, G., McLeod, J.D., Patel, Y.I., Ellwood, C.N., Walker, L.S., and Sansom, D.M. (1999). IL-2-independent activation and proliferation in human T cells induced by CD28. J Immunol *163*, 1809-1816.

Boyman, O., and Sprent, J. (2012). The role of interleukin-2 during homeostasis and activation of the immune system. Nat Rev Immunol *12*, 180-190.

Brennan, P., Babbage, J.W., Burgering, B.M., Groner, B., Reif, K., and Cantrell, D.A. (1997). Phosphatidylinositol 3-kinase couples the interleukin-2 receptor to the cell cycle regulator E2F. Immunity *7*, 679-689.

Burnet, F.M. (1959). The Clonal Selection Theory of Acquired Immunity (Cambridge, UK: Cambridge Univ. Press).

Burr, J.S., Savage, N.D., Messah, G.E., Kimzey, S.L., Shaw, A.S., Arch, R.H., and Green, J.M. (2001). Cutting edge: distinct motifs within CD28 regulate T cell proliferation and induction of Bcl-XL. J Immunol *166*, 5331-5335.

Carreno, B.M., and Collins, M. (2002). The B7 family of ligands and its receptors: new pathways for costimulation and inhibition of immune responses. Annu Rev Immunol *20*, 29-53.

Catron, D.M., Itano, A.A., Pape, K.A., Mueller, D.L., and Jenkins, M.K. (2004). Visualizing the first 50 hr of the primary immune response to a soluble antigen. Immunity *21*, 341-347.

Catron, D.M., Rusch, L.K., Hataye, J., Itano, A.A., and Jenkins, M.K. (2006). CD4+ T cells that enter the draining lymph nodes after antigen injection participate in the primary response and become central-memory cells. J Exp Med *203*, 1045-1054.

Chang, J.T., Palanivel, V.R., Kinjyo, I., Schambach, F., Intlekofer, A.M., Banerjee, A., Longworth, S.A., Vinup, K.E., Mrass, P., Oliaro, J*., et al.* (2007). Asymmetric T lymphocyte division in the initiation of adaptive immune responses. Science *315*, 1687-1691.

Chen, C., Edelstein, L.C., and Gelinas, C. (2000). The Rel/NF-kappaB family directly activates expression of the apoptosis inhibitor Bcl-x(L). Mol Cell Biol *20*, 2687-2695.

Chevalier, N., Jarrossay, D., Ho, E., Avery, D.T., Ma, C.S., Yu, D., Sallusto, F., Tangye, S.G., and Mackay, C.R. (2011). CXCR5 expressing human central memory CD4 T cells and their relevance for humoral immune responses. J Immunol *186*, 5556-5568.

Choi, Y.S., Kageyama, R., Eto, D., Escobar, T.C., Johnston, R.J., Monticelli, L., Lao, C., and Crotty, S. (2011). ICOS receptor instructs T follicular helper cell versus effector cell differentiation via induction of the transcriptional repressor Bcl6. Immunity *34*, 932-946.

Christensen, J.E., Christensen, J.P., Kristensen, N.N., Hansen, N.J., Stryhn, A., and Thomsen, A.R. (2002). Role of CD28 co-stimulation in generation and maintenance of virus-specific T cells. Int Immunol *14*, 701-711.

Cosma, C.L., Sherman, D.R., and Ramakrishnan, L. (2003). The secret lives of the pathogenic mycobacteria. Annu Rev Microbiol *57*, 641-676.

Costello, R., Cerdan, C., Lipcey, C., Algarte, M., Martin, Y., Baeuerle, P.A., Olive, D., and Imbert, J. (1993). The role of NF-kappa B1 (p50/p105) gene expression in activation of human blood T-lymphocytes via CD2 and CD28 adhesion molecules. Cell Growth Differ *4*, 947-954.

Coyle, A.J., Lehar, S., Lloyd, C., Tian, J., Delaney, T., Manning, S., Nguyen, T., Burwell, T., Schneider, H., Gonzalo, J.A*., et al.* (2000). The CD28-related molecule ICOS is required for effective T cell-dependent immune responses. Immunity *13*, 95-105.

Crotty, S. (2011). Follicular helper CD4 T cells (TFH). Annu Rev Immunol *29*, 621-663.

Cunningham, A.F., Gaspal, F., Serre, K., Mohr, E., Henderson, I.R., Scott-Tucker, A., Kenny, S.M., Khan, M., Toellner, K.M., Lane, P.J., and MacLennan, I.C. (2007). Salmonella induces a switched antibody response without germinal centers that impedes the extracellular spread of infection. J Immunol *178*, 6200-6207.

Dahl, A.M., Klein, C., Andres, P.G., London, C.A., Lodge, M.P., Mulligan, R.C., and Abbas, A.K. (2000). Expression of bcl-X(L) restores cell survival, but not proliferation off effector differentiation, in CD28-deficient T lymphocytes. J Exp Med *191*, 2031-2038.

De Smedt, T., Pajak, B., Muraille, E., Lespagnard, L., Heinen, E., De Baetselier, P., Urbain, J., Leo, O., and Moser, M. (1996). Regulation of dendritic cell numbers and maturation by lipopolysaccharide in vivo. J Exp Med *184*, 1413-1424.

Deenick, E.K., Chan, A., Ma, C.S., Gatto, D., Schwartzberg, P.L., Brink, R., and Tangye, S.G. (2010). Follicular helper T cell differentiation requires continuous antigen presentation that is independent of unique B cell signaling. Immunity *33*, 241-253.

Dent, A.L., Shaffer, A.L., Yu, X., Allman, D., and Staudt, L.M. (1997). Control of inflammation, cytokine expression, and germinal center formation by BCL-6. Science *276*, 589-592.

Dodson, L.F., Boomer, J.S., Deppong, C.M., Shah, D.D., Sim, J., Bricker, T.L., Russell, J.H., and Green, J.M. (2009). Targeted knock-in mice expressing mutations of CD28 reveal an essential pathway for costimulation. Mol Cell Biol *29*, 3710-3721.

Dooms, H., Wolslegel, K., Lin, P., and Abbas, A.K. (2007). Interleukin-2 enhances CD4+ T cell memory by promoting the generation of IL-7R alpha-expressing cells. J Exp Med *204*, 547-557.

Edinger, A.L., and Thompson, C.B. (2002). Akt maintains cell size and survival by increasing mTOR-dependent nutrient uptake. Mol Biol Cell *13*, 2276-2288.

Egawa, T., Albrecht, B., Favier, B., Sunshine, M.J., Mirchandani, K., O'Brien, W., Thome, M., and Littman, D.R. (2003). Requirement for CARMA1 in antigen receptor-induced NF-kappa B activation and lymphocyte proliferation. Curr Biol *13*, 1252-1258.

Ertelt, J.M., Rowe, J.H., Johanns, T.M., Lai, J.C., McLachlan, J.B., and Way, S.S. (2009). Selective priming and expansion of antigen-specific Foxp3- CD4+ T cells during Listeria monocytogenes infection. J Immunol *182*, 3032-3038.

Fazilleau, N., McHeyzer-Williams, L.J., Rosen, H., and McHeyzer-Williams, M.G. (2009). The function of follicular helper T cells is regulated by the strength of T cell antigen receptor binding. Nat Immunol *10*, 375-384.

Ferguson, S.E., Han, S., Kelsoe, G., and Thompson, C.B. (1996). CD28 is required for germinal center formation. J Immunol *156*, 4576-4581.

Fos, C., Salles, A., Lang, V., Carrette, F., Audebert, S., Pastor, S., Ghiotto, M., Olive, D., Bismuth, G., and Nunes, J.A. (2008). ICOS ligation recruits the p50alpha PI3K regulatory subunit to the immunological synapse. J Immunol *181*, 1969-1977.

Frauwirth, K.A., Riley, J.L., Harris, M.H., Parry, R.V., Rathmell, J.C., Plas, D.R., Elstrom, R.L., June, C.H., and Thompson, C.B. (2002). The CD28 signaling pathway regulates glucose metabolism. Immunity *16*, 769-777.

Friend, L.D., Shah, D.D., Deppong, C., Lin, J., Bricker, T.L., Juehne, T.I., Rose, C.M., and Green, J.M. (2006). A dose-dependent requirement for the proline motif of CD28 in cellular and humoral immunity revealed by a targeted knockin mutant. J Exp Med *203*, 2121-2133.

Fuse, S., Zhang, W., and Usherwood, E.J. (2008). Control of memory CD8+ T cell differentiation by CD80/CD86-CD28 costimulation and restoration by IL-2 during the recall response. J Immunol *180*, 1148-1157.

Gaffen, S.L. (2001). Signaling domains of the interleukin 2 receptor. Cytokine *14*, 63-77.

Garcia, Z., Pradelli, E., Celli, S., Beuneu, H., Simon, A., and Bousso, P. (2007). Competition for antigen determines the stability of T cell-dendritic cell interactions during clonal expansion. Proc Natl Acad Sci U S A *104*, 4553-4558.

Garcon, F., Patton, D.T., Emery, J.L., Hirsch, E., Rottapel, R., Sasaki, T., and Okkenhaug, K. (2008). CD28 provides T-cell costimulation and enhances PI3K activity at the immune synapse independently of its capacity to interact with the p85/p110 heterodimer. Blood *111*, 1464-1471.

Geginat, G., Schenk, S., Skoberne, M., Goebel, W., and Hof, H. (2001). A novel approach of direct ex vivo epitope mapping identifies dominant and subdominant CD4 and CD8 T cell epitopes from Listeria monocytogenes. J Immunol *166*, 1877-1884.

Ghosh, P., Tan, T.H., Rice, N.R., Sica, A., and Young, H.A. (1993). The interleukin 2 CD28-responsive complex contains at least three members of the NF kappa B family: c-Rel, p50, and p65. Proc Natl Acad Sci U S A *90*, 1696-1700.

Gigoux, M., Shang, J., Pak, Y., Xu, M., Choe, J., Mak, T.W., and Suh, W.K. (2009). Inducible costimulator promotes helper T-cell differentiation through phosphoinositide 3-kinase. Proc Natl Acad Sci U S A *106*, 20371-20376.

Goenka, R., Barnett, L.G., Silver, J.S., O'Neill, P.J., Hunter, C.A., Cancro, M.P., and Laufer, T.M. (2011). Cutting edge: dendritic cell-restricted antigen presentation initiates the follicular helper T cell program but cannot complete ultimate effector differentiation. J Immunol *187*, 1091-1095.

Gong, D., and Malek, T.R. (2007). Cytokine-dependent Blimp-1 expression in activated T cells inhibits IL-2 production. J Immunol *178*, 242-252.

Gonzalez, S.F., Degn, S.E., Pitcher, L.A., Woodruff, M., Heesters, B.A., and Carroll, M.C. (2011). Trafficking of B cell antigen in lymph nodes. Annu Rev Immunol *29*, 215-233.

Gonzalo, J.A., Delaney, T., Corcoran, J., Goodearl, A., Gutierrez-Ramos, J.C., and Coyle, A.J. (2001). Cutting edge: the related molecules CD28 and inducible costimulator deliver both unique and complementary signals required for optimal T cell activation. J Immunol *166*, 1-5.

Greenwald, R.J., Freeman, G.J., and Sharpe, A.H. (2005). The B7 family revisited. Annu Rev Immunol *23*, 515-548.

Grimbacher, B., Hutloff, A., Schlesier, M., Glocker, E., Warnatz, K., Drager, R., Eibel, H., Fischer, B., Schaffer, A.A., Mages, H.W.*, et al.* (2003). Homozygous loss of ICOS is associated with adult-onset common variable immunodeficiency. Nat Immunol *4*, 261-268.

Gudmundsdottir, H., Wells, A.D., and Turka, L.A. (1999). Dynamics and requirements of T cell clonal expansion in vivo at the single-cell level: effector function is linked to proliferative capacity. J Immunol *162*, 5212-5223.

Harada, Y., Ohgai, D., Watanabe, R., Okano, K., Koiwai, O., Tanabe, K., Toma, H., Altman, A., and Abe, R. (2003). A single amino acid alteration in cytoplasmic domain determines IL-2 promoter activation by ligation of CD28 but not inducible costimulator (ICOS). J Exp Med *197*, 257-262.

Harada, Y., Tokushima, M., Matsumoto, Y., Ogawa, S., Otsuka, M., Hayashi, K., Weiss, B.D., June, C.H., and Abe, R. (2001). Critical requirement for the membrane-proximal cytosolic tyrosine residue for CD28-mediated costimulation in vivo. J Immunol *166*, 3797-3803.

Harding, F.A., McArthur, J.G., Gross, J.A., Raulet, D.H., and Allison, J.P. (1992). CD28-mediated signalling co-stimulates murine T cells and prevents induction of anergy in T-cell clones. Nature *356*, 607-609.

Harhaj, E.W., Maggirwar, S.B., Good, L., and Sun, S.C. (1996). CD28 mediates a potent costimulatory signal for rapid degradation of IkappaBbeta which is associated with accelerated activation of various NF-kappaB/Rel heterodimers. Mol Cell Biol *16*, 6736-6743.

Harrington, L.E., Janowski, K.M., Oliver, J.R., Zajac, A.J., and Weaver, C.T. (2008). Memory CD4 T cells emerge from effector T-cell progenitors. Nature *452*, 356-360.

Hataye, J., Moon, J.J., Khoruts, A., Reilly, C., and Jenkins, M.K. (2006). Naive and memory CD4+ T cell survival controlled by clonal abundance. Science *312*, 114-116.

Hogquist, K.A., Baldwin, T.A., and Jameson, S.C. (2005). Central tolerance: learning self-control in the thymus. Nat Rev Immunol *5*, 772-782.

Holdorf, A.D., Lee, K.H., Burack, W.R., Allen, P.M., and Shaw, A.S. (2002). Regulation of Lck activity by CD4 and CD28 in the immunological synapse. Nat Immunol *3*, 259-264.

Homann, D., Teyton, L., and Oldstone, M.B. (2001). Differential regulation of antiviral T-cell immunity results in stable CD8+ but declining CD4+ T-cell memory. Nat Med *7*, 913-919.

Hou, J., Schindler, U., Henzel, W.J., Wong, S.C., and McKnight, S.L. (1995). Identification and purification of human Stat proteins activated in response to interleukin-2. Immunity *2*, 321-329.

Hutloff, A., Dittrich, A.M., Beier, K.C., Eljaschewitsch, B., Kraft, R., Anagnostopoulos, I., and Kroczek, R.A. (1999). ICOS is an inducible T-cell co-stimulator structurally and functionally related to CD28. Nature *397*, 263-266.

Ichii, H., Sakamoto, A., Kuroda, Y., and Tokuhisa, T. (2004). Bcl6 acts as an amplifier for the generation and proliferative capacity of central memory CD8+ T cells. J Immunol *173*, 883-891.

Iezzi, G., Karjalainen, K., and Lanzavecchia, A. (1998). The duration of antigenic stimulation determines the fate of naive and effector T cells. Immunity *8*, 89-95.

Iwai, H., Kozono, Y., Hirose, S., Akiba, H., Yagita, H., Okumura, K., Kohsaka, H., Miyasaka, N., and Azuma, M. (2002). Amelioration of collagen-induced arthritis by blockade of inducible costimulator-B7 homologous protein costimulation. J Immunol *169*, 4332-4339.

Jameson, S.C., Hogquist, K.A., and Bevan, M.J. (1995). Positive selection of thymocytes. Annu Rev Immunol *13*, 93-126.

Janeway, C.A., Jr., and Medzhitov, R. (2002). Innate immune recognition. Annu Rev Immunol *20*, 197-216.

Jenkins, M.K., Chen, C.A., Jung, G., Mueller, D.L., and Schwartz, R.H. (1990). Inhibition of antigen-specific proliferation of type 1 murine T cell clones after stimulation with immobilized anti-CD3 monoclonal antibody. J Immunol *144*, 16-22.

Jenkins, M.K., Chu, H.H., McLachlan, J.B., and Moon, J.J. (2010). On the composition of the preimmune repertoire of T cells specific for Peptide-major histocompatibility complex ligands. Annu Rev Immunol *28*, 275-294.

Jenkins, M.K., Khoruts, A., Ingulli, E., Mueller, D.L., McSorley, S.J., Reinhardt, R.L., Itano, A., and Pape, K.A. (2001). In vivo activation of antigen-specific CD4 T cells. Annu Rev Immunol *19*, 23-45.

Johnston, R.J., Choi, Y.S., Diamond, J.A., Yang, J.A., and Crotty, S. (2012). STAT5 is a potent negative regulator of TFH cell differentiation. J Exp Med *209*, 243-250.

Johnston, R.J., Poholek, A.C., DiToro, D., Yusuf, I., Eto, D., Barnett, B., Dent, A.L., Craft, J., and Crotty, S. (2009). Bcl6 and Blimp-1 are reciprocal and antagonistic regulators of T follicular helper cell differentiation. Science *325*, 1006-1010.

Jones, R.G., Parsons, M., Bonnard, M., Chan, V.S., Yeh, W.C., Woodgett, J.R., and Ohashi, P.S. (2000). Protein kinase B regulates T lymphocyte survival, nuclear factor kappaB activation, and Bcl-X(L) levels in vivo. J Exp Med *191*, 1721-1734.

June, C.H., Ledbetter, J.A., Gillespie, M.M., Lindsten, T., and Thompson, C.B. (1987). T-cell proliferation involving the CD28 pathway is associated with cyclosporine-resistant interleukin 2 gene expression. Mol Cell Biol *7*, 4472-4481.

Jung, Y.J., Ryan, L., LaCourse, R., and North, R.J. (2005). Properties and protective value of the secondary versus primary T helper type 1 response to airborne Mycobacterium tuberculosis infection in mice. J Exp Med *201*, 1915-1924.

Kalia, V., Sarkar, S., Subramaniam, S., Haining, W.N., Smith, K.A., and Ahmed, R. (2010). Prolonged interleukin-2Ralpha expression on virus-specific CD8+ T cells favors terminal-effector differentiation in vivo. Immunity *32*, 91-103.

Kallies, A., Xin, A., Belz, G.T., and Nutt, S.L. (2009). Blimp-1 transcription factor is required for the differentiation of effector CD8(+) T cells and memory responses. Immunity *31*, 283-295.

Kaplan, D.H., Jenison, M.C., Saeland, S., Shlomchik, W.D., and Shlomchik, M.J. (2005). Epidermal langerhans cell-deficient mice develop enhanced contact hypersensitivity. Immunity *23*, 611-620.

Kearney, E.R., Pape, K.A., Loh, D.Y., and Jenkins, M.K. (1994). Visualization of peptide-specific T cell immunity and peripheral tolerance induction in vivo. Immunity *1*, 327-339.

Kearney, E.R., Walunas, T.L., Karr, R.W., Morton, P.A., Loh, D.Y., Bluestone, J.A., and Jenkins, M.K. (1995). Antigen-dependent clonal expansion of a trace population of antigen-specific CD4+ T cells in vivo is dependent on CD28 costimulation and inhibited by CTLA-4. J Immunol *155*, 1032-1036.

Kerfoot, S.M., Yaari, G., Patel, J.R., Johnson, K.L., Gonzalez, D.G., Kleinstein, S.H., and Haberman, A.M. (2011). Germinal center B cell and T follicular helper cell development initiates in the interfollicular zone. Immunity *34*, 947-960.

Khanna, K.M., and Lefrancois, L. (2008). Geography and plumbing control the T cell response to infection. Immunol Cell Biol *86*, 416-422.

Khoruts, A., Mondino, A., Pape, K.A., Reiner, S.L., and Jenkins, M.K. (1998). A natural immunological adjuvant enhances T cell clonal expansion through a CD28-dependent, interleukin (IL)-2-independent mechanism. J Exp Med *187*, 225-236.

Khoshnan, A., Tindell, C., Laux, I., Bae, D., Bennett, B., and Nel, A.E. (2000). The NF-kappa B cascade is important in Bcl-xL expression and for the anti-apoptotic effects of the CD28 receptor in primary human CD4+ lymphocytes. J Immunol *165*, 1743-1754.

Kitamura, D., Roes, J., Kuhn, R., and Rajewsky, K. (1991). A B cell-deficient mouse by targeted disruption of the membrane exon of the immunoglobulin mu chain gene. Nature *350*, 423-426.

Kitano, M., Moriyama, S., Ando, Y., Hikida, M., Mori, Y., Kurosaki, T., and Okada, T. (2011). Bcl6 protein expression shapes pre-germinal center B cell dynamics and follicular helper T cell heterogeneity. Immunity *34*, 961-972.

Klein, L., Hinterberger, M., Wirnsberger, G., and Kyewski, B. (2009). Antigen presentation in the thymus for positive selection and central tolerance induction. Nat Rev Immunol *9*, 833-844.

Kontgen, F., Grumont, R.J., Strasser, A., Metcalf, D., Li, R., Tarlinton, D., and Gerondakis, S. (1995). Mice lacking the c-rel proto-oncogene exhibit defects in lymphocyte proliferation, humoral immunity, and interleukin-2 expression. Genes Dev *9*, 1965-1977.

Lazarevic, V., and Glimcher, L.H. (2011). T-bet in disease. Nat Immunol *12*, 597-606.

Lee, S.K., Rigby, R.J., Zotos, D., Tsai, L.M., Kawamoto, S., Marshall, J.L., Ramiscal, R.R., Chan, T.D., Gatto, D., Brink, R., *et al.* (2011). B cell priming for extrafollicular antibody responses requires Bcl-6 expression by T cells. J Exp Med *208*, 1377-1388.

Li, Q.J., Chau, J., Ebert, P.J., Sylvester, G., Min, H., Liu, G., Braich, R., Manoharan, M., Soutschek, J., Skare, P., *et al.* (2007). miR-181a is an intrinsic modulator of T cell sensitivity and selection. Cell *129*, 147-161.

Liao, W., Lin, J.X., Wang, L., Li, P., and Leonard, W.J. (2011). Modulation of cytokine receptors by IL-2 broadly regulates differentiation into helper T cell lineages. Nat Immunol *12*, 551-559.

Lin, J.X., Migone, T.S., Tsang, M., Friedmann, M., Weatherbee, J.A., Zhou, L., Yamauchi, A., Bloom, E.T., Mietz, J., John, S., and et al. (1995). The role of shared receptor motifs and common Stat proteins in the generation of cytokine pleiotropy and redundancy by IL-2, IL-4, IL-7, IL-13, and IL-15. Immunity *2*, 331-339.

Lindstein, T., June, C.H., Ledbetter, J.A., Stella, G., and Thompson, C.B. (1989). Regulation of lymphokine messenger RNA stability by a surface-mediated T cell activation pathway. Science *244*, 339-343.

Linterman, M.A., Rigby, R.J., Wong, R., Silva, D., Withers, D., Anderson, G., Verma, N.K., Brink, R., Hutloff, A., Goodnow, C.C., and Vinuesa, C.G. (2009). Roquin differentiates the specialized functions of duplicated T cell costimulatory receptor genes CD28 and ICOS. Immunity *30*, 228-241.

Linton, P.J., Harbertson, J., and Bradley, L.M. (2000). A critical role for B cells in the development of memory CD4 cells. J. Immunol. *165*, 5558-5565.

Lio, C.W., Dodson, L.F., Deppong, C.M., Hsieh, C.S., and Green, J.M. (2010). CD28 facilitates the generation of Foxp3(-) cytokine responsive regulatory T cell precursors. J Immunol *184*, 6007-6013.

Lohning, M., Hegazy, A.N., Pinschewer, D.D., Busse, D., Lang, K.S., Hofer, T., Radbruch, A., Zinkernagel, R.M., and Hengartner, H. (2008). Long-lived virus-reactive memory T cells generated from purified cytokine-secreting T helper type 1 and type 2 effectors. J. Exp. Med. *205*, 53-61.

Love, P.E., and Bhandoola, A. (2011). Signal integration and crosstalk during thymocyte migration and emigration. Nat Rev Immunol *11*, 469-477.

Luthje, K., Kallies, A., Shimohakamada, Y., GT, T.B., Light, A., Tarlinton, D.M., and Nutt, S.L. (2012). The development and fate of follicular helper T cells defined by an IL-21 reporter mouse. Nat Immunol *13*, 491-498.

MacLeod, M.K., Clambey, E.T., Kappler, J.W., and Marrack, P. (2009). CD4 memory T cells: what are they and what can they do? Semin Immunol *21*, 53-61.

MacLeod, M.K., David, A., McKee, A.S., Crawford, F., Kappler, J.W., and Marrack, P. (2011). Memory CD4 T cells that express CXCR5 provide accelerated help to B cells. J Immunol *186*, 2889-2896.

Mak, T.W., Shahinian, A., Yoshinaga, S.K., Wakeham, A., Boucher, L.M., Pintilie, M., Duncan, G., Gajewska, B.U., Gronski, M., Eriksson, U.*, et al.* (2003). Costimulation through the inducible costimulator ligand is essential for both T helper and B cell functions in T cell-dependent B cell responses. Nat Immunol *4*, 765-772.

Marshall, H.D., Chandele, A., Jung, Y.W., Meng, H., Poholek, A.C., Parish, I.A., Rutishauser, R., Cui, W., Kleinstein, S.H., Craft, J., and Kaech, S.M. (2011). Differential expression of Ly6C and T-bet distinguish effector and memory Th1 CD4(+) cell properties during viral infection. Immunity *35*, 633-646.

Marzo, A.L., Klonowski, K.D., Le Bon, A., Borrow, P., Tough, D.F., and Lefrancois, L. (2005). Initial T cell frequency dictates memory CD8+ T cell lineage commitment. Nat Immunol *6*, 793-799.

McAdam, A.J., Chang, T.T., Lumelsky, A.E., Greenfield, E.A., Boussiotis, V.A., Duke-Cohan, J.S., Chernova, T., Malenkovich, N., Jabs, C., Kuchroo, V.K.*, et al.* (2000). Mouse inducible costimulatory molecule (ICOS) expression is enhanced by CD28 costimulation and regulates differentiation of CD4+ T cells. J Immunol *165*, 5035-5040.

McAdam, A.J., Greenwald, R.J., Levin, M.A., Chernova, T., Malenkovich, N., Ling, V., Freeman, G.J., and Sharpe, A.H. (2001). ICOS is critical for CD40-mediated antibody class switching. Nature *409*, 102-105.

McSorley, S.J., and Jenkins, M.K. (2000). Antibody is required for protection against virulent but not attenuated Salmonella enterica serovar typhimurium. Infect Immun *68*, 3344-3348.

Medeiros, R.B., Burbach, B.J., Mueller, K.L., Srivastava, R., Moon, J.J., Highfill, S., Peterson, E.J., and Shimizu, Y. (2007). Regulation of NF-kappaB activation in T cells via association of the adapter proteins ADAP and CARMA1. Science *316*, 754-758.

Michel, F., Attal-Bonnefoy, G., Mangino, G., Mise-Omata, S., and Acuto, O. (2001). CD28 as a molecular amplifier extending TCR ligation and signaling capabilities. Immunity *15*, 935-945.

Mittrucker, H.W., Kursar, M., Kohler, A., Yanagihara, D., Yoshinaga, S.K., and Kaufmann, S.H. (2002). Inducible costimulator protein controls the protective T cell response against Listeria monocytogenes. J Immunol *169*, 5813-5817.

Mombaerts, P., Iacomini, J., Johnson, R.S., Herrup, K., Tonegawa, S., and Papaioannou, V.E. (1992). RAG-1-deficient mice have no mature B and T lymphocytes. Cell *68*, 869-877.

Monack, D.M., Mueller, A., and Falkow, S. (2004). Persistent bacterial infections: the interface of the pathogen and the host immune system. Nat. Rev. Microbiol. *2*, 747-765.

Moon, J.J., Chu, H.H., Hataye, J., Pagan, A.J., Pepper, M., McLachlan, J.B., Zell, T., and Jenkins, M.K. (2009). Tracking epitope-specific T cells. Nat Protoc *4*, 565-581.

Moon, J.J., Chu, H.H., Pepper, M., McSorley, S.J., Jameson, S.C., Kedl, R.M., and Jenkins, M.K. (2007). Naive CD4(+) T cell frequency varies for different epitopes and predicts repertoire diversity and response magnitude. Immunity *27*, 203-213.

Morita, R., Schmitt, N., Bentebibel, S.E., Ranganathan, R., Bourdery, L., Zurawski, G., Foucat, E., Dullaers, M., Oh, S., Sabzghabaei, N., *et al.* (2011). Human blood CXCR5(+)CD4(+) T cells are counterparts of T follicular cells and contain specific subsets that differentially support antibody secretion. Immunity *34*, 108-121.

Mueller, D.L., Jenkins, M.K., and Schwartz, R.H. (1989a). An accessory cell-derived costimulatory signal acts independently of protein kinase C activation to allow T cell proliferation and prevent the induction of unresponsiveness. J Immunol *142*, 2617-2628.

Mueller, D.L., Jenkins, M.K., and Schwartz, R.H. (1989b). Clonal expansion versus functional clonal inactivation: a costimulatory signalling pathway determines the outcome of T cell antigen receptor occupancy. Annu Rev Immunol *7*, 445-480.

Nakayamada, S., Kanno, Y., Takahashi, H., Jankovic, D., Lu, K.T., Johnson, T.A., Sun, H.W., Vahedi, G., Hakim, O., Handon, R.*, et al.* (2011). Early Th1 cell differentiation is marked by a Tfh cell-like transition. Immunity *35*, 919-931.

Narayan, P., Holt, B., Tosti, R., and Kane, L.P. (2006). CARMA1 is required for Akt-mediated NF-kappaB activation in T cells. Mol Cell Biol *26*, 2327-2336.

Nikolich-Zugich, J., Slifka, M.K., and Messaoudi, I. (2004). The many important facets of T-cell repertoire diversity. Nat Rev Immunol *4*, 123-132.

Nurieva, R.I., Chung, Y., Hwang, D., Yang, X.O., Kang, H.S., Ma, L., Wang, Y.H., Watowich, S.S., Jetten, A.M., Tian, Q., and Dong, C. (2008). Generation of T follicular helper cells is mediated by interleukin-21 but independent of T helper 1, 2, or 17 cell lineages. Immunity *29*, 138-149.

Nurieva, R.I., Chung, Y., Martinez, G.J., Yang, X.O., Tanaka, S., Matskevitch, T.D., Wang, Y.H., and Dong, C. (2009). Bcl6 mediates the development of T follicular helper cells. Science *325*, 1001-1005.

Nurieva, R.I., Podd, A., Chen, Y., Alekseev, A.M., Yu, M., Qi, X., Huang, H., Wen, R., Wang, J., Li, H.S.*, et al.* (2012). STAT5 Protein Negatively Regulates T Follicular Helper (Tfh) Cell Generation and Function. J Biol Chem *287*, 11234-11239.

Obar, J.J., Molloy, M.J., Jellison, E.R., Stoklasek, T.A., Zhang, W., Usherwood, E.J., and Lefrancois, L. (2010). CD4+ T cell regulation of CD25 expression controls development of short-lived effector CD8+ T cells in primary and secondary responses. Proc Natl Acad Sci U S A *107*, 193-198.

Oestreich, K.J., Mohn, S.E., and Weinmann, A.S. (2012). Molecular mechanisms that control the expression and activity of Bcl-6 in TH1 cells to regulate flexibility with a TFH-like gene profile. Nat Immunol *13*, 405-411.

Okkenhaug, K., Wu, L., Garza, K.M., La Rose, J., Khoo, W., Odermatt, B., Mak, T.W., Ohashi, P.S., and Rottapel, R. (2001). A point mutation in CD28 distinguishes proliferative signals from survival signals. Nat Immunol *2*, 325-332.

Pages, F., Ragueneau, M., Rottapel, R., Truneh, A., Nunes, J., Imbert, J., and Olive, D. (1994). Binding of phosphatidylinositol-3-OH kinase to CD28 is required for T-cell signalling. Nature *369*, 327-329.

Pamer, E.G. (2004). Immune responses to Listeria monocytogenes. Nat Rev Immunol *4*, 812-823.

Pape, K.A., Catron, D.M., Itano, A.A., and Jenkins, M.K. (2007). The humoral immune response is initiated in lymph nodes by B cells that acquire soluble antigen directly in the follicles. Immunity *26*, 491-502.

Park, S.G., Schulze-Luehrman, J., Hayden, M.S., Hashimoto, N., Ogawa, W., Kasuga, M., and Ghosh, S. (2009). The kinase PDK1 integrates T cell antigen receptor and CD28 coreceptor signaling to induce NF-kappaB and activate T cells. Nat Immunol *10*, 158-166.

Parry, R.V., Rumbley, C.A., Vandenberghe, L.H., June, C.H., and Riley, J.L. (2003). CD28 and inducible costimulatory protein Src homology 2 binding domains show distinct regulation of phosphatidylinositol 3-kinase, Bcl-xL, and IL-2 expression in primary human CD4 T lymphocytes. J Immunol *171*, 166-174.

Pearce, E.L., Walsh, M.C., Cejas, P.J., Harms, G.M., Shen, H., Wang, L.S., Jones, R.G., and Choi, Y. (2009). Enhancing CD8 T-cell memory by modulating fatty acid metabolism. Nature *460*, 103-107.

Pepper, M., and Jenkins, M.K. (2011). Origins of CD4(+) effector and central memory T cells. Nat Immunol *131*, 467-471.

Pepper, M., Linehan, J.L., Pagan, A.J., Zell, T., Dileepan, T., Cleary, P.P., and Jenkins, M.K. (2010). Different routes of bacterial infection induce long-lived TH1 memory cells and short-lived TH17 cells. Nat Immunol *11*, 83-89.

Pepper, M., Pagan, A.J., Igyarto, B.Z., Taylor, J.J., and Jenkins, M.K. (2011). Opposing signals from the Bcl6 transcription factor and the interleukin-2 receptor generate T helper 1 central and effector memory cells. Immunity *35*, 583-595.

Pipkin, M.E., Sacks, J.A., Cruz-Guilloty, F., Lichtenheld, M.G., Bevan, M.J., and Rao, A. (2010). Interleukin-2 and inflammation induce distinct transcriptional programs that promote the differentiation of effector cytolytic T cells. Immunity *32*, 79-90.

Pobezinsky, L.A., Angelov, G.S., Tai, X., Jeurling, S., Van Laethem, F., Feigenbaum, L., Park, J.H., and Singer, A. (2012). Clonal deletion and the fate of autoreactive thymocytes that survive negative selection. Nat Immunol *13*, 569-578.

Portnoy, D.A., Auerbuch, V., and Glomski, I.J. (2002). The cell biology of Listeria monocytogenes infection: the intersection of bacterial pathogenesis and cell-mediated immunity. J Cell Biol *158*, 409-414.

Punt, J.A., Havran, W., Abe, R., Sarin, A., and Singer, A. (1997). T cell receptor (TCR)-induced death of immature CD4+CD8+ thymocytes by two distinct mechanisms differing in their requirement for CD28 costimulation: implications for negative selection in the thymus. J Exp Med *186*, 1911-1922.

Punt, J.A., Osborne, B.A., Takahama, Y., Sharrow, S.O., and Singer, A. (1994). Negative selection of CD4+CD8+ thymocytes by T cell receptor-induced apoptosis requires a costimulatory signal that can be provided by CD28. J Exp Med *179*, 709-713.

Quah, B.J., Warren, H.S., and Parish, C.R. (2007). Monitoring lymphocyte proliferation in vitro and in vivo with the intracellular fluorescent dye carboxyfluorescein diacetate succinimidyl ester. Nat Protoc *2*, 2049-2056.

Racine, R., Jones, D.D., Chatterjee, M., McLaughlin, M., Macnamara, K.C., and Winslow, G.M. (2010). Impaired germinal center responses and suppression of local IgG production during intracellular bacterial infection. J Immunol *184*, 5085-5093.

Rasheed, A.U., Rahn, H.P., Sallusto, F., Lipp, M., and Muller, G. (2006). Follicular B helper T cell activity is confined to CXCR5(hi)ICOS(hi) CD4 T cells and is independent of CD57 expression. Eur J Immunol *36*, 1892-1903.

Rathmell, J.C., Elstrom, R.L., Cinalli, R.M., and Thompson, C.B. (2003). Activated Akt promotes increased resting T cell size, CD28-independent T cell growth, and development of autoimmunity and lymphoma. Eur J Immunol *33*, 2223-2232.

Rees, W., Bender, J., Teague, T.K., Kedl, R.M., Crawford, F., Marrack, P., and Kappler, J. (1999). An inverse relationship between T cell receptor affinity and antigen dose during CD4(+) T cell responses in vivo and in vitro. Proc Natl Acad Sci U S A *96*, 9781-9786.

Reinhardt, R.L., Khoruts, A., Merica, R., Zell, T., and Jenkins, M.K. (2001). Visualizing the generation of memory CD4 T cells in the whole body. Nature *410*, 101-105.

Riley, J.L., Mao, M., Kobayashi, S., Biery, M., Burchard, J., Cavet, G., Gregson, B.P., June, C.H., and Linsley, P.S. (2002). Modulation of TCR-induced transcriptional profiles by ligation of CD28, ICOS, and CTLA-4 receptors. Proc Natl Acad Sci U S A *99*, 11790-11795.

Rogers, P.R., Song, J., Gramaglia, I., Killeen, N., and Croft, M. (2001). OX40 promotes Bcl-xL and Bcl-2 expression and is essential for long-term survival of CD4 T cells. Immunity *15*, 445-455.

Rolf, J., Bell, S.E., Kovesdi, D., Janas, M.L., Soond, D.R., Webb, L.M., Santinelli, S., Saunders, T., Hebeis, B., Killeen, N., *et al.* (2010). Phosphoinositide 3-kinase activity in

T cells regulates the magnitude of the germinal center reaction. J Immunol *185*, 4042-4052.

Rubtsov, Y.P., Niec, R.E., Josefowicz, S., Li, L., Darce, J., Mathis, D., Benoist, C., and Rudensky, A.Y. (2010). Stability of the regulatory T cell lineage in vivo. Science *329*, 1667-1671.

Rudd, C.E., and Schneider, H. (2003). Unifying concepts in CD28, ICOS and CTLA4 co-receptor signalling. Nat Rev Immunol *3*, 544-556.

Rutishauser, R.L., Martins, G.A., Kalachikov, S., Chandele, A., Parish, I.A., Meffre, E., Jacob, J., Calame, K., and Kaech, S.M. (2009). Transcriptional repressor Blimp-1 promotes CD8(+) T cell terminal differentiation and represses the acquisition of central memory T cell properties. Immunity *31*, 296-308.

Sallusto, F., Geginat, J., and Lanzavecchia, A. (2004). Central memory and effector memory T cell subsets: function, generation, and maintenance. Annu Rev Immunol *22*, 745-763.

Sallusto, F., Lenig, D., Forster, R., Lipp, M., and Lanzavecchia, A. (1999). Two subsets of memory T lymphocytes with distinct homing potentials and effector functions. Nature *401*, 708-712.

Sallusto, F., and Mackay, C.R. (2004). Chemoattractants and their receptors in homeostasis and inflammation. Curr Opin Immunol *16*, 724-731.

Sanchez-Lockhart, M., Graf, B., and Miller, J. (2008). Signals and sequences that control CD28 localization to the central region of the immunological synapse. J Immunol *181*, 7639-7648.

Sanchez-Lockhart, M., Marin, E., Graf, B., Abe, R., Harada, Y., Sedwick, C.E., and Miller, J. (2004). Cutting edge: CD28-mediated transcriptional and posttranscriptional regulation of IL-2 expression are controlled through different signaling pathways. J Immunol *173*, 7120-7124.

Sarkar, S., Teichgraber, V., Kalia, V., Polley, A., Masopust, D., Harrington, L.E., Ahmed, R., and Wherry, E.J. (2007). Strength of stimulus and clonal competition impact the rate of memory CD8 T cell differentiation. J Immunol *179*, 6704-6714.

Schatz, D.G., and Ji, Y. (2011). Recombination centres and the orchestration of V(D)J recombination. Nat Rev Immunol *11*, 251-263.

Schmelzle, T., and Hall, M.N. (2000). TOR, a central controller of cell growth. Cell *103*, 253-262.

Sette, A., Moutaftsi, M., Moyron-Quiroz, J., McCausland, M.M., Davies, D.H., Johnston, R.J., Peters, B., Rafii-El-Idrissi Benhnia, M., Hoffmann, J., Su, H.P., *et al.* (2008). Selective CD4+ T cell help for antibody responses to a large viral pathogen: deterministic linkage of specificities. Immunity *28*, 847-858.

Sha, W.C., Liou, H.C., Tuomanen, E.I., and Baltimore, D. (1995). Targeted disruption of the p50 subunit of NF-kappa B leads to multifocal defects in immune responses. Cell *80*, 321-330.

Shaffer, A.L., Lin, K.I., Kuo, T.C., Yu, X., Hurt, E.M., Rosenwald, A., Giltnane, J.M., Yang, L., Zhao, H., Calame, K., and Staudt, L.M. (2002). Blimp-1 orchestrates plasma cell differentiation by extinguishing the mature B cell gene expression program. Immunity *17*, 51-62.

Shaffer, A.L., Yu, X., He, Y., Boldrick, J., Chan, E.P., and Staudt, L.M. (2000). BCL-6 represses genes that function in lymphocyte differentiation, inflammation, and cell cycle control. Immunity *13*, 199-212.

Shahinian, A., Pfeffer, K., Lee, K.P., Kundig, T.M., Kishihara, K., Wakeham, A., Kawai, K., Ohashi, P.S., Thompson, C.B., and Mak, T.W. (1993). Differential T cell costimulatory requirements in CD28-deficient mice. Science *261*, 609-612.

Shin, H., Blackburn, S.D., Intlekofer, A.M., Kao, C., Angelosanto, J.M., Reiner, S.L., and Wherry, E.J. (2009). A role for the transcriptional repressor Blimp-1 in CD8(+) T cell exhaustion during chronic viral infection. Immunity *31*, 309-320.

Siggs, O.M., Makaroff, L.E., and Liston, A. (2006). The why and how of thymocyte negative selection. Curr Opin Immunol *18*, 175-183.

Singer, A., Adoro, S., and Park, J.H. (2008). Lineage fate and intense debate: myths, models and mechanisms of CD4- versus CD8-lineage choice. Nat Rev Immunol *8*, 788-801.

Snapper, C.M., and Paul, W.E. (1987). Interferon-gamma and B cell stimulatory factor-1 reciprocally regulate Ig isotype production. Science *236*, 944-947.

Song, J., Salek-Ardakani, S., So, T., and Croft, M. (2007). The kinases aurora B and mTOR regulate the G1-S cell cycle progression of T lymphocytes. Nat Immunol *8*, 64-73.

Sperling, A.I., Auger, J.A., Ehst, B.D., Rulifson, I.C., Thompson, C.B., and Bluestone, J.A. (1996). CD28/B7 interactions deliver a unique signal to naive T cells that regulates cell survival but not early proliferation. J Immunol *157*, 3909-3917.

Srinivas, S., Watanabe, T., Lin, C.S., William, C.M., Tanabe, Y., Jessell, T.M., and Costantini, F. (2001). Cre reporter strains produced by targeted insertion of EYFP and ECFP into the ROSA26 locus. BMC Dev. Biol. *1*, 4.

Stadinski, B.D., Zhang, L., Crawford, F., Marrack, P., Eisenbarth, G.S., and Kappler, J.W. (2010). Diabetogenic T cells recognize insulin bound to IAg7 in an unexpected, weakly binding register. Proc Natl Acad Sci U S A *107*, 10978-10983.

Suh, W.K., Tafuri, A., Berg-Brown, N.N., Shahinian, A., Plyte, S., Duncan, G.S., Okada, H., Wakeham, A., Odermatt, B., Ohashi, P.S., and Mak, T.W. (2004). The inducible costimulator plays the major costimulatory role in humoral immune responses in the absence of CD28. J Immunol *172*, 5917-5923.

Sun, Z., Arendt, C.W., Ellmeier, W., Schaeffer, E.M., Sunshine, M.J., Gandhi, L., Annes, J., Petrzilka, D., Kupfer, A., Schwartzberg, P.L., and Littman, D.R. (2000). PKC-theta is required for TCR-induced NF-kappaB activation in mature but not immature T lymphocytes. Nature *404*, 402-407.

Surh, C.D., and Sprent, J. (2008). Homeostasis of naive and memory T cells. Immunity *29*, 848-862.

Suzuki, A., Yamaguchi, M.T., Ohteki, T., Sasaki, T., Kaisho, T., Kimura, Y., Yoshida, R., Wakeham, A., Higuchi, T., Fukumoto, M*., et al.* (2001). T cell-specific loss of Pten leads to defects in central and peripheral tolerance. Immunity *14*, 523-534.

Swain, S.L., McKinstry, K.K., and Strutt, T.M. (2012). Expanding roles for CD4(+) T cells in immunity to viruses. Nat Rev Immunol *12*, 136-148.

Tafuri, A., Shahinian, A., Bladt, F., Yoshinaga, S.K., Jordana, M., Wakeham, A., Boucher, L.M., Bouchard, D., Chan, V.S., Duncan, G*., et al.* (2001). ICOS is essential for effective T-helper-cell responses. Nature *409*, 105-109.

Tai, X., Cowan, M., Feigenbaum, L., and Singer, A. (2005). CD28 costimulation of developing thymocytes induces Foxp3 expression and regulatory T cell differentiation independently of interleukin 2. Nat Immunol *6*, 152-162.

Tai, X., Van Laethem, F., Sharpe, A.H., and Singer, A. (2007). Induction of autoimmune disease in CTLA-4-/- mice depends on a specific CD28 motif that is required for in vivo costimulation. Proc Natl Acad Sci U S A *104*, 13756-13761.

Tavano, R., Contento, R.L., Baranda, S.J., Soligo, M., Tuosto, L., Manes, S., and Viola, A. (2006). CD28 interaction with filamin-A controls lipid raft accumulation at the T-cell immunological synapse. Nat Cell Biol *8*, 1270-1276.

Thompson, C.B., Lindsten, T., Ledbetter, J.A., Kunkel, S.L., Young, H.A., Emerson, S.G., Leiden, J.M., and June, C.H. (1989). CD28 activation pathway regulates the production of multiple T-cell-derived lymphokines/cytokines. Proc Natl Acad Sci U S A *86*, 1333-1337.

Trumpfheller, C., Longhi, M.P., Caskey, M., Idoyaga, J., Bozzacco, L., Keler, T., Schlesinger, S.J., and Steinman, R.M. (2012). Dendritic cell-targeted protein vaccines: a novel approach to induce T-cell immunity. J Intern Med *271*, 183-192.

Tsien, R.Y. (1998). The green fluorescent protein. Annu Rev Biochem *67*, 509-544.

Umlauf, S.W., Beverly, B., Lantz, O., and Schwartz, R.H. (1995). Regulation of interleukin 2 gene expression by CD28 costimulation in mouse T-cell clones: both nuclear and cytoplasmic RNAs are regulated with complex kinetics. Mol Cell Biol *15*, 3197-3205.

van Berkel, M.E., and Oosterwegel, M.A. (2006). CD28 and ICOS: similar or separate costimulators of T cells? Immunol Lett *105*, 115-122.

van Berkel, M.E., Schrijver, E.H., Hofhuis, F.M., Sharpe, A.H., Coyle, A.J., Broeren, C.P., Tesselaar, K., and Oosterwegel, M.A. (2005). ICOS contributes to T cell expansion in CTLA-4 deficient mice. J Immunol *175*, 182-188.

van Faassen, H., Saldanha, M., Gilbertson, D., Dudani, R., Krishnan, L., and Sad, S. (2005). Reducing the stimulation of CD8+ T cells during infection with intracellular bacteria promotes differentiation primarily into a central (CD62LhighCD44high) subset. J Immunol *174*, 5341-5350.

Vang, K.B., Yang, J., Pagan, A.J., Li, L.X., Wang, J., Green, J.M., Beg, A.A., and Farrar, M.A. (2010). Cutting edge: CD28 and c-Rel-dependent pathways initiate regulatory T cell development. J Immunol *184*, 4074-4077.

Vinuesa, C.G., Cook, M.C., Angelucci, C., Athanasopoulos, V., Rui, L., Hill, K.M., Yu, D., Domaschenz, H., Whittle, B., Lambe, T., *et al.* (2005). A RING-type ubiquitin ligase family member required to repress follicular helper T cells and autoimmunity. Nature *435*, 452-458.

Viola, A., and Lanzavecchia, A. (1996). T cell activation determined by T cell receptor number and tunable thresholds. Science *273*, 104-106.

von Boehmer, H., Aifantis, I., Azogui, O., Feinberg, J., Saint-Ruf, C., Zober, C., Garcia, C., and Buer, J. (1998). Crucial function of the pre-T-cell receptor (TCR) in TCR beta selection, TCR beta allelic exclusion and alpha beta versus gamma delta lineage commitment. Immunol Rev *165*, 111-119.

Waldmann, T.A. (1989). The multi-subunit interleukin-2 receptor. Annu Rev Biochem *58*, 875-911.

Walker, L.S., and Abbas, A.K. (2002). The enemy within: keeping self-reactive T cells at bay in the periphery. Nat Rev Immunol *2*, 11-19.

Weinblatt, M., Combe, B., Covucci, A., Aranda, R., Becker, J.C., and Keystone, E. (2006). Safety of the selective costimulation modulator abatacept in rheumatoid arthritis patients receiving background biologic and nonbiologic disease-modifying antirheumatic drugs: A one-year randomized, placebo-controlled study. Arthritis Rheum *54*, 2807-2816.

Wells, A.D., Gudmundsdottir, H., and Turka, L.A. (1997). Following the fate of individual T cells throughout activation and clonal expansion. Signals from T cell receptor and CD28 differentially regulate the induction and duration of a proliferative response. J Clin Invest *100*, 3173-3183.

Wherry, E.J., Blattman, J.N., Murali-Krishna, K., van der Most, R., and Ahmed, R. (2003). Viral persistence alters CD8 T-cell immunodominance and tissue distribution and results in distinct stages of functional impairment. J Virol *77*, 4911-4927.

Whitmire, J.K., Asano, M.S., Kaech, S.M., Sarkar, S., Hannum, L.G., Shlomchik, M.J., and Ahmed, R. (2009). Requirement of B cells for generating CD4+ T cell memory. J Immunol *182*, 1868-1876.

Willerford, D.M., Chen, J., Ferry, J.A., Davidson, L., Ma, A., and Alt, F.W. (1995). Interleukin-2 receptor alpha chain regulates the size and content of the peripheral lymphoid compartment. Immunity *3*, 521-530.

Williams, M.A., Tyznik, A.J., and Bevan, M.J. (2006). Interleukin-2 signals during priming are required for secondary expansion of CD8+ memory T cells. Nature *441*, 890-893.

Yan, J., Wolff, M.J., Unternaehrer, J., Mellman, I., and Mamula, M.J. (2005). Targeting antigen to CD19 on B cells efficiently activates T cells. Int Immunol *17*, 869-877.

Yokosuka, T., Kobayashi, W., Sakata-Sogawa, K., Takamatsu, M., Hashimoto-Tane, A., Dustin, M.L., Tokunaga, M., and Saito, T. (2008). Spatiotemporal regulation of T cell costimulation by TCR-CD28 microclusters and protein kinase C theta translocation. Immunity *29*, 589-601.

Yoshinaga, S.K., Whoriskey, J.S., Khare, S.D., Sarmiento, U., Guo, J., Horan, T., Shih, G., Zhang, M., Coccia, M.A., Kohno, T., *et al.* (1999). T-cell co-stimulation through B7RP-1 and ICOS. Nature *402*, 827-832.

Yu, D., Rao, S., Tsai, L.M., Lee, S.K., He, Y., Sutcliffe, E.L., Srivastava, M., Linterman, M., Zheng, L., Simpson, N., *et al.* (2009). The transcriptional repressor Bcl-6 directs T follicular helper cell lineage commitment. Immunity *31*, 457-468.

Yusuf, I., Kageyama, R., Monticelli, L., Johnston, R.J., Ditoro, D., Hansen, K., Barnett, B., and Crotty, S. (2010). Germinal center T follicular helper cell IL-4 production is dependent on signaling lymphocytic activation molecule receptor (CD150). J Immunol *185*, 190-202.

Zang, X., Loke, P., Kim, J., Wojnoonski, K., Kusdra, L., and Allison, J.P. (2006). A genetic library screen for signaling proteins that interact with phosphorylated T cell costimulatory receptors. Genomics *88*, 841-845.

Zaph, C., Uzonna, J., Beverley, S.M., and Scott, P. (2004). Central memory T cells mediate long-term immunity to Leishmania major in the absence of persistent parasites. Nat Med *10*, 1104-1110.

Zheng, Y., Collins, S.L., Lutz, M.A., Allen, A.N., Kole, T.P., Zarek, P.E., and Powell, J.D. (2007). A role for mammalian target of rapamycin in regulating T cell activation versus anergy. J Immunol *178*, 2163-2170.